A Methodology for Predicting Post-earthquake Traffic Capacity of Simply-Supported Girder Bridge Groups on Regional High-Speed Railways

Lingxu Wu[1] 、Lizhong Jiang[2,3] 、Wangbao Zhou[2]、Yulin Feng[4]

1. Zhejiang University of Water Resources and Electric Power, Hangzhou, Zhejiang;
2. Central South University, Changsha, Hunan;
3. Hunan University of Science and Technology, Xiangtan, Hunan;
4. East China Jiaotong University, Nanchang, Jiangxi

June 2026

Presentation Outline

Background and State of the Art

Data-Driven Seismic Damage Prediction Method for High-Speed Railway Simply Supported Girder Bridge Systems

Seismic Response Prediction and Uncertainty Quantification for High-Speed Railway Simply Supported Girder Bridge System

Seismic Reliability Assessment Method for High-Speed Railway Simply Supported Girder Bridge Systems

Regional Seismic Reliability Assessment of High-Speed Railway Simply Supported Girder Bridge Systems

Research Background and Significance

- High-speed railways often replace embankments with bridges to ensure running smoothness, resulting in long bridge sections and a high bridge proportion.
- Many planned and under-construction high-speed railways extend into seismic fault zones and high-seismic-intensity regions, with several routes in the “Eight Vertical and Eight Horizontal” network passing through such areas.

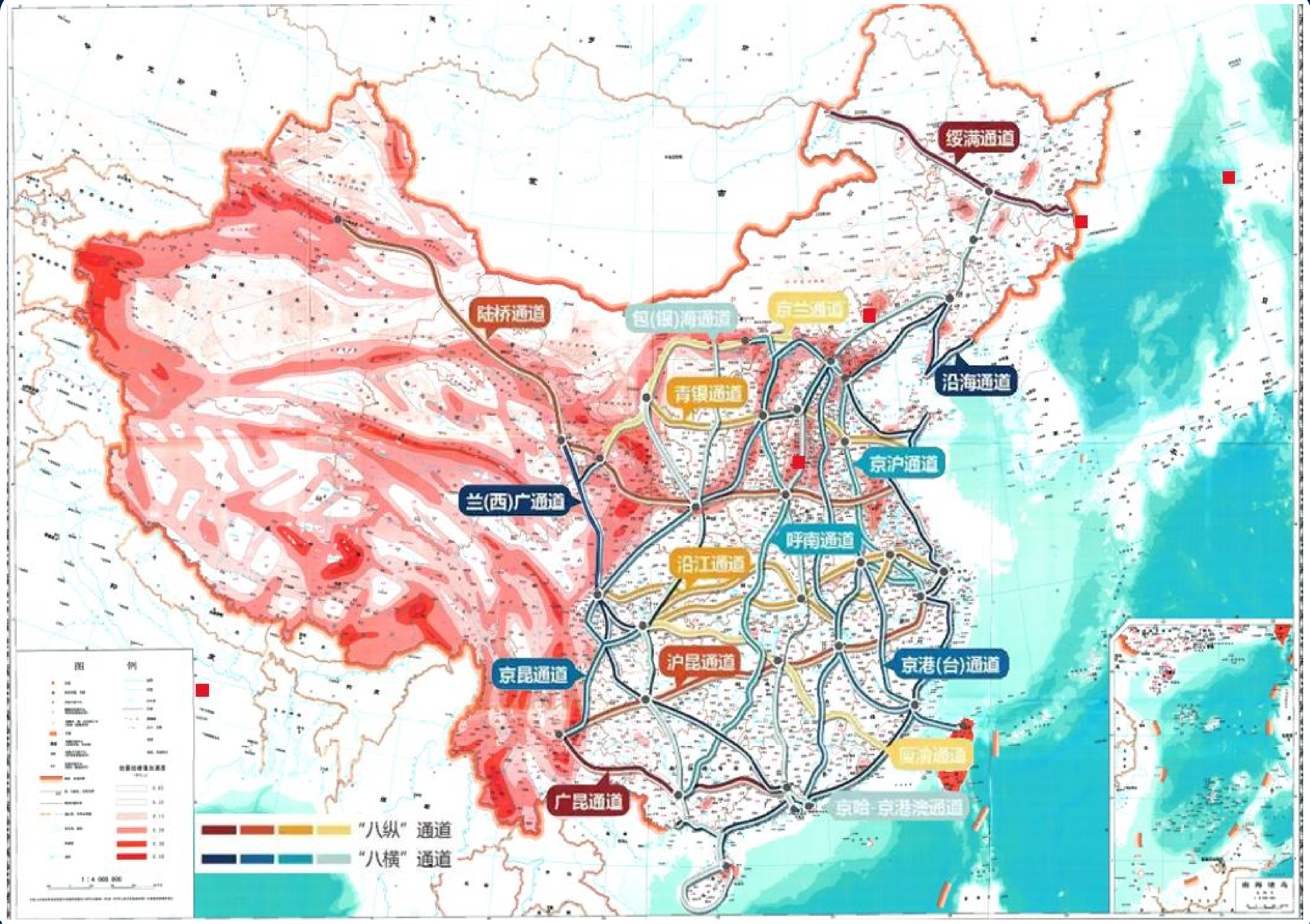

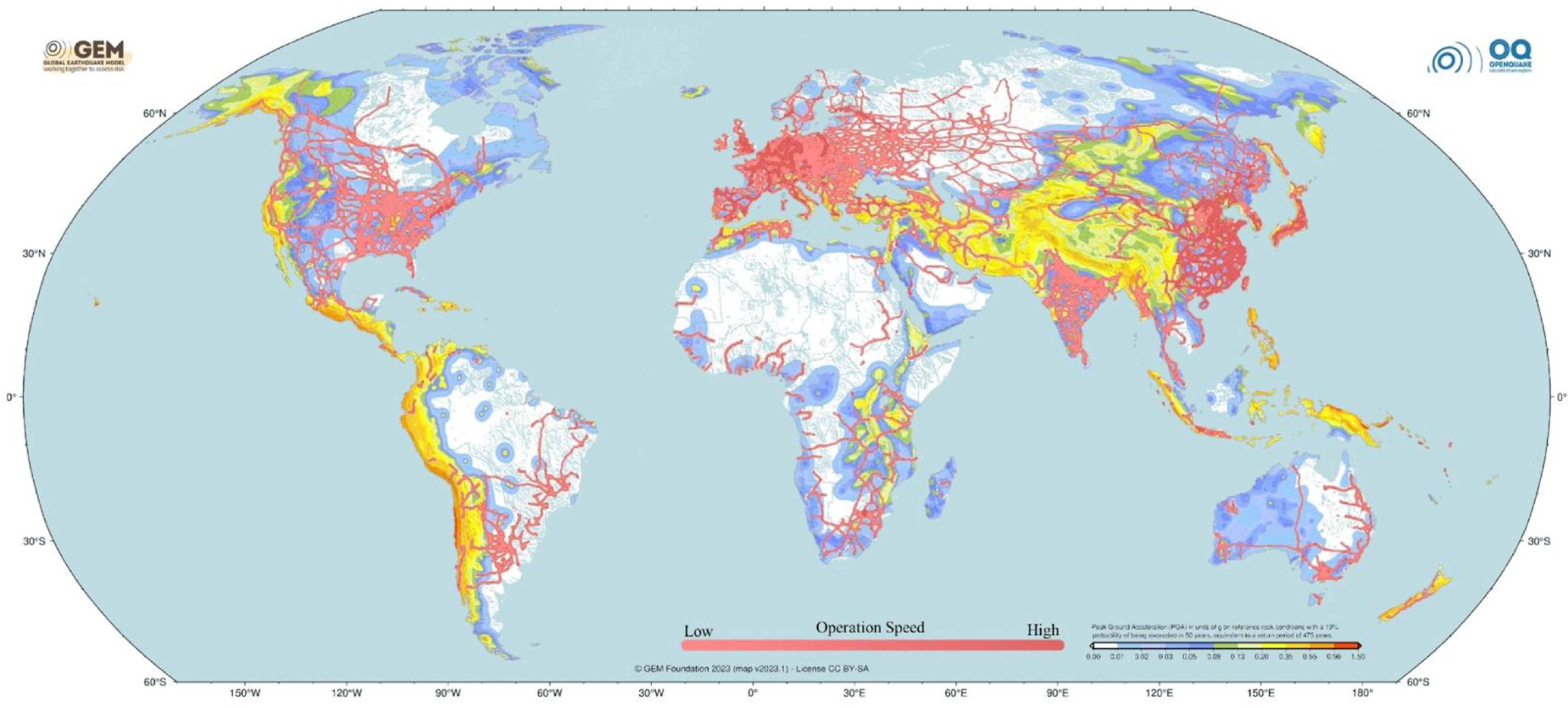

Research Background and Significance

- High-speed railway serves as a key means of **transporting emergency supplies and personnel** after earthquakes, owing to its high transport capacity, speed, and efficiency.
- Rapid prediction of component responses and damage states is critical for assessing **regional transport capacity**, supporting rescue decisions, guiding repairs, and restoring railway operability and bridge safety.

Seismic Damage of High-Speed Railway Bridges

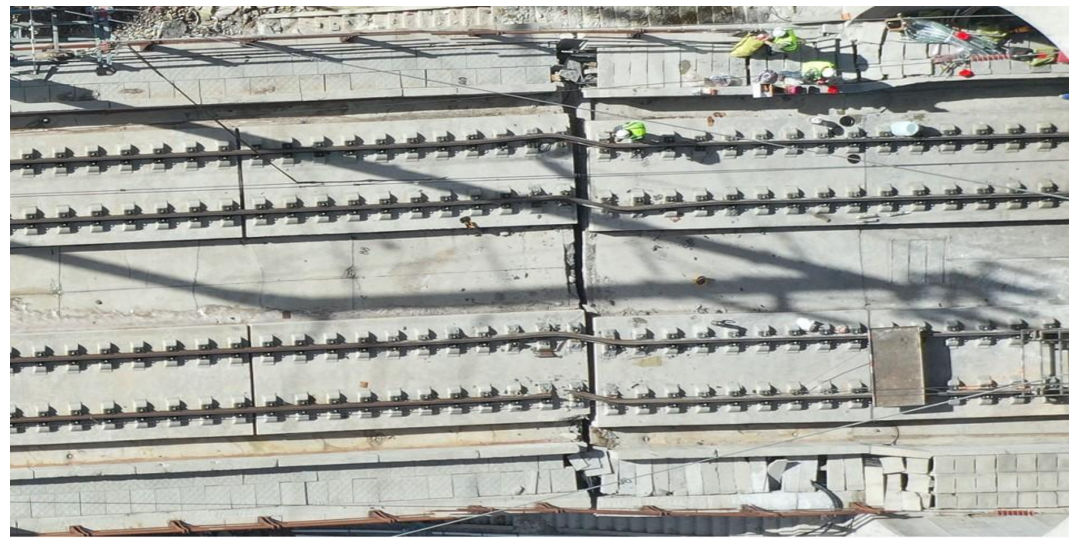

Train Suspensions and Delays

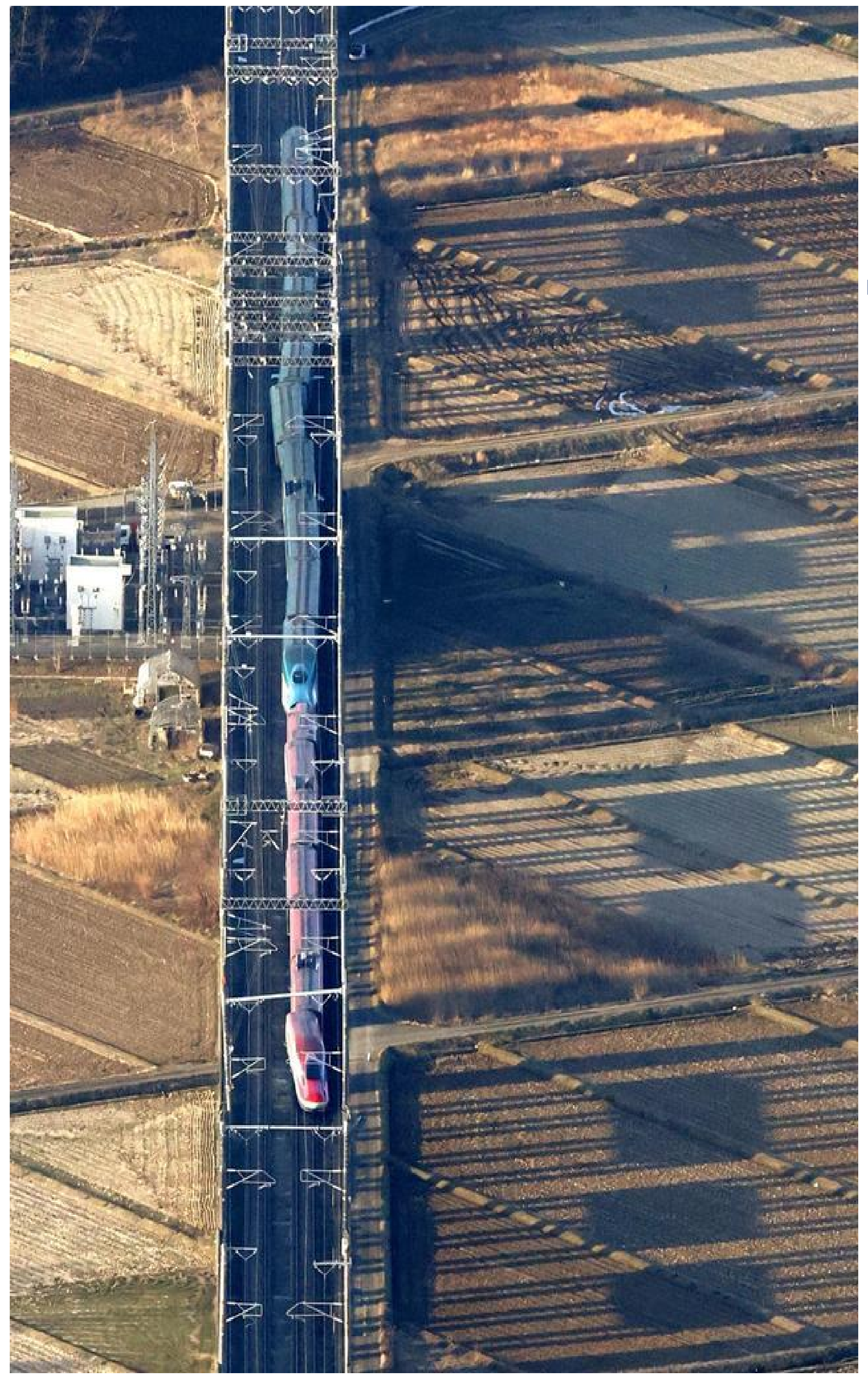

Threatening Bridge Train Operation Safety

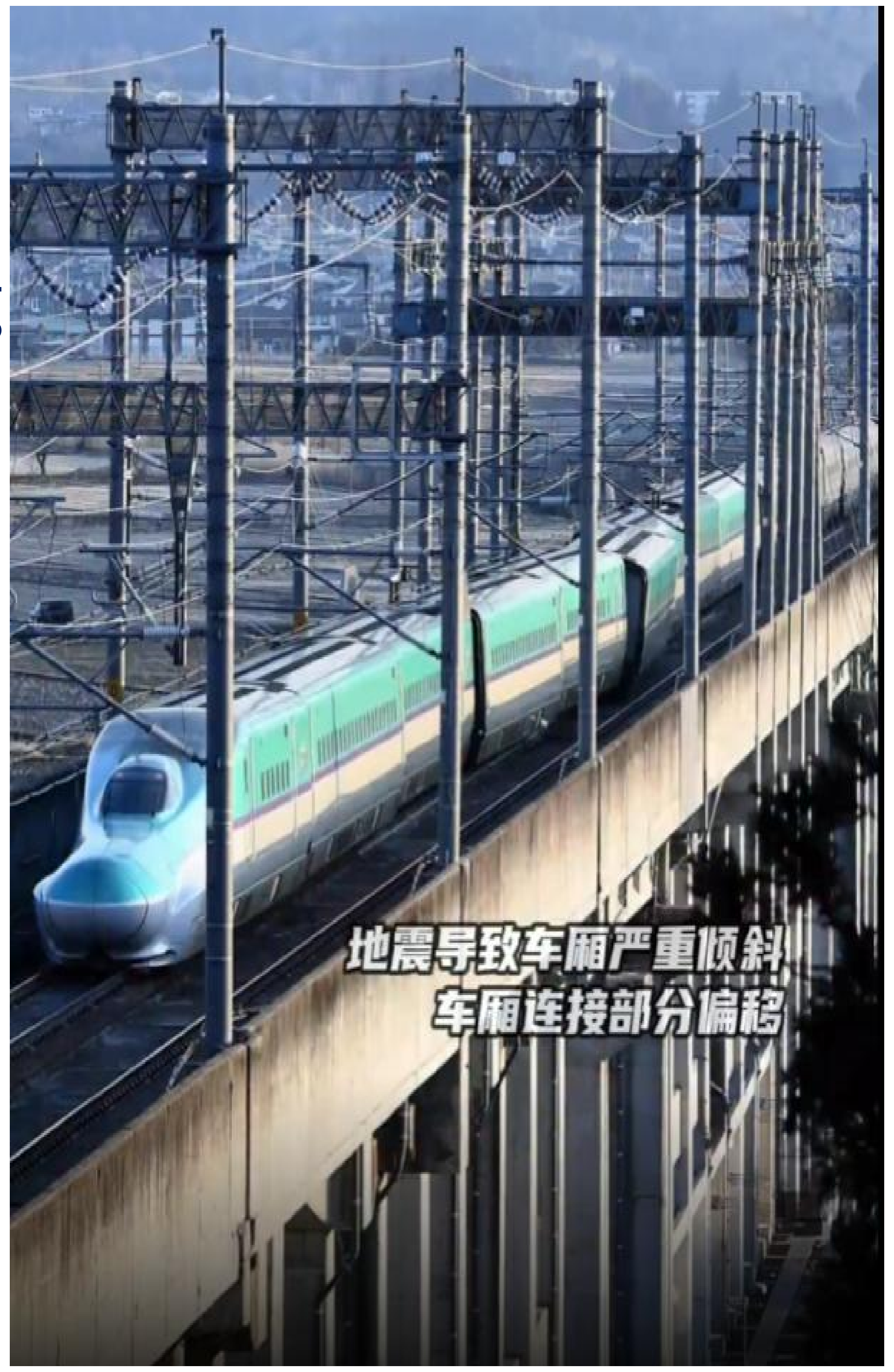

Research Background and Significance

浙江水利水電學院
Zhejiang University of Water Resources and Electric Power

- Sparse station deployment has caused a severe shortage of natural ground-motion records, limiting the characterization of regional propagation–attenuation patterns and spatiotemporal evolution mechanisms.
- It further falls short of supporting post-earthquake structural damage mechanism analysis with sufficient high-fidelity samples, resulting in a regional high-risk–low-data-density mismatch.

Limited Natural Ground-Motion Samples

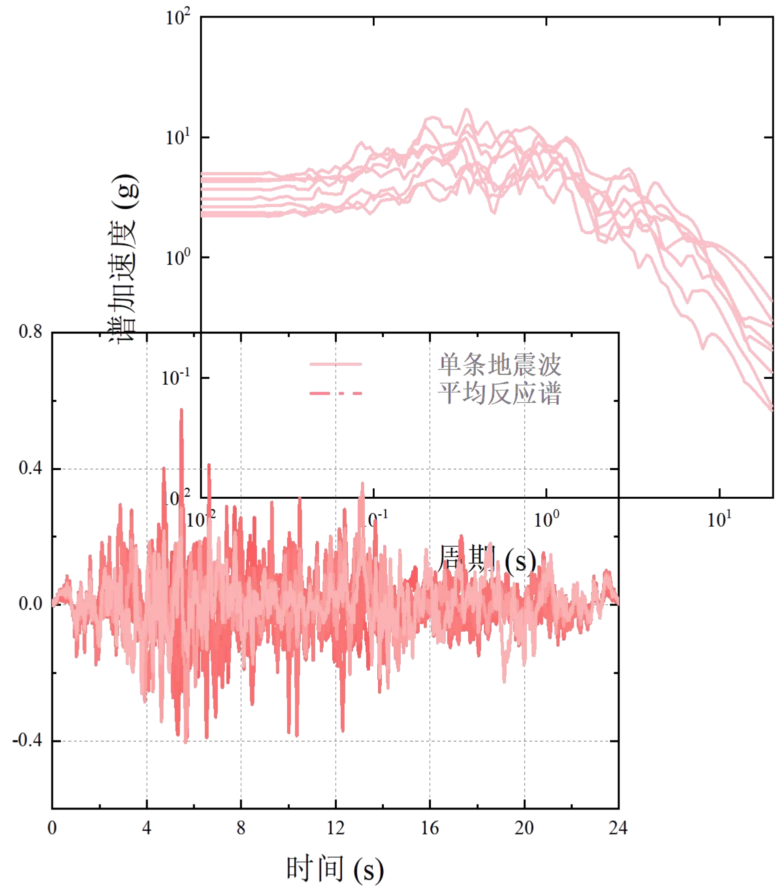

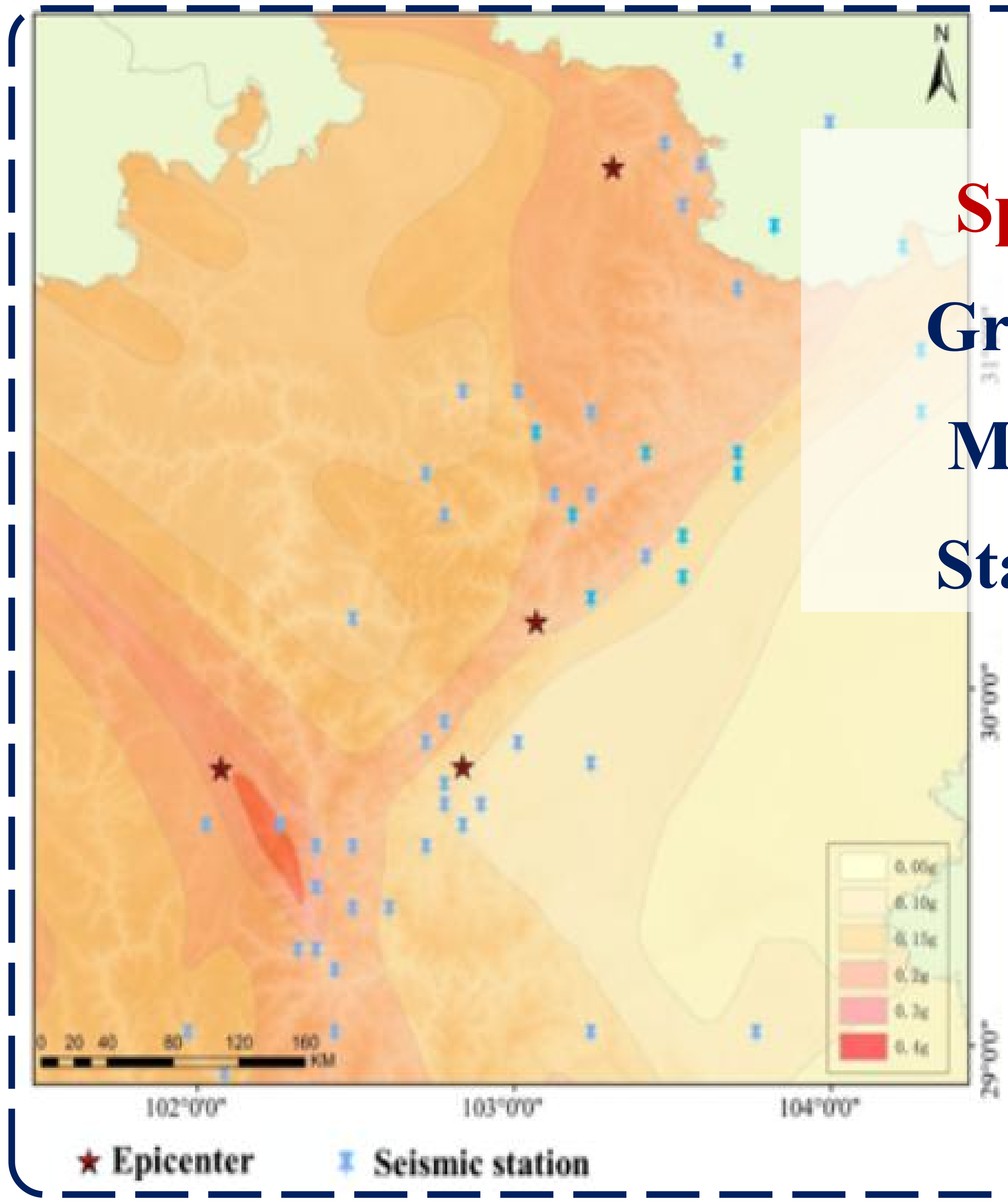

Sparse Ground-Motion Stations

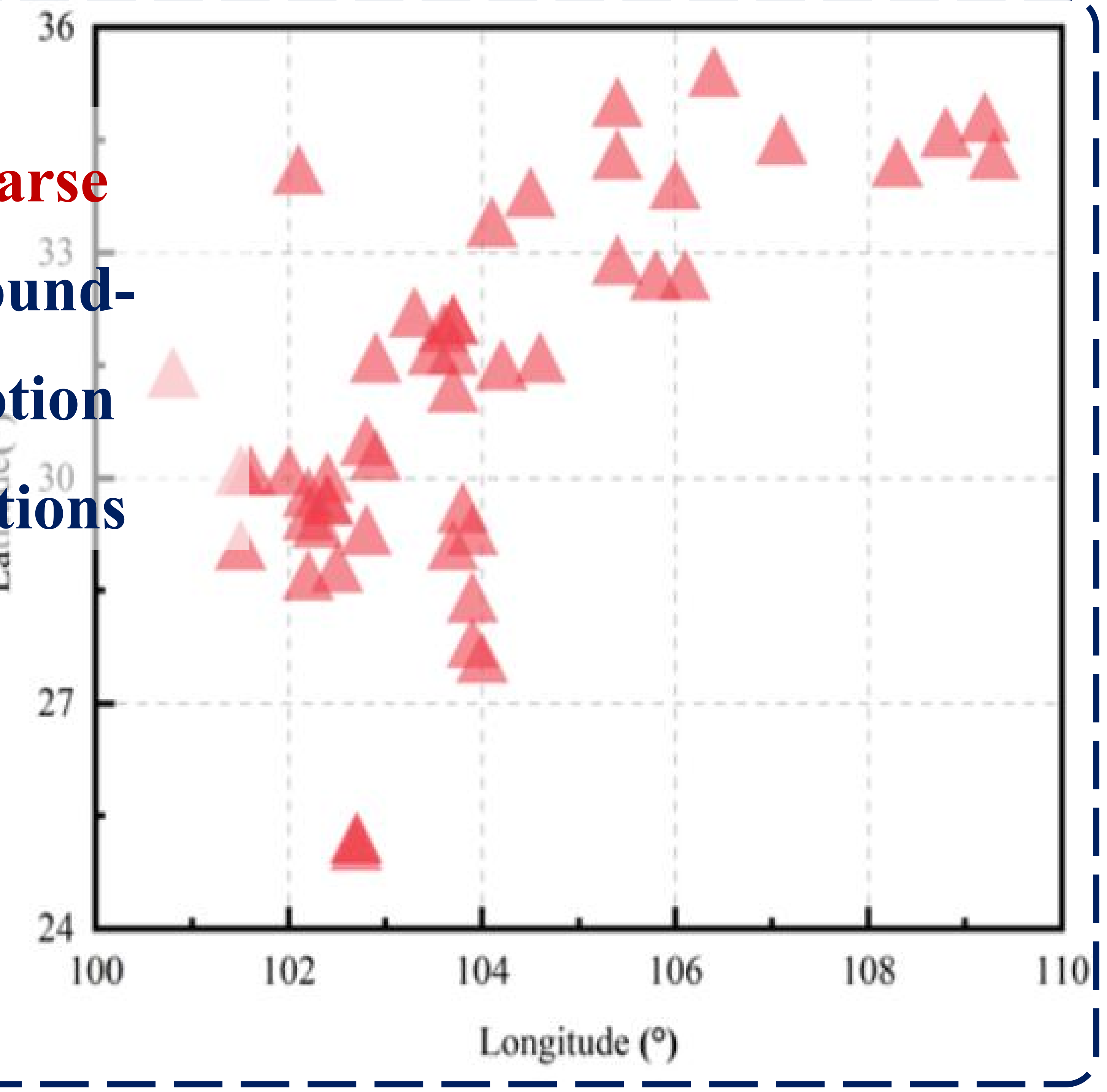

Domestic and International Research Progress

Natural Ground-Motion Sample Generation Methods

- **Physics-Based** Ground-Motion Simulation
- **Statistical** Ground-Motion Models
- **NN-Based (Neural Network-Based)** Ground-Motion Generation

System-Level Seismic Damage Assessment Methods

System Degradation Seismic Damage → Seismic Fragility Analysis Methods → NN-Based Rapid Prediction

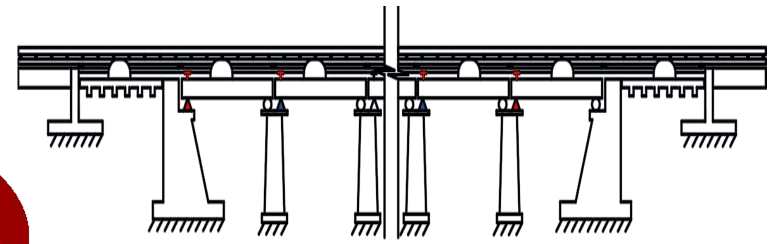

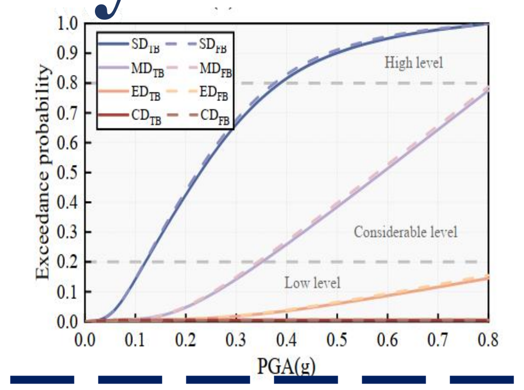

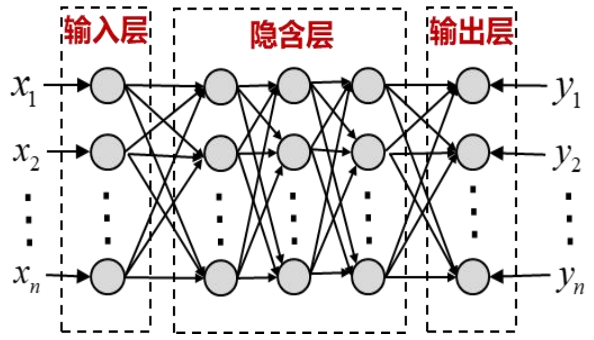

System-Level Post-Earthquake Train Operation Performance Assessment Methods

Seismic Structural Damage
↓
Operability Loss

NN-Based Rapid Prediction

NN Surrogate Model Performance

NN Performance	**Prediction Reliability**
many	**less**

Limitations of Existing Research

(1) Existing studies on natural ground-motion samples often overlook scenario-dependent time costs and lack validation of generated samples in terms of ground-motion characteristics and network performance.

(2) Existing assessments mainly rely on fragility analysis, limiting the applicability, efficiency, and accuracy of post-earthquake performance evaluation for high-speed railway simply supported girder bridge systems.

(3) The credibility of neural network surrogate-based assessment remains insufficiently studied in complex post-earthquake scenarios involving multi-source stochastic variables and high efficiency requirements.

(4) Existing regional studies mainly focus on uncertainties in ground-motion and structural parameters, while overlooking the effects of regional topography and prior parameter distributions.

Methodological Framework

Foundation

System

Region

Input

Natural Ground-Motion Records

System (Single Bridge) Seismic Reliability

Rapid System-Level Seismic Reliability Assessment Based on Uncertainty Quantification

System Seismic Reliability Assessment across Different Regions

Presentation Outline

Background and State of the Art

Data-Driven Seismic Damage Prediction Method for High-Speed Railway Simply Supported Girder Bridge Systems

Seismic Response Prediction and Uncertainty Quantification for High-Speed Railway Simply Supported Girder Bridge System

Seismic Reliability Assessment Method for High-Speed Railway Simply Supported Girder Bridge Systems

Regional Seismic Reliability Assessment of High-Speed Railway Simply Supported Girder Bridge Systems

CRTS II Slab Ballastless Track Simply-supported Girder Bridge System

浙江水利水電學院
Zhejiang University of Water Resources and Electric Power

- The high-speed railway CRTS II slab ballastless track–simply supported girder bridge system consists of three subsystems: the simply supported girder bridge, CRTS II slab ballastless track, and subgrade section subsystems

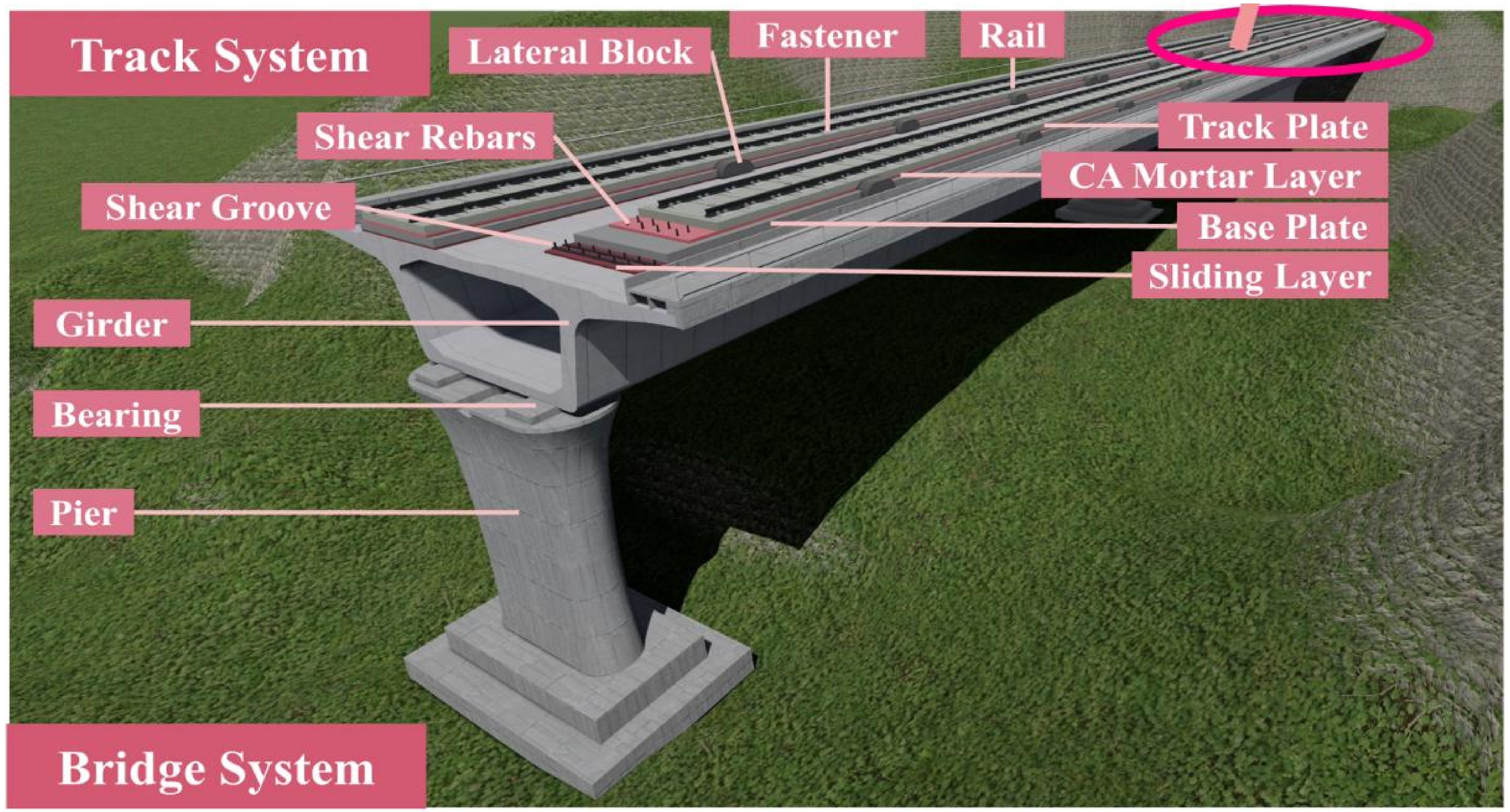

High-Speed Railway Simply Supported Girder Bridge System and Subsystems

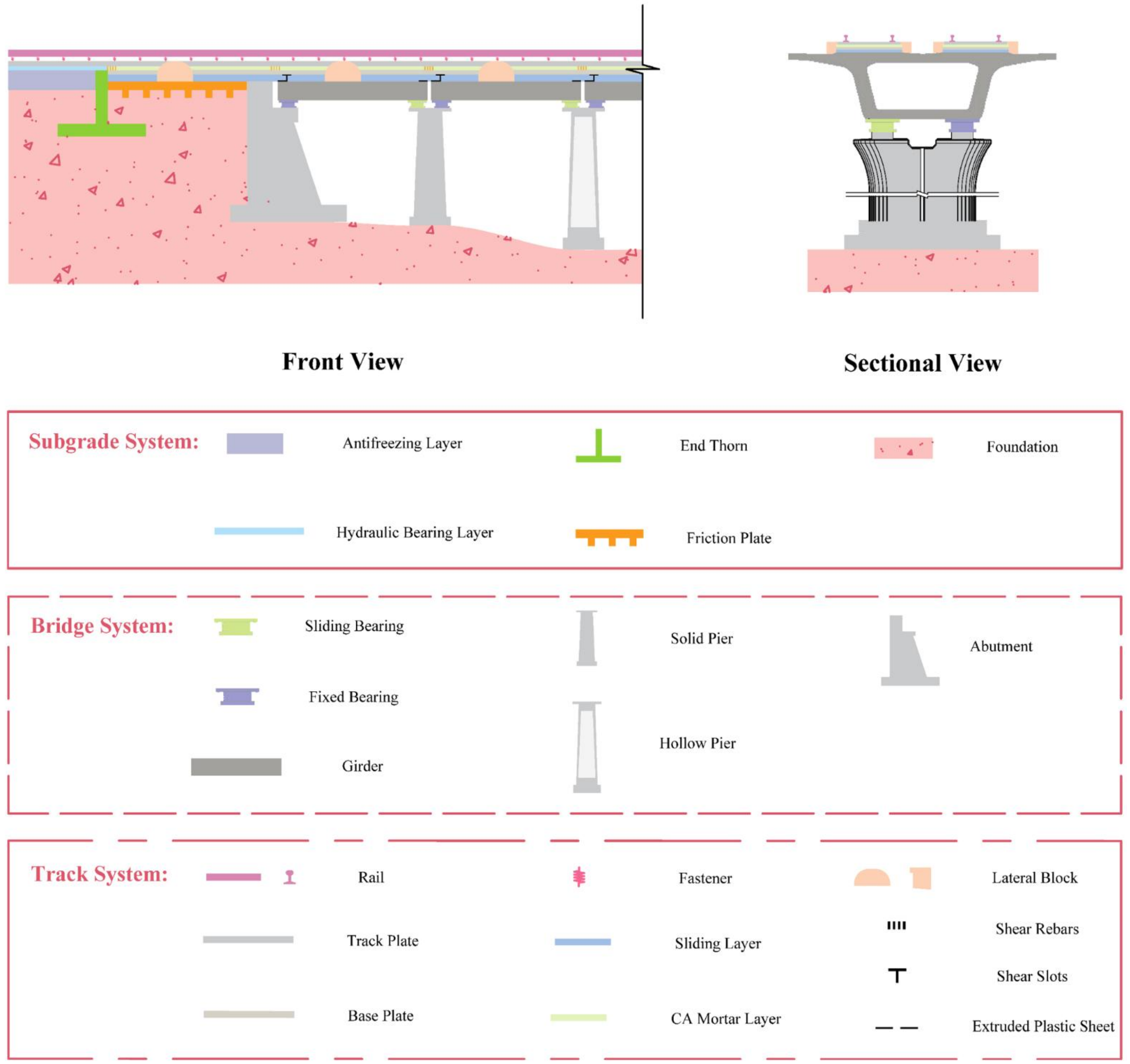

Simulation Model of the High-Speed Railway Simply Supported Girder Bridge

✓ Simulation Model Development for the High-Speed Railway Simply Supported Girder Bridge System

Model Validation

- Real earthquake-induced damage data for high-speed railway systems are difficult to investigate and collect, leaving limited valid samples, while neural network surrogate models require large datasets. A finite element model was therefore developed for dynamic seismic damage simulation and validated through scaled model tests.

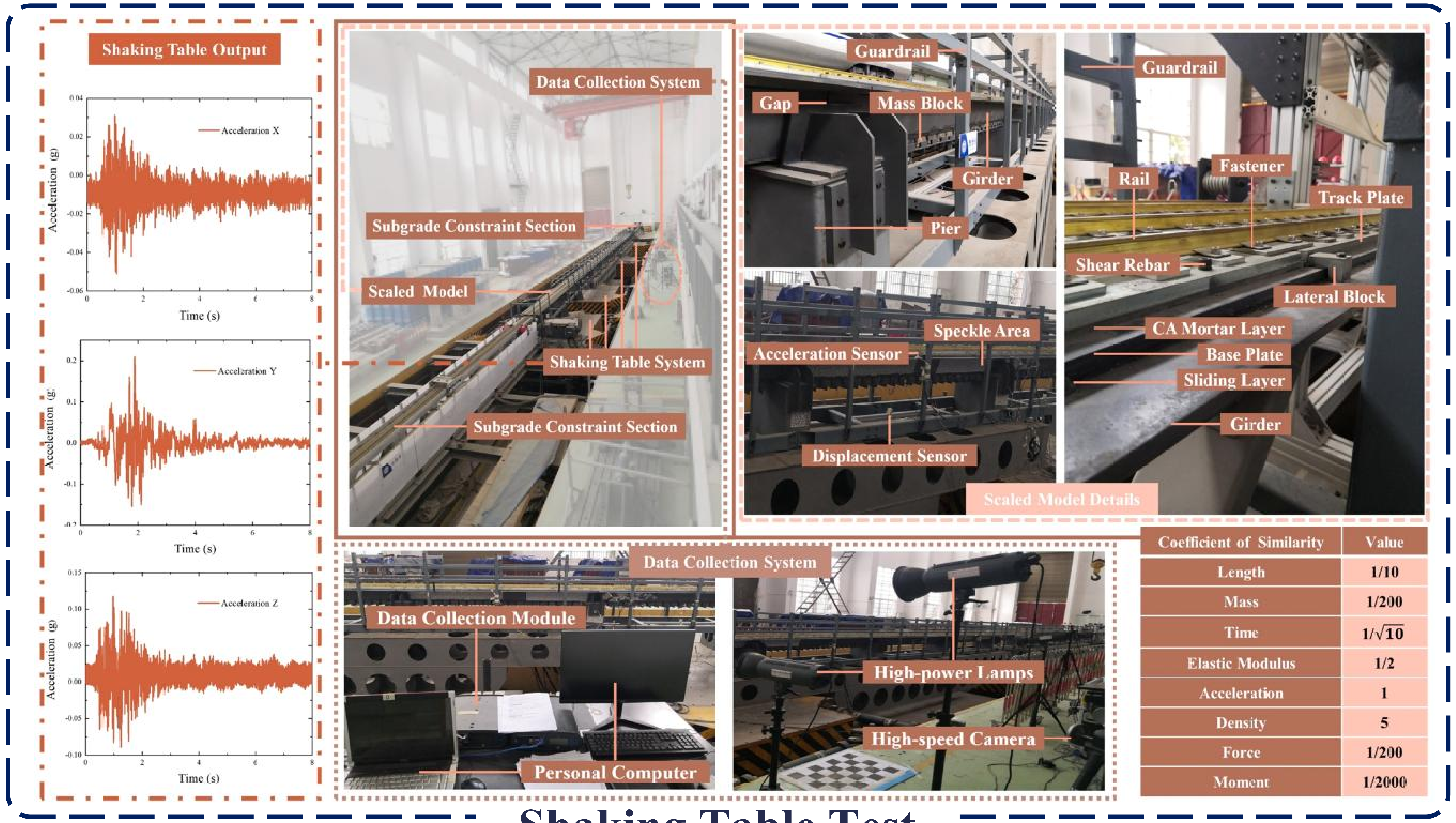

Coefficient of Similarity	Value
Length	1/10
Mass	1/200
Time	$1/\sqrt{10}$
Elastic Modulus	1/2
Acceleration	1
Density	5
Force	1/200
Moment	1/2000

Shaking Table Test

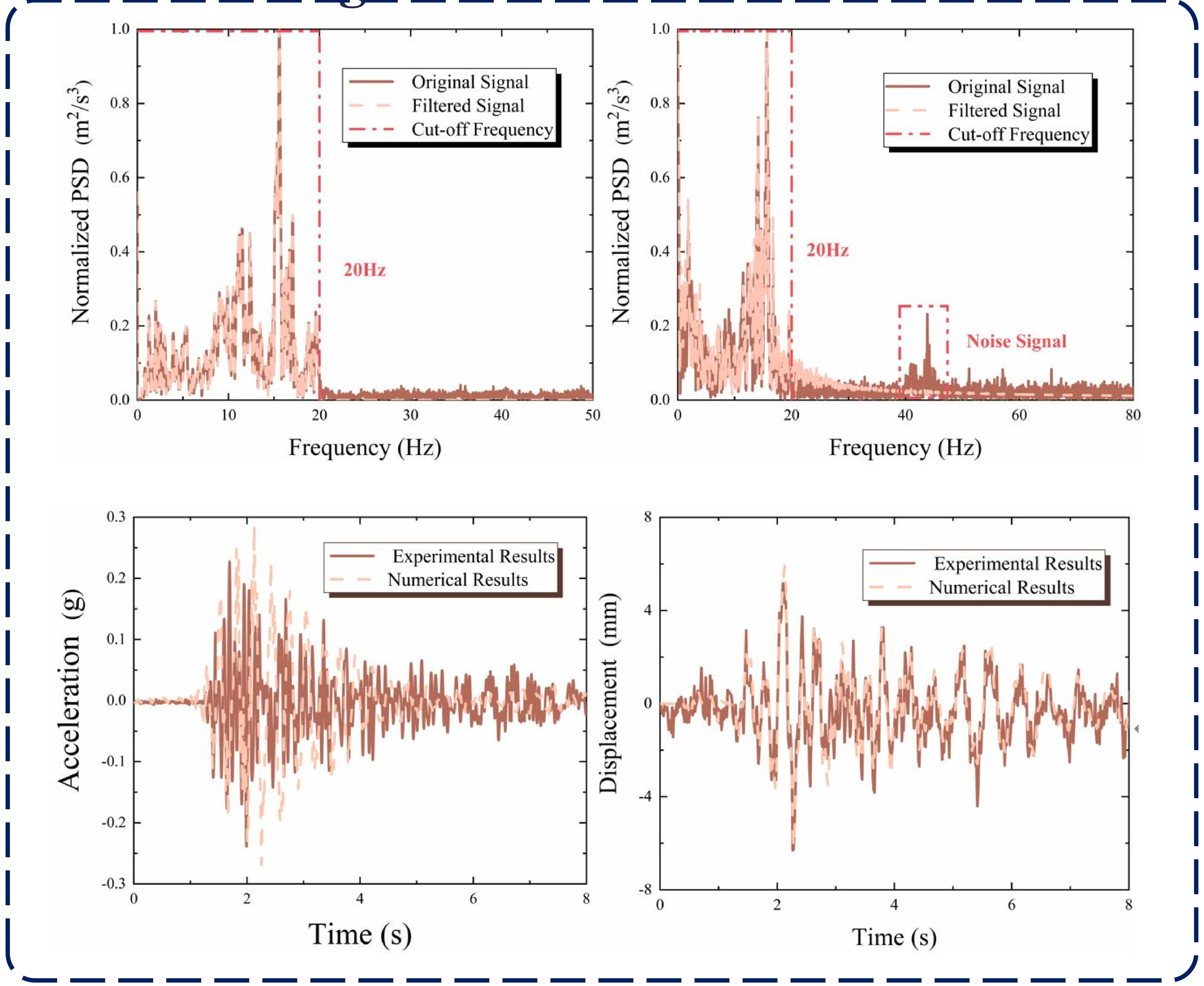

✓ Validated Model Providing Reliable and **Sufficient Samples** for NN surrogate-based rapid seismic damage prediction

Limited-Sample Seismic Damage Prediction for Track–Bridge Systems

- Existing natural ground-motion records are insufficient for seismic analysis, and this limitation is amplified in neural network surrogate-based seismic damage prediction of high-speed railway simply supported girder bridge systems. A deep convolutional generative adversarial network (DCGAN)-based ground-motion generation method was therefore proposed.

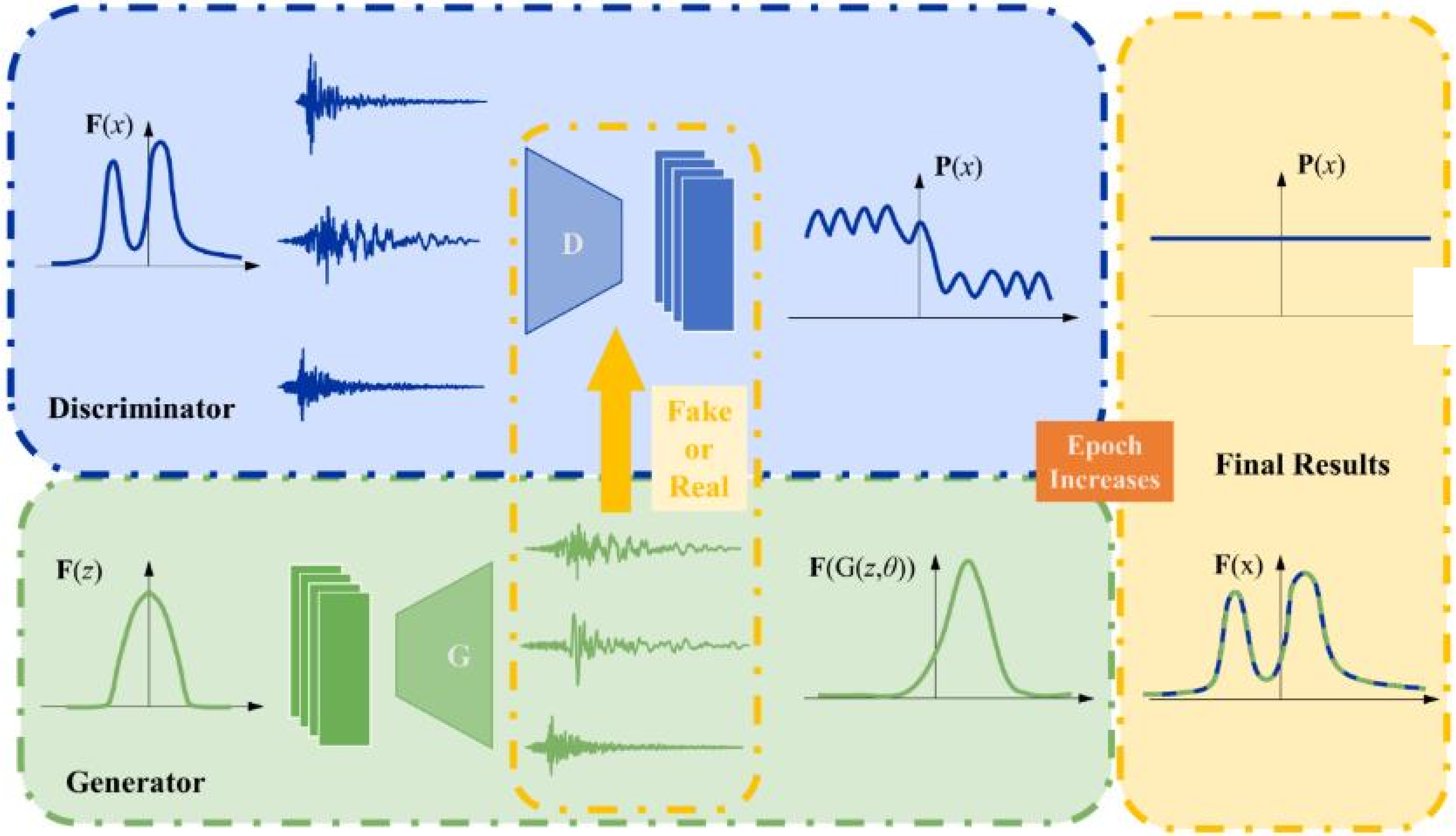

Validation

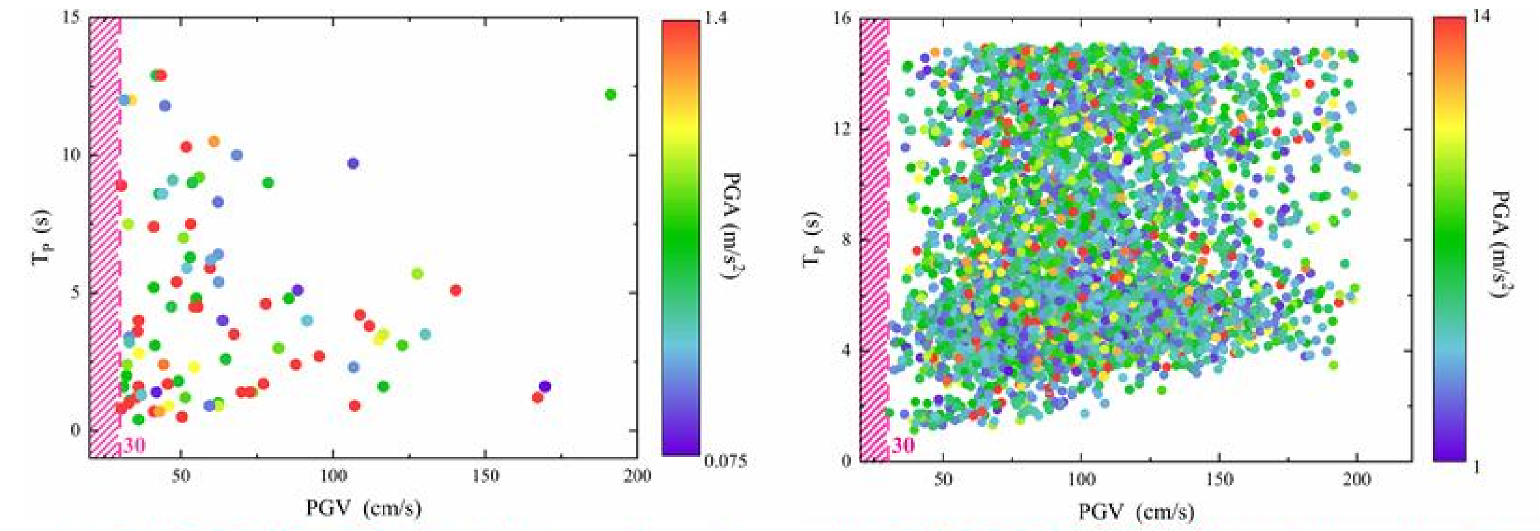

(a) The PGV-Tp-PGA distribution plot of seismic motions provided by references (Baker, 2007)

(b) The PGV-Tp-PGA distribution plot of seismic motions generated by the proposed method

$$PI = \frac{1}{1+e^{-23.3+14.6*PR+20.5*ER}}$$

$$t_{10\%\sum E_{pluse}} < t_{20\%\sum E_{total}}$$

$$PGV > 30cm/s$$

Pulse Characteristics

Neural Network Prediction Results

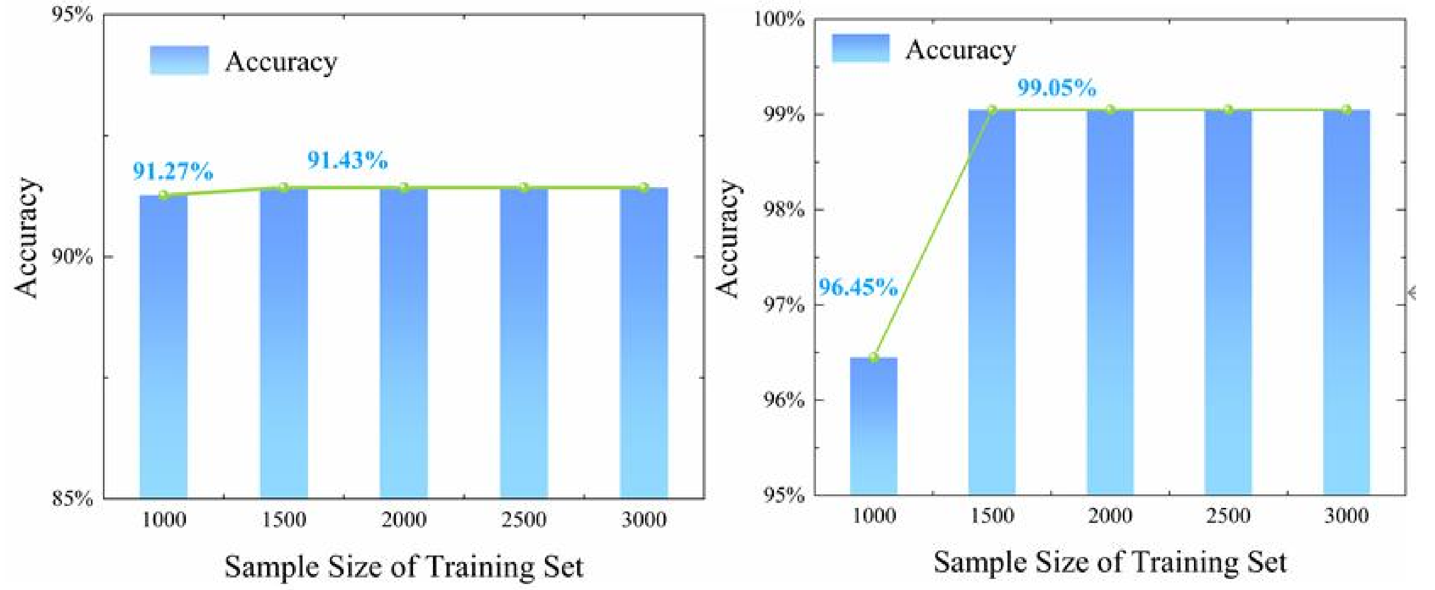

(a) Fixed Bearing #3

(b) Fixed Bearing #5

✓ Sufficient ground-motion samples were generated, and their physical plausibility was validated

Limited-Sample Seismic Damage Prediction for Track–Bridge Systems

浙江水利水電学院
Zhejiang University of Water Resources and Electric Power

- For different regions, the effects of training-set size and composition on prediction results were analyzed, and the predictive performance of neural network models with different architectures was compared across regions.

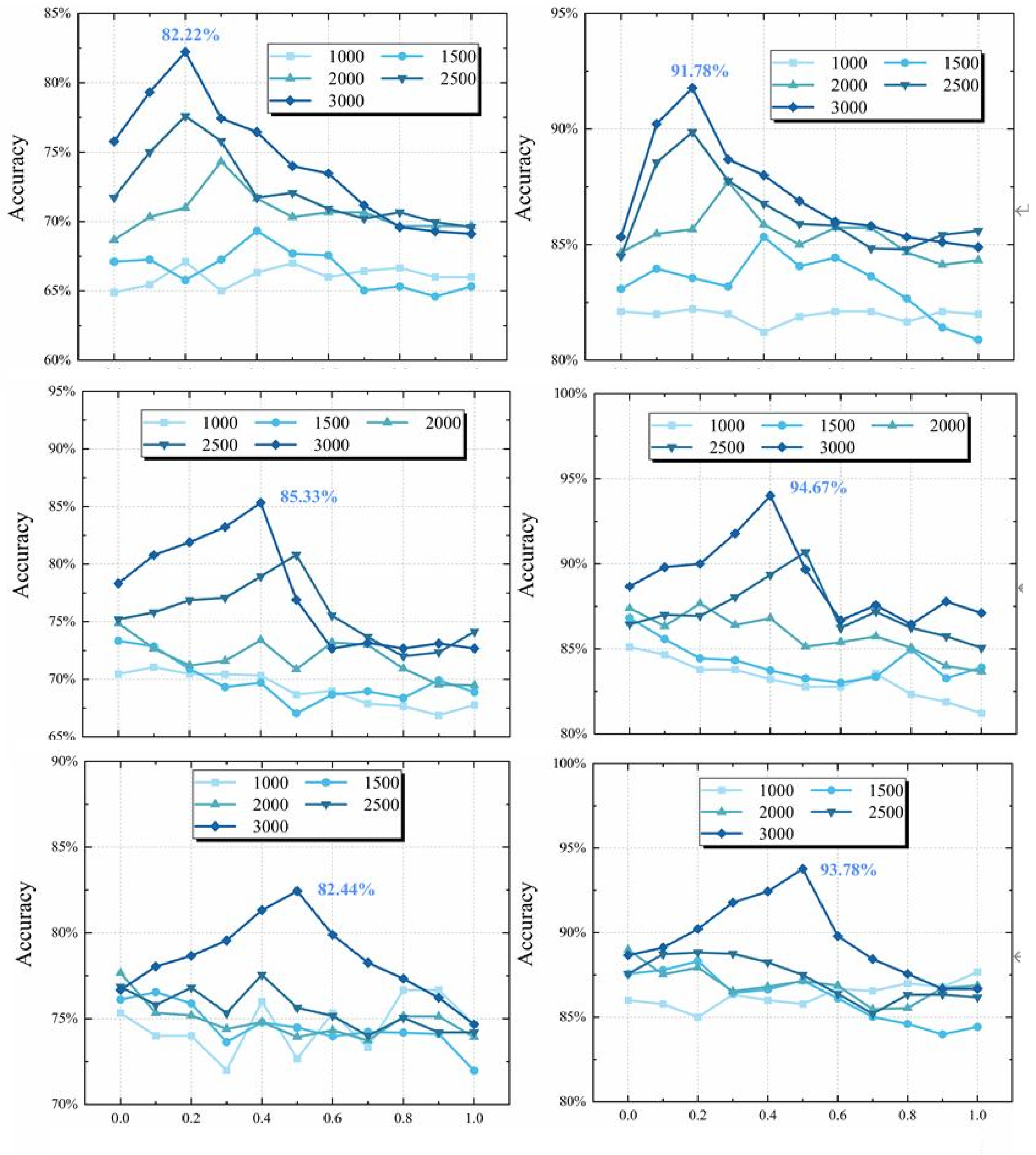

Influence of Training Samples on Seismic Damage Prediction

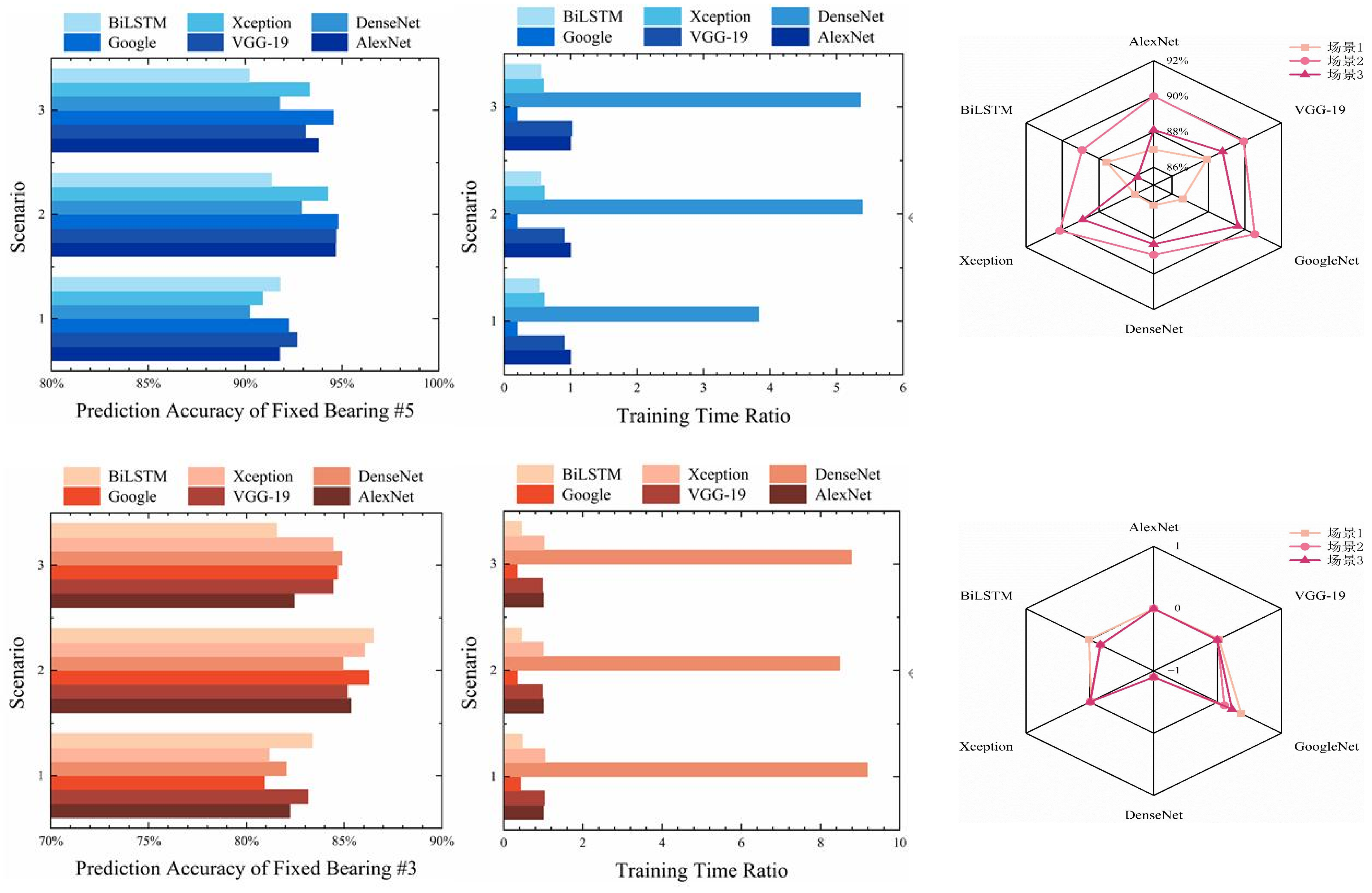

Network Architecture Effects on Seismic Damage Prediction

✓ Effects of training samples and network architecture on system-level seismic damage prediction across regions were analyzed

Presentation Outline

- Background and State of the Art
- Data-Driven Seismic Damage Prediction Method for High-Speed Railway Simply Supported Girder Bridge Systems
- Seismic Response Prediction and Uncertainty Quantification for High-Speed Railway Simply Supported Girder Bridge System
- Seismic Reliability Assessment Method for High-Speed Railway Simply Supported Girder Bridge Systems
- Regional Seismic Reliability Assessment of High-Speed Railway Simply Supported Girder Bridge Systems

Seismic Response Prediction for High-Speed Railway Simply Supported Girder Bridge Systems

浙江水利水電學院
Zhejiang University of Water Resources and Electric Power

☐ A NN Surrogate Model for Seismic Response Prediction of High-Speed Railway Simply Supported Girder Bridge Systems

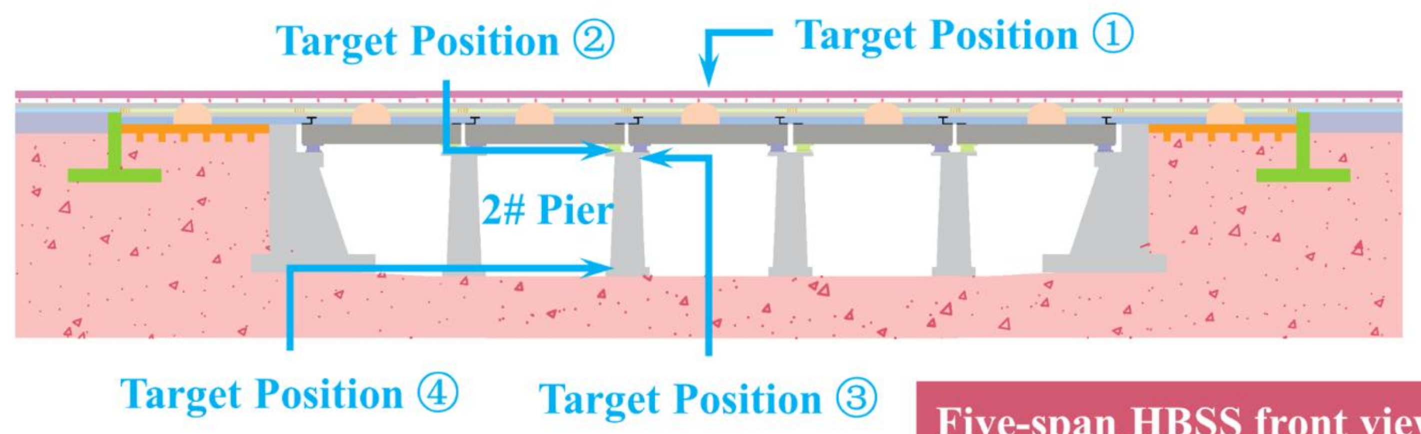

Five-span HBSS front view

Explanations

Predicted Target Position:

① Rail displacement at the mid-span

② Displacement of fixed bearing on top of pier 2 #

③ Displacement at pier top of pier 2 #

④ Shear force at the bottom of pier 2 #

Seismic Motions

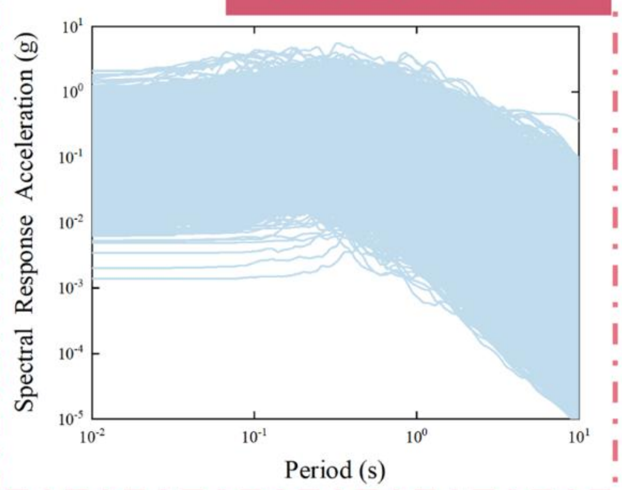

Surrogate Model

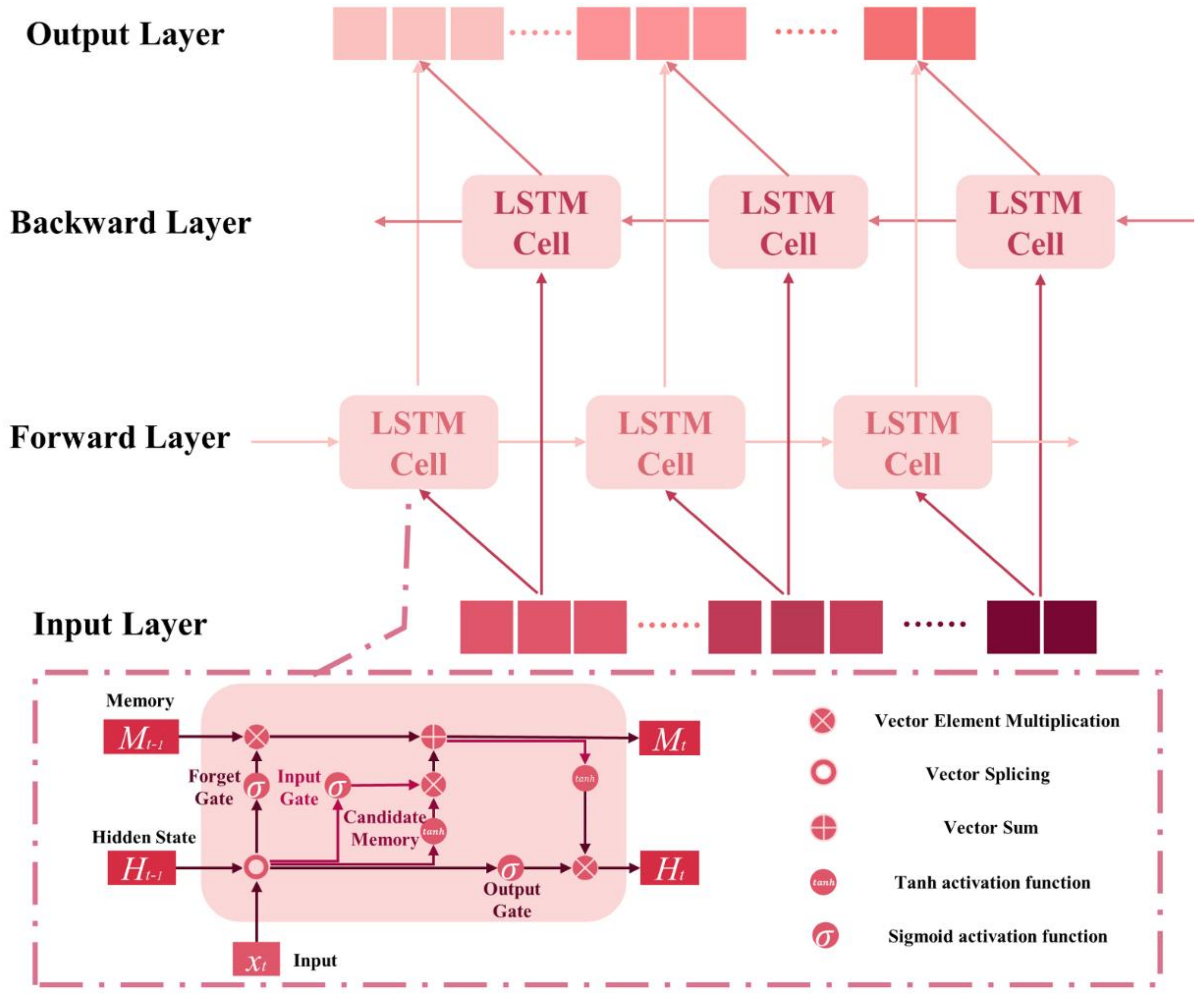

Prediction Results

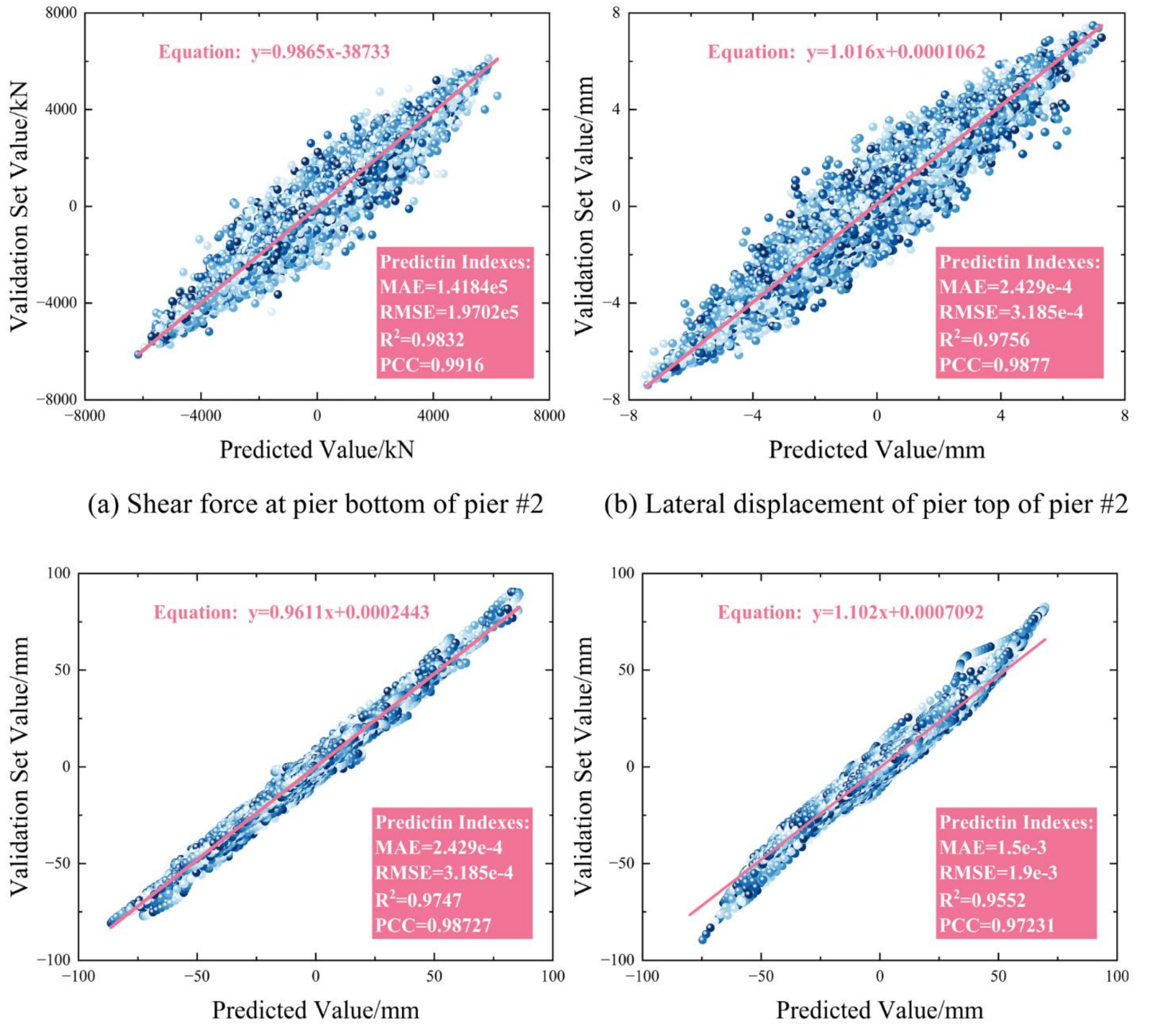

(a) Shear force at pier bottom of pier #2 (b) Lateral displacement of pier top of pier #2

(c) Lateral displacement of fixed bearing (d) Lateral displacement of rail

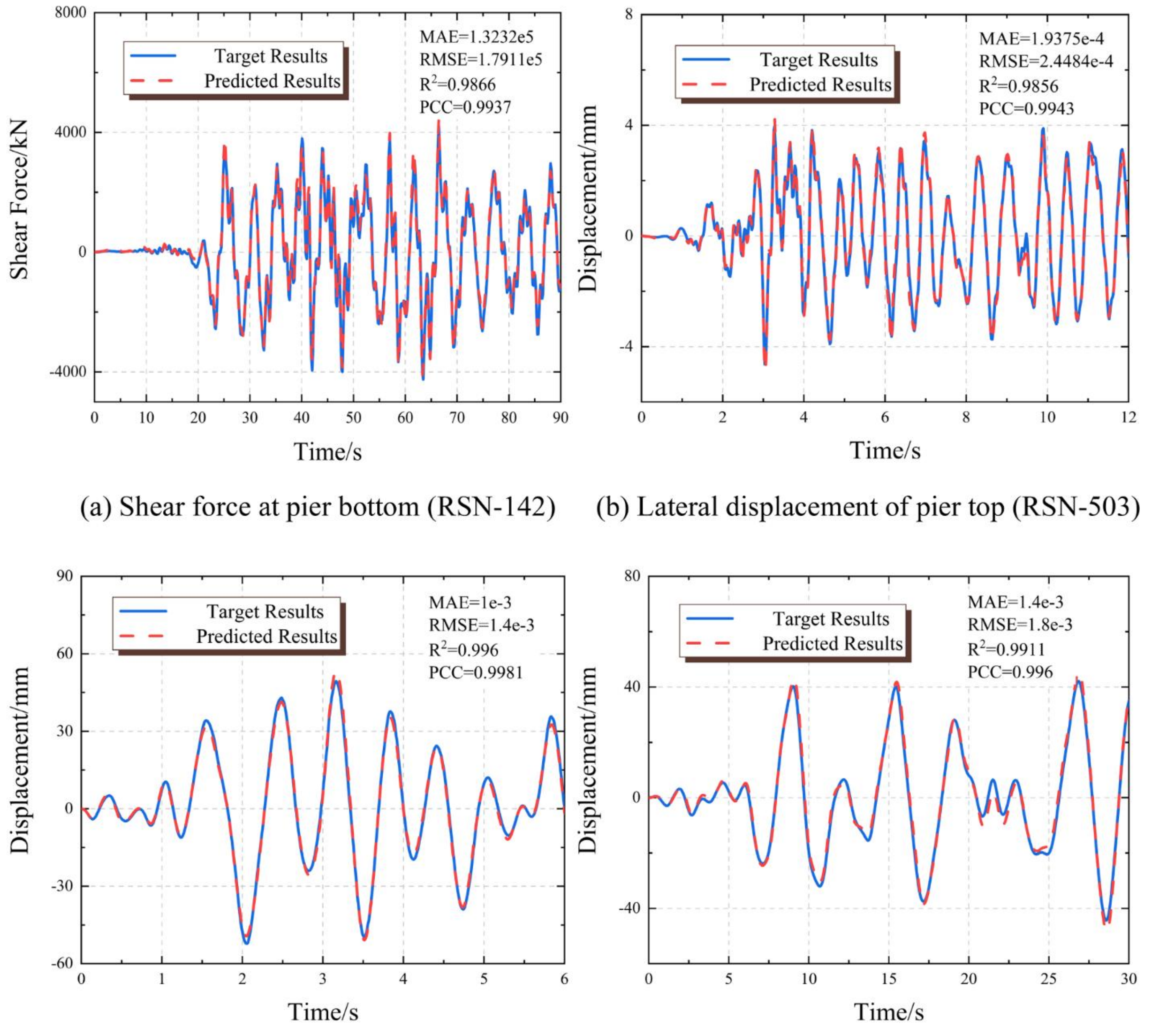

(a) Shear force at pier bottom (RSN-142) (b) Lateral displacement of pier top (RSN-503)

(c) Displacement of fixed bearing (RSN-219) (d) Displacement of rail (RSN-593)

For the validation set at the target location, both the coefficient of determination and the correlation coefficient exceed 0.95. The seismic responses predicted by Bi-LSTM agree well with the finite element results, demonstrating the rationality of NN surrogate model-based rapid seismic damage prediction for HRSBS.

✓ **An NN surrogate model was developed for seismic response prediction, supporting the uncertainty quantification framework**

Seismic Response Time-History Prediction and Uncertainty Quantification

☐ Uncertainty Quantification Framework for Neural Network-Based Seismic Response Prediction

Seismic Events	Index	Prediction	Prediction Interval 1	Prediction Interval 2	Prediction Interval 3
	I_b	0	12%	100%	100%
RSN-TEST1	M_b	/	0.0480	0.192	0.276
	C_b	/	1.46	0.192	0.276
	I_b	0	18.7%	100%	100%
RSN-TEST2	M_b	/	0.03	0.12	0.17
	C_b	/	0.74	0.12	0.17
	I_b	0	9.00%	100%	100%
RSN-TEST3	M_b	/	0.04	0.16	0.24
	C_b	/	1.26	0.16	0.24
	I_b	0	17.0%	100%	100%
RSN-TEST4	M_b	/	0.03	0.11	0.16
	C_b	/	0.74	0.11	0.16
	I_b	0	19.2%	100%	100%
RSN-TEST5	M_b	/	0.04	0.15	0.21
	C_b	/	0.89	0.15	0.21
	I_b	0	13.0%	100%	100%
RSN-TEST6	M_b	/	0.05	0.20	0.28
	C_b	/	1.45	0.20	0.28
	I_b	0	18.8%	100%	100%
RSN-TEST7	M_b	/	0.04	0.14	0.21
	C_b	/	0.88	0.14	0.21

Interval Prediction

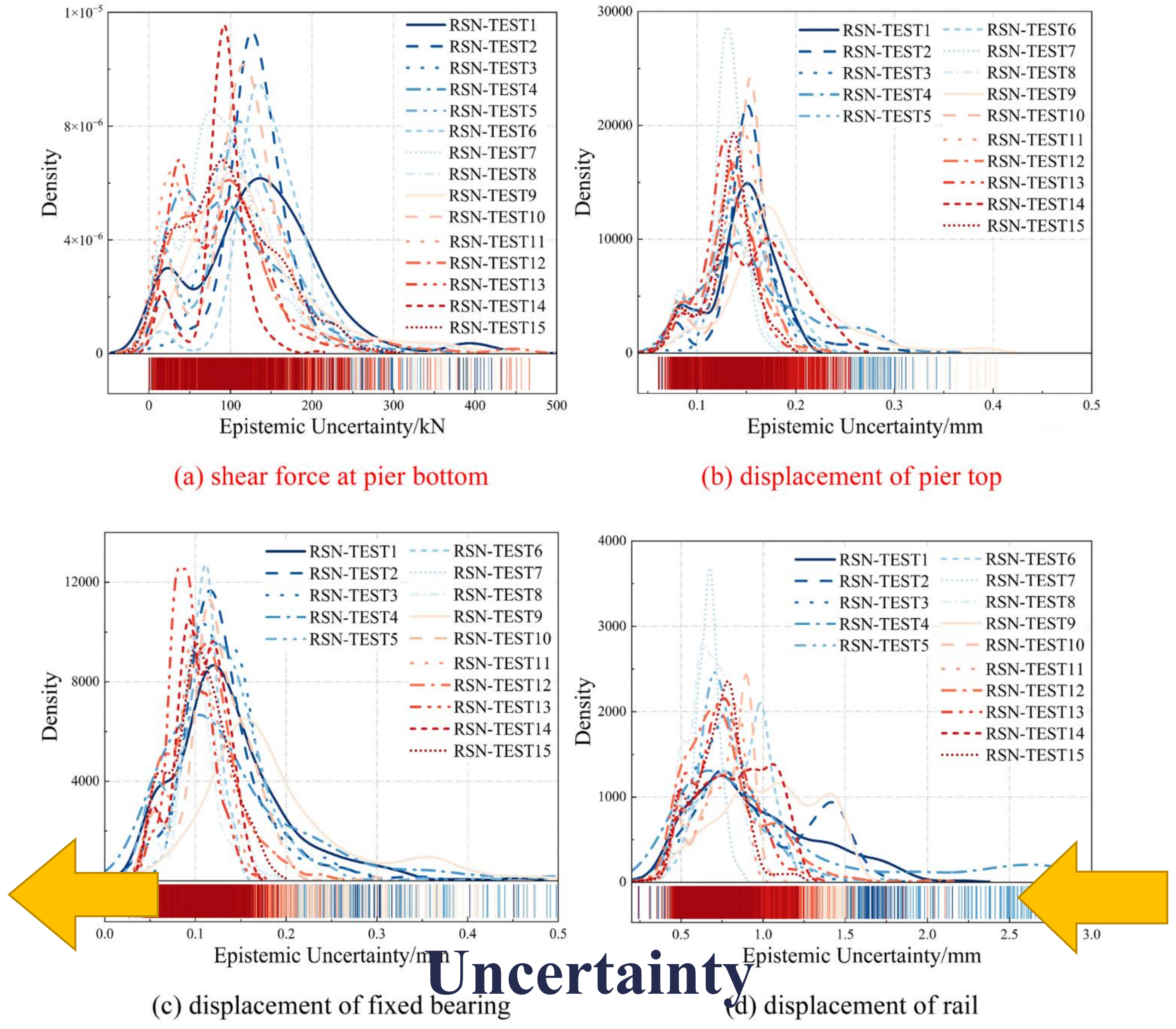

(a) shear force at pier bottom
(b) displacement of pier top
(c) displacement of fixed bearing
(d) displacement of rail

Uncertainty Quantification

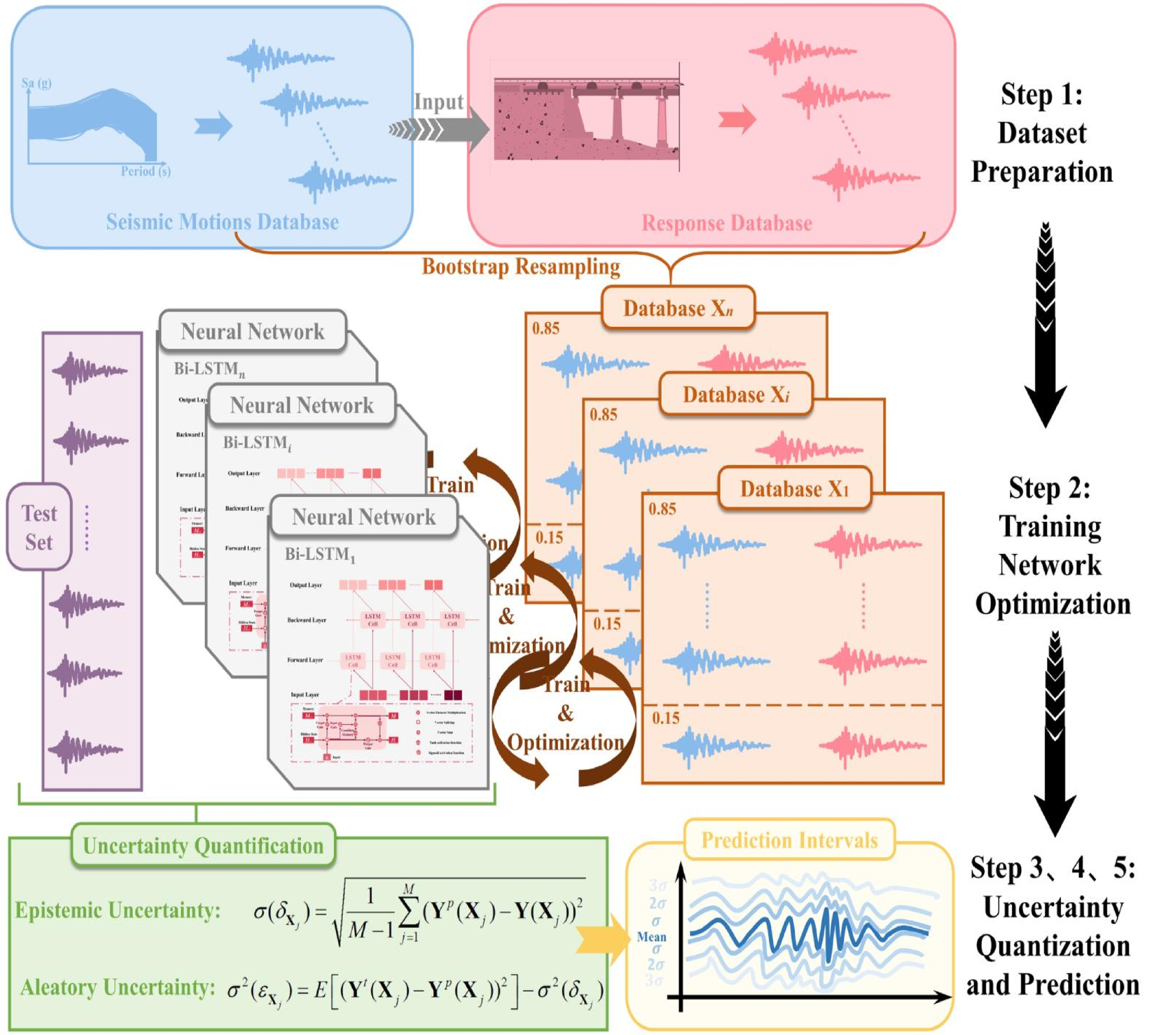

- Quantified aleatory uncertainty in rapid seismic response prediction.
- Identified component location as a source of aleatory uncertainty.
- Obtained prediction intervals at different confidence levels.

✓ Seismic response **prediction uncertainty** was quantified, **yielding prediction intervals** for HRSBS

Seismic Response Peak Prediction and Uncertainty Quantification

□ Uncertainty-Embedded Response Prediction for high-speed railway simply supported girder bridge systems.

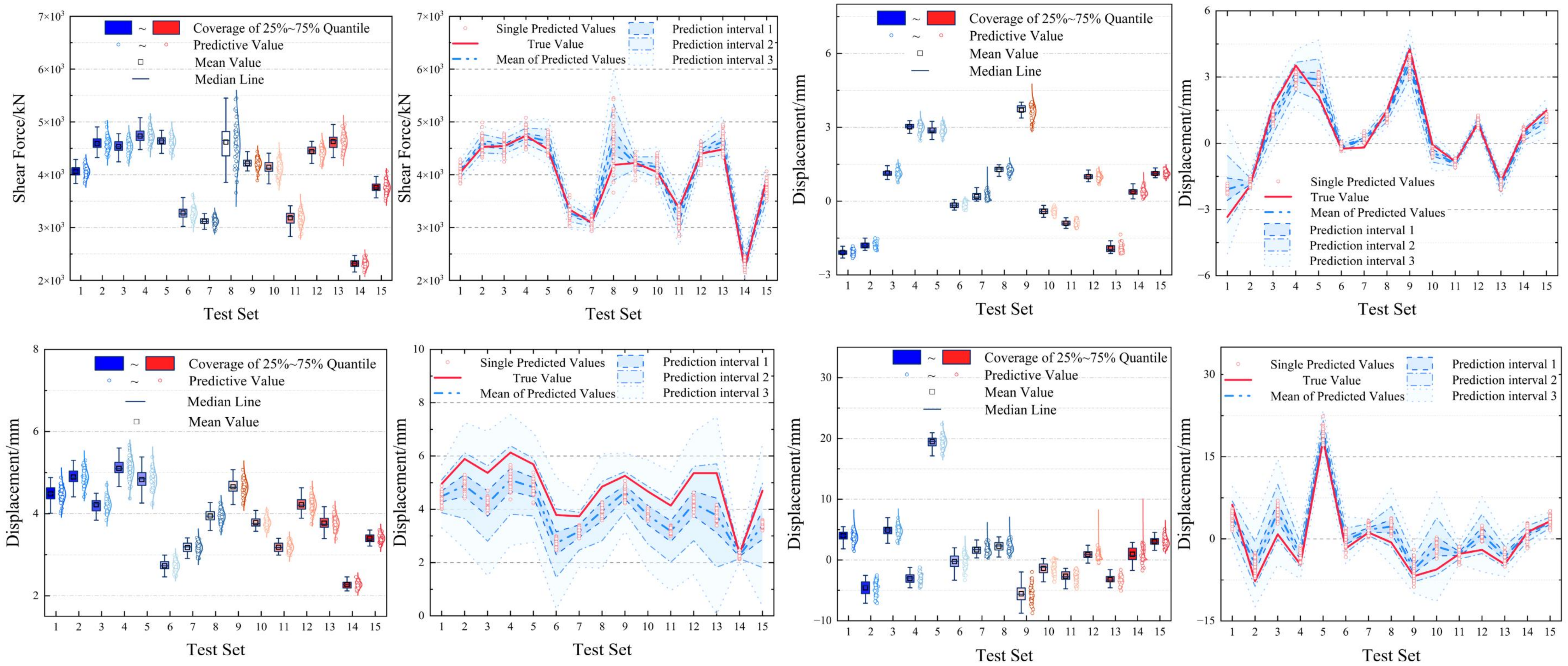

Surrogate Model

$$MR_p = \frac{N_i}{N_a} \quad (3\text{-}5)$$

$$MR_e = (1-c) * \int_v^{\infty} f(x)dx + c * \left(1 - \int_v^{\infty} f(x)dx\right) \quad (3\text{-}6)$$

$$MR_b = (1-c) * P(x < v_i) + c * (1 - P(x < v_i)) \quad (3\text{-}7)$$

$$P(x < v_i) = \Phi\left(\frac{N_a \ln(v_i) - \sum_{i=1}^{N_a} \ln(Y^p)}{N_a \sigma}\right) \quad (3\text{-}8)$$

Bearing Damage Identification

Misjudgment rate of fixed bearing damage state by different methods.

Condition	Actual Damage State	ESM	EP	ETBR	BBL
RSN-TEST1	Damage	14%	17.89%	24%	0.3%
RSN-TEST2	Safe	2%	2.22%	2%	0%
RSN-TEST13	Safe	32%	27.84%	42%	2.59%

- Prediction intervals with different coverage probabilities were obtained.
- The 95% prediction interval satisfies the prediction requirements for most scenarios.
- The accuracy of component critical-state identification was significantly improved.

✓ Confidence-dependent **prediction intervals** were constructed, improving component **damage-state identification accuracy**

Applicability Analysis

浙江水利水電學院
Zhejiang University of Water Resources and Electric Power

☐ Applicability of Bi-LSTM-Based Peak Response Prediction with a Single Ground-Motion Input

- **Proposed evaluation metrics for the applicability domain of NN surrogate models.**
- **Determined the applicability domain of Bi-LSTM peak prediction with a single acceleration time-history input;**

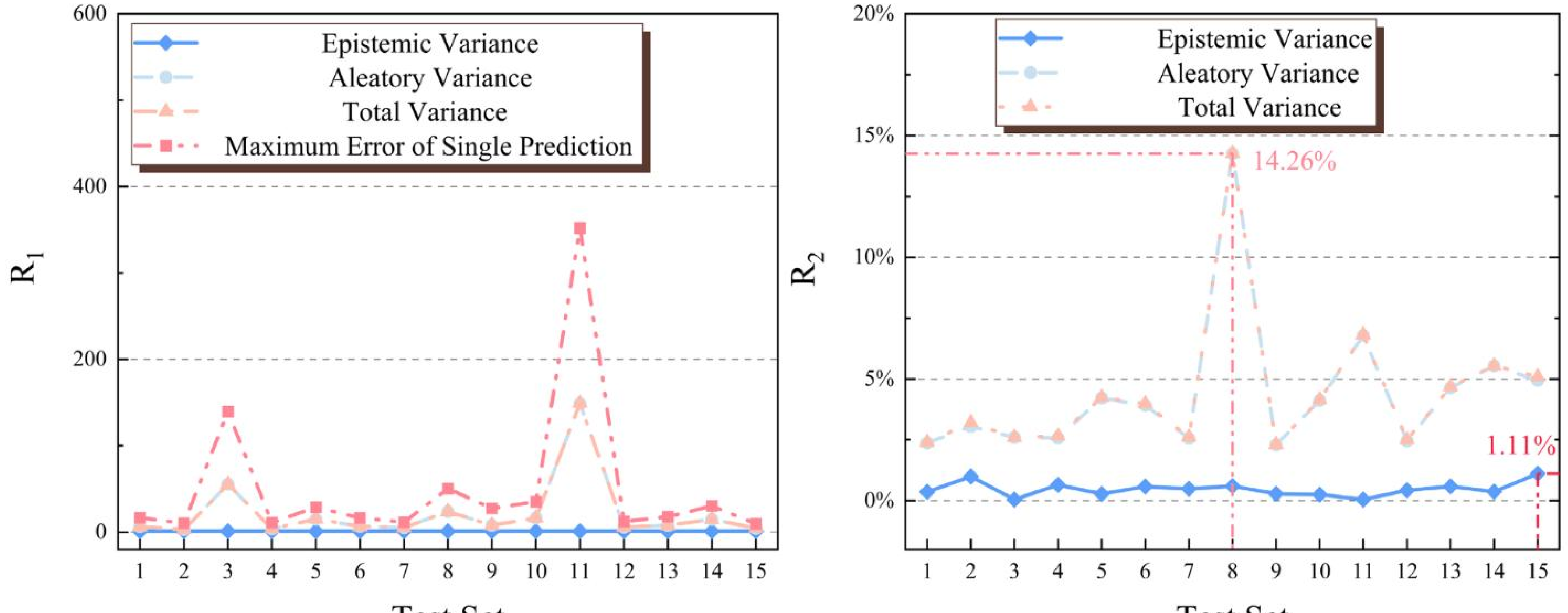

Pier Base Shear Force

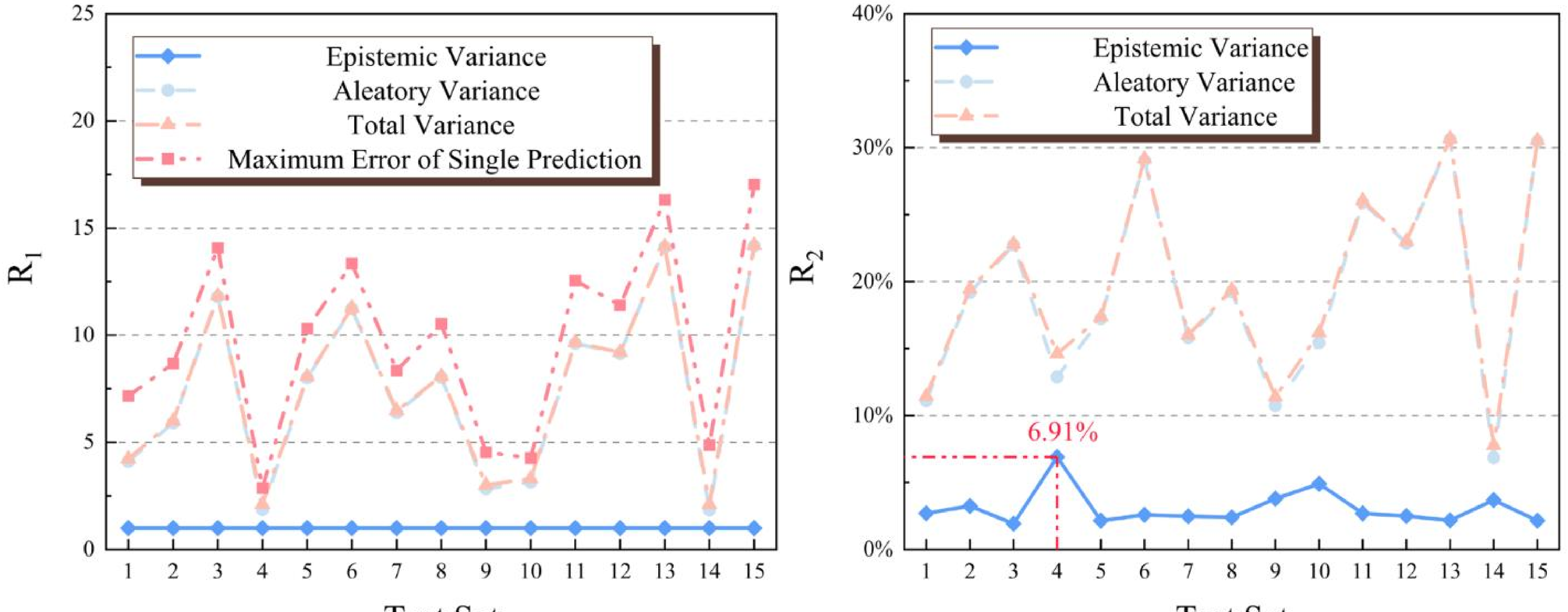

Bearing Displacement

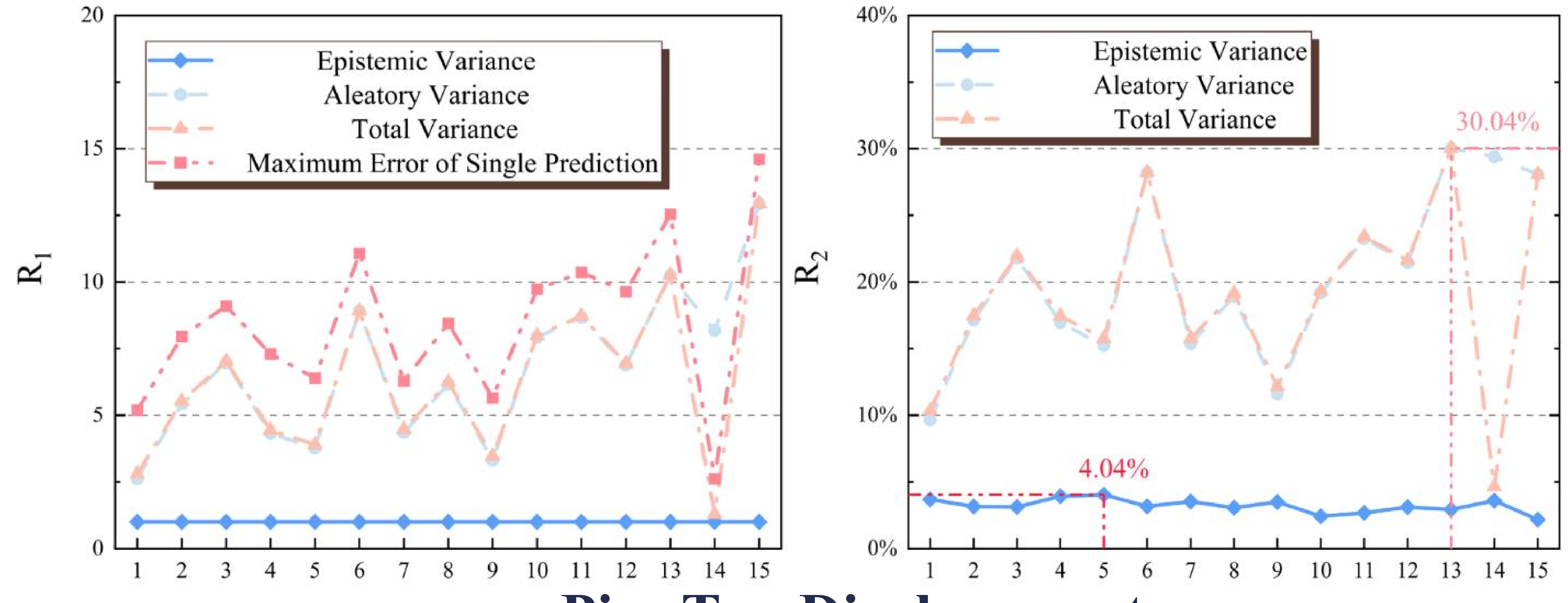

Pier Top Displacement

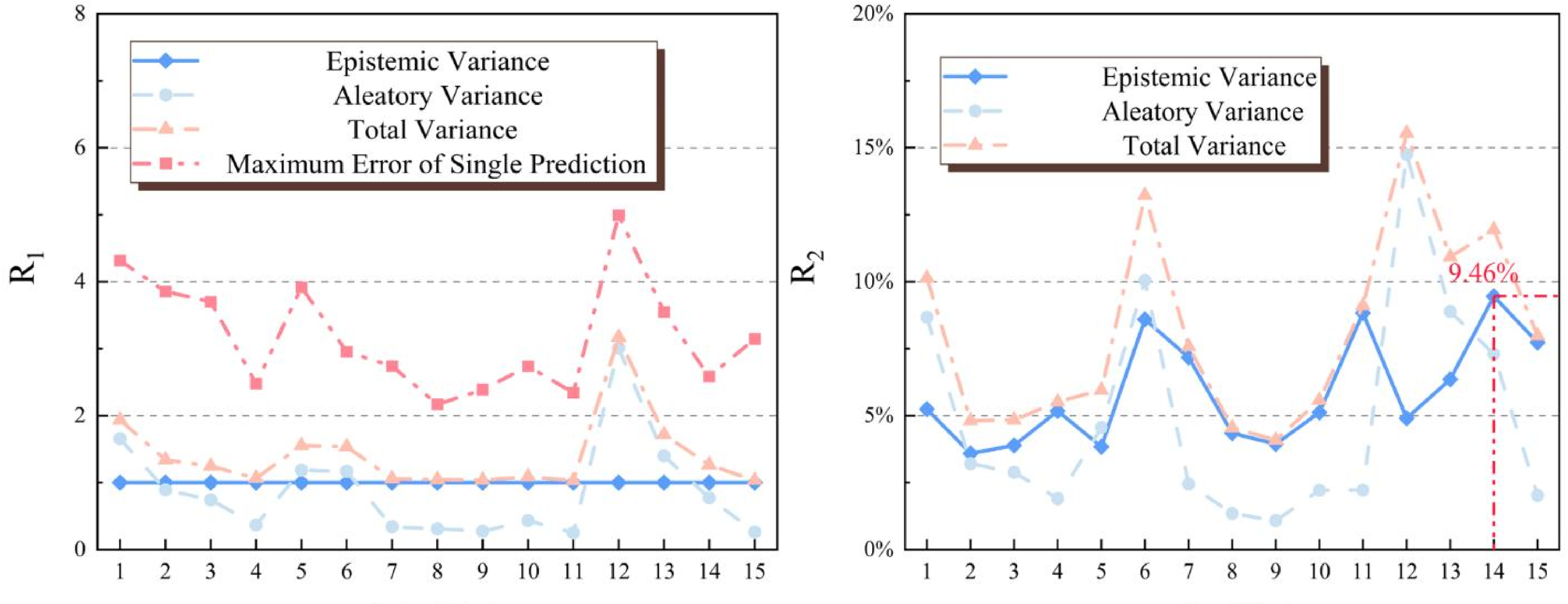

Rail Displacement

✓ Quantified **uncertainty** in seismic **peak response** prediction for HRSBS and clarified the NN **applicability domain**

Presentation Outline

Background and State of the Art

Data-Driven Seismic Damage Prediction Method for High-Speed Railway Simply Supported Girder Bridge Systems

Seismic Response Prediction and Uncertainty Quantification for High-Speed Railway Simply Supported Girder Bridge System

Seismic Reliability Assessment Method for High-Speed Railway Simply Supported Girder Bridge Systems

Regional Seismic Reliability Assessment of High-Speed Railway Simply Supported Girder Bridge Systems

Post-Earthquake Operability Prediction

A neural network surrogate model was developed to predict post-earthquake train operability on railway bridges

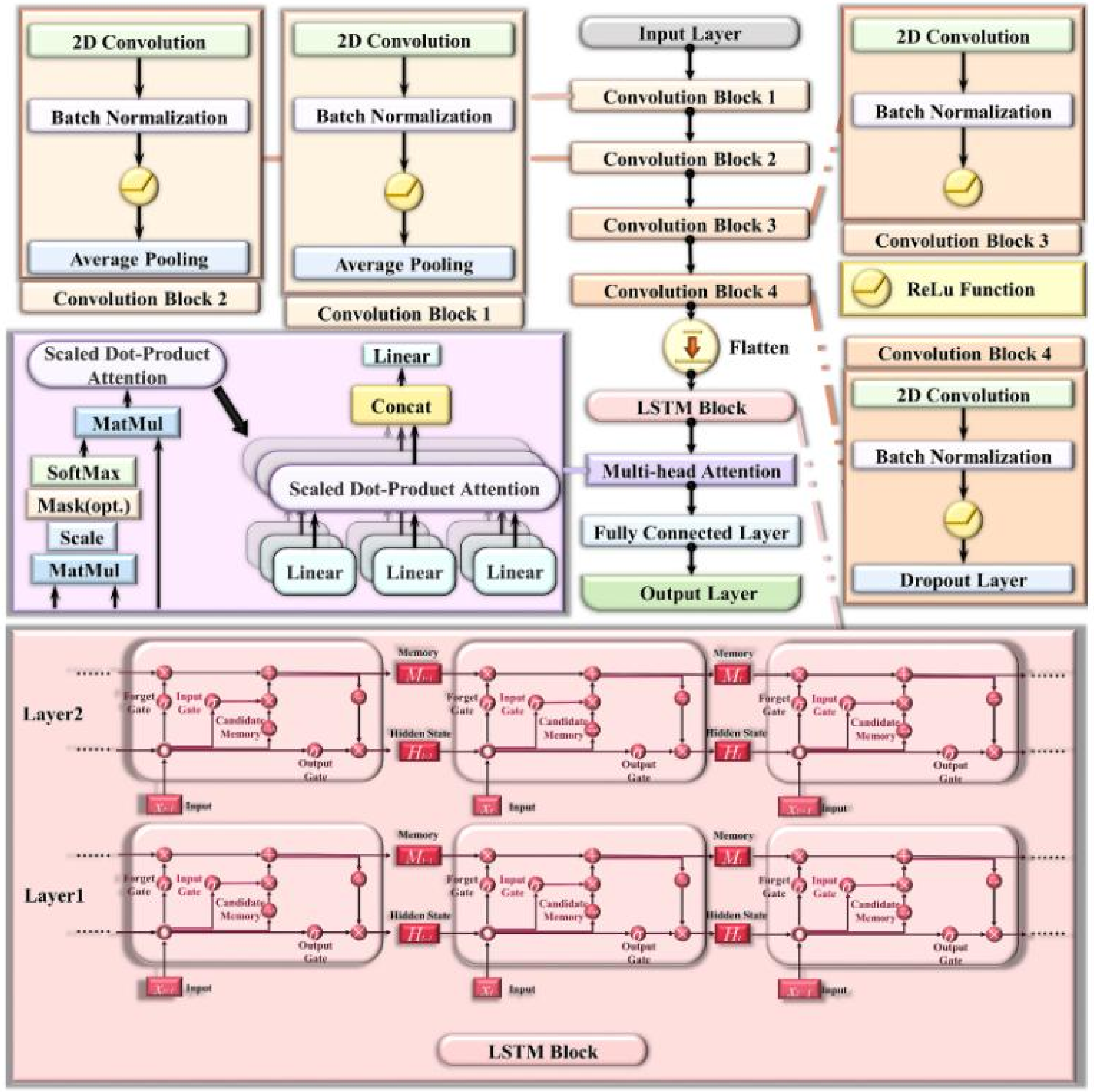

Prediction Accuracy

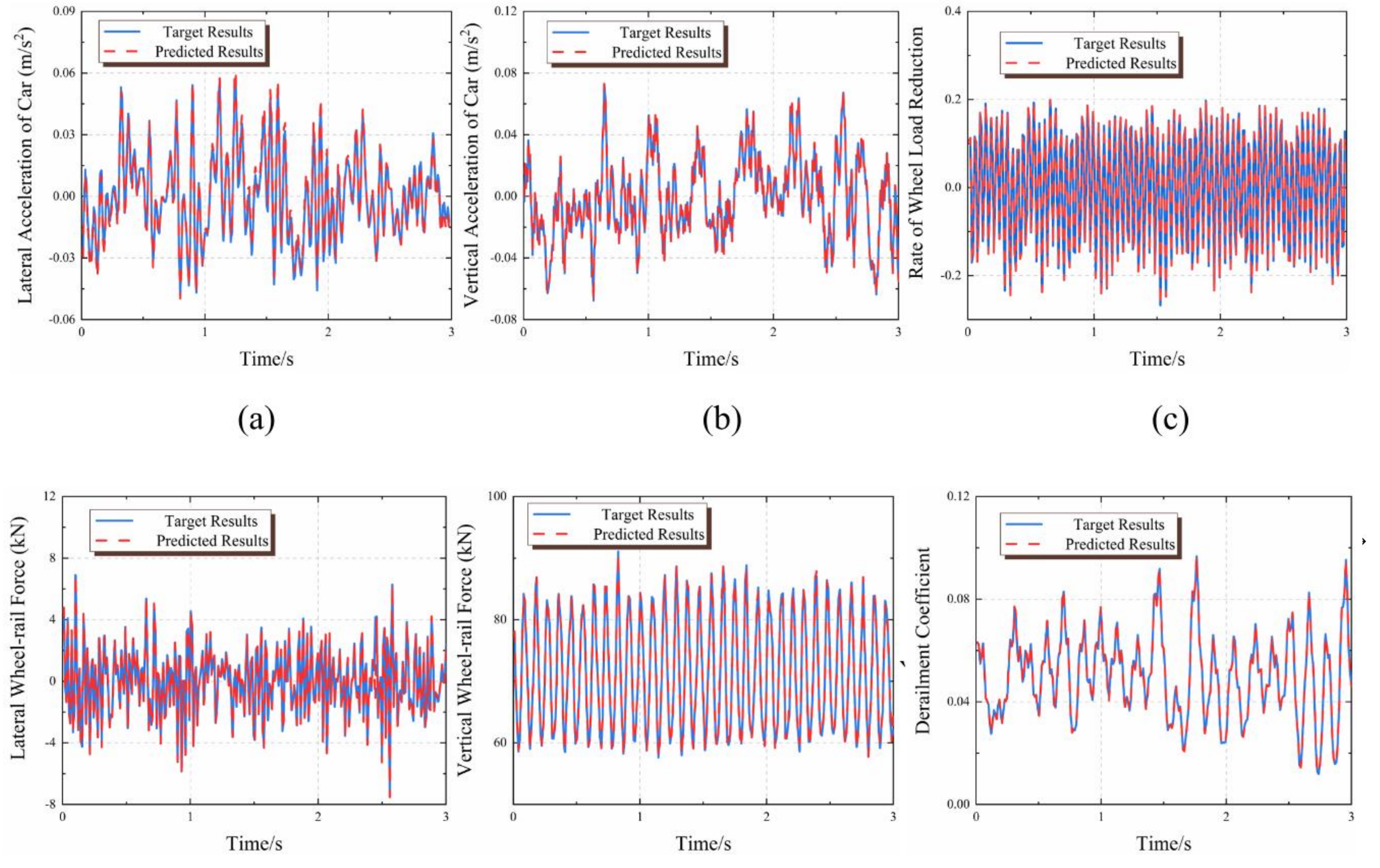

(a) (b) (c) (d) (e) (f)

$$R_{MAE}=\frac{\sum_{j=1}^{G^{Te}}\left|\mathbf{Y}^{p}(\mathbf{S}_j^{Te})-\mathbf{Y}^{t}(\mathbf{S}_j^{Te})\right|}{G^{Te}}$$

$$R_{RMSE}=\sqrt{\frac{\sum_{j=1}^{G^{Te}}(\mathbf{Y}^{p}(\mathbf{S}_j^{Te})-\mathbf{Y}^{t}(\mathbf{S}_j^{Te}))^2}{G^{Te}}}$$

$$\Re^2=1-\frac{\sum_{j=1}^{G^{Te}}(\mathbf{Y}^{t}(\mathbf{S}_j^{Te})-\mathbf{Y}^{p}(\mathbf{S}_j^{Te}))^2}{\sum_{j=1}^{G^{Te}}(\mathbf{Y}^{t}(\mathbf{S}_j^{Te})-\bar{\mathbf{Y}}^{t}(\mathbf{S}_j^{Te}))^2}$$

$$C=\frac{\sum_{j=1}^{G^{Te}}(\mathbf{Y}^{p}(\mathbf{S}_j^{Te})-\bar{\mathbf{Y}}^{p}(\mathbf{S}_j^{Te}))(\mathbf{Y}^{t}(\mathbf{S}_j^{Te})-\bar{\mathbf{Y}}^{t}(\mathbf{S}_j^{Te}))}{\sqrt{\sum_{j=1}^{G^{Te}}(\mathbf{Y}^{p}(\mathbf{S}_j^{Te})-\bar{\mathbf{Y}}^{p}(\mathbf{S}_j^{Te}))^2}\sqrt{\sum_{j=1}^{G^{Te}}(\mathbf{Y}^{t}(\mathbf{S}_j^{Te})-\bar{\mathbf{Y}}^{t}(\mathbf{S}_j^{Te}))^2}}$$

Validation

Robustness

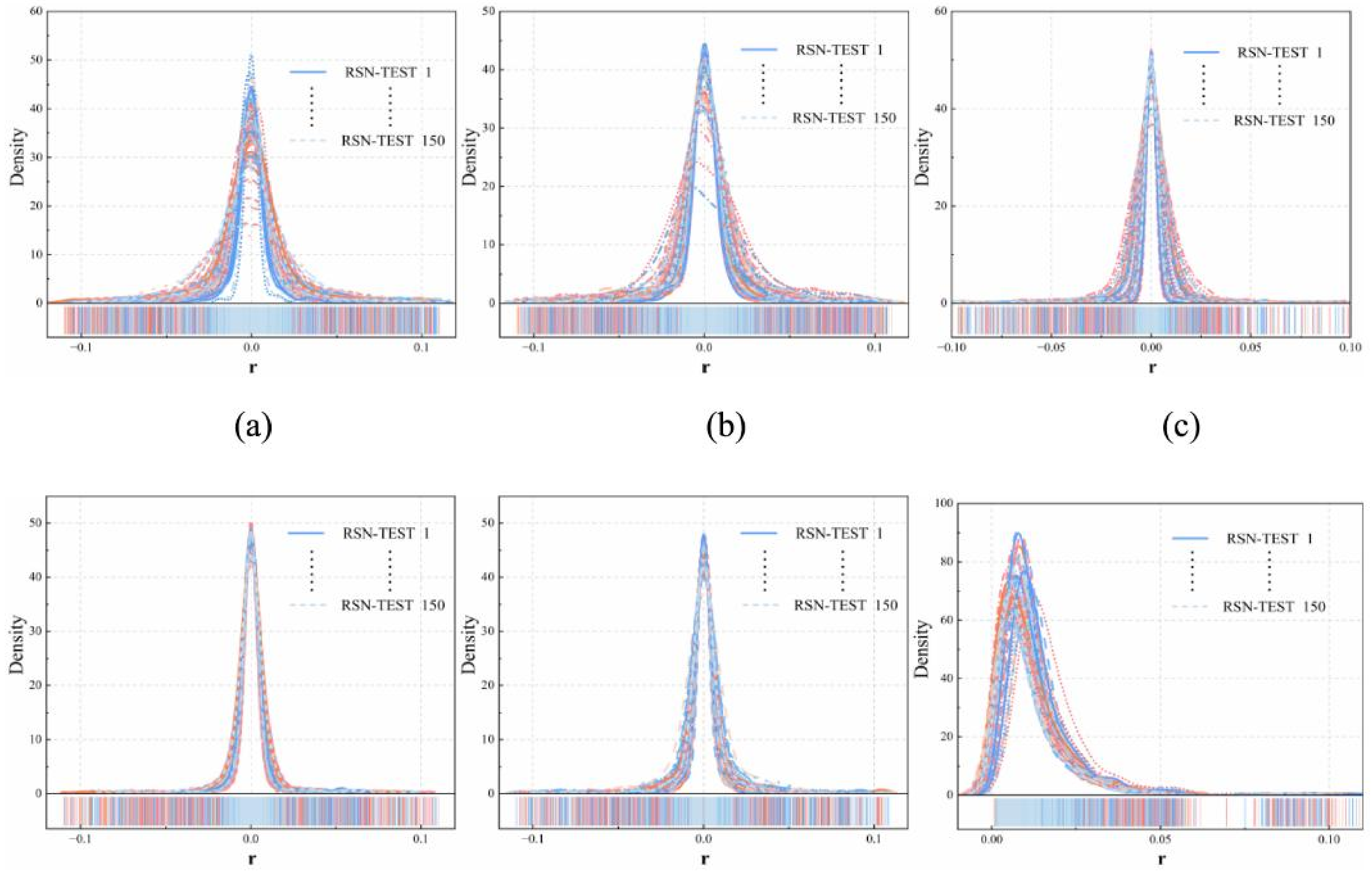

(a) (b) (c) (d) (e) (f)

$$\mathbf{r}(j)=\frac{\sigma(\delta_{\mathbf{S}_j^{Te}})}{\mathbf{Y}^{t}(\mathbf{S}_j^{Te})}$$

✓ The proposed NN surrogate model provides **accurate and robust** predictions of post-earthquake train operability time histories

Sensitivity Analysis of Peak Response Prediction

☐ Quantified uncertainty in peak response prediction and analyzed factors affecting robustness.

Time-History Prediction Results

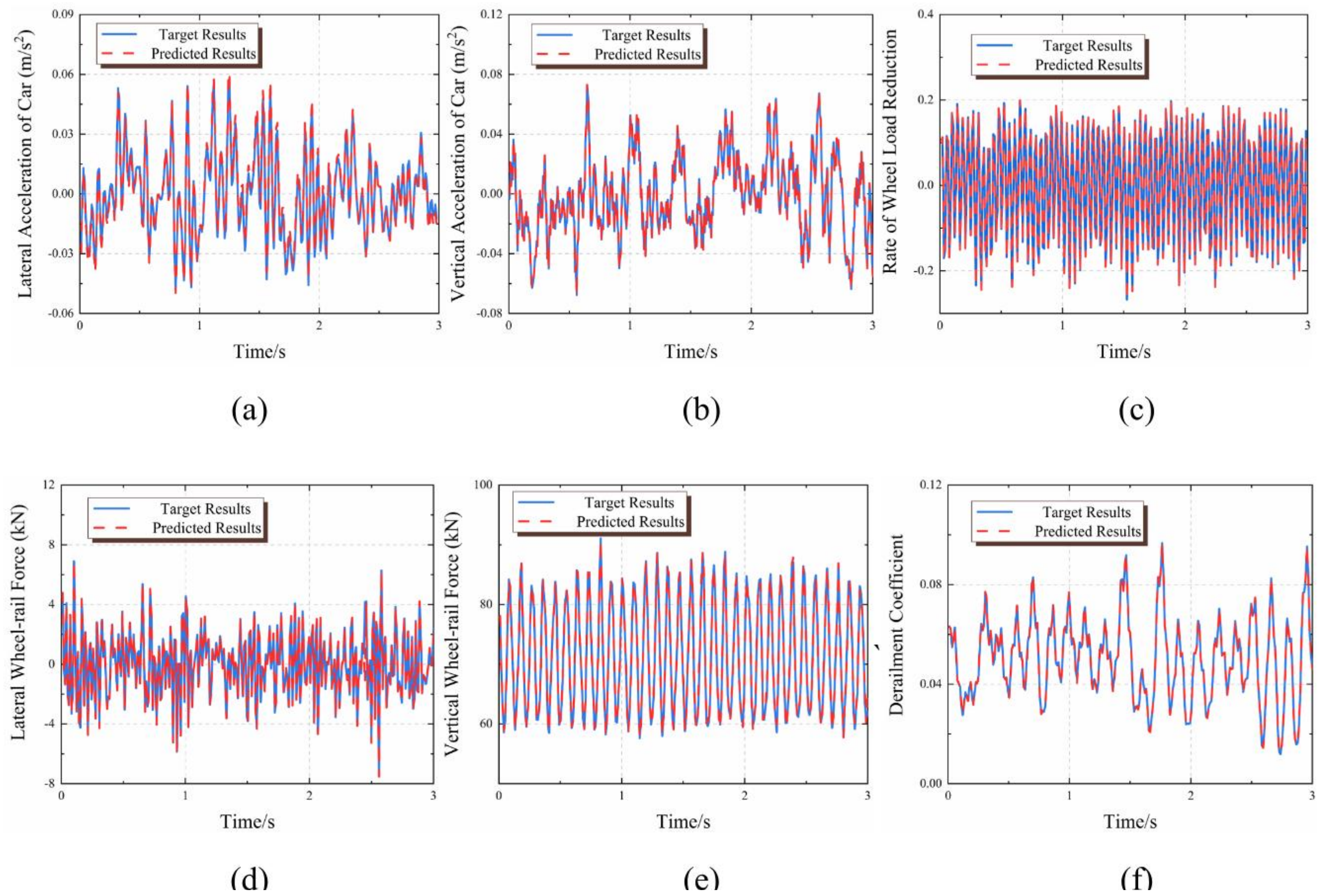

Peak Response Prediction Results

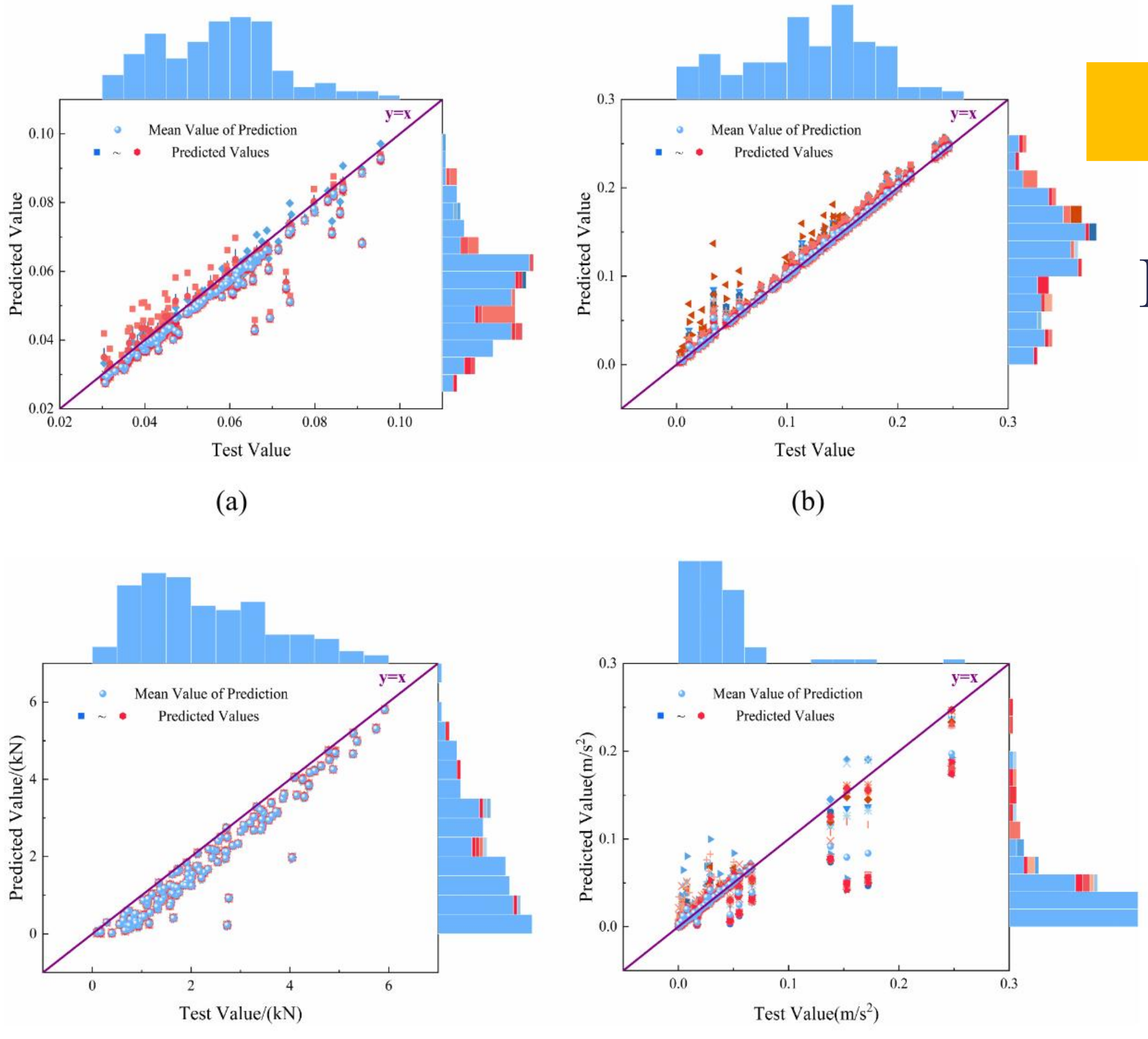

Uncertainty Quantification

Influencing Factor Analysis

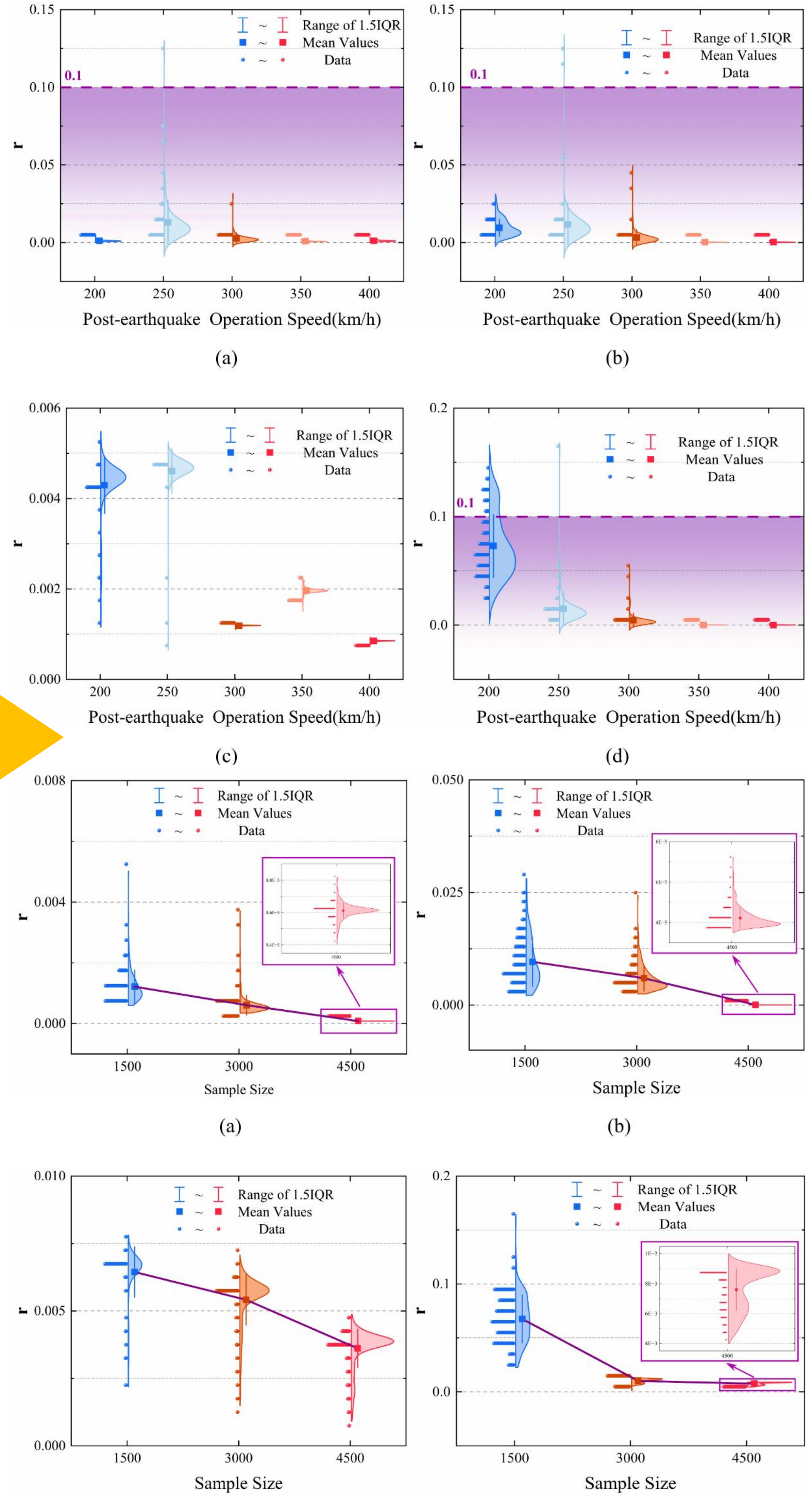

Post-Earthquake Operating Speed

Sample Size

✓ Uncertainty in post-earthquake operability peak prediction is non-negligible; increasing sample size most effectively improves NN robustness

Uncertainty-Embedded Peak Response Prediction

- A neural network surrogate model was developed to predict the total peak-value error of train operation indicators.

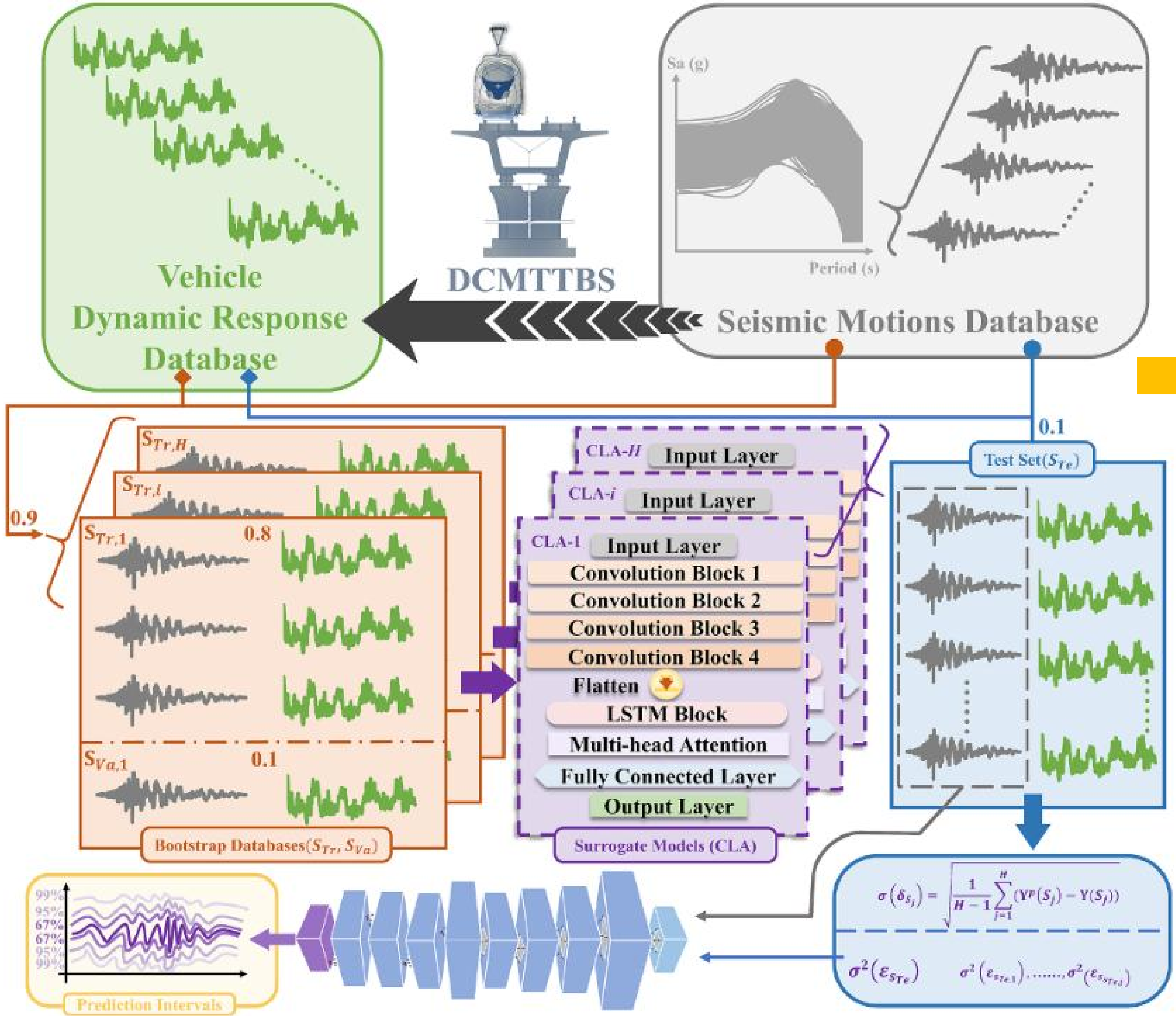

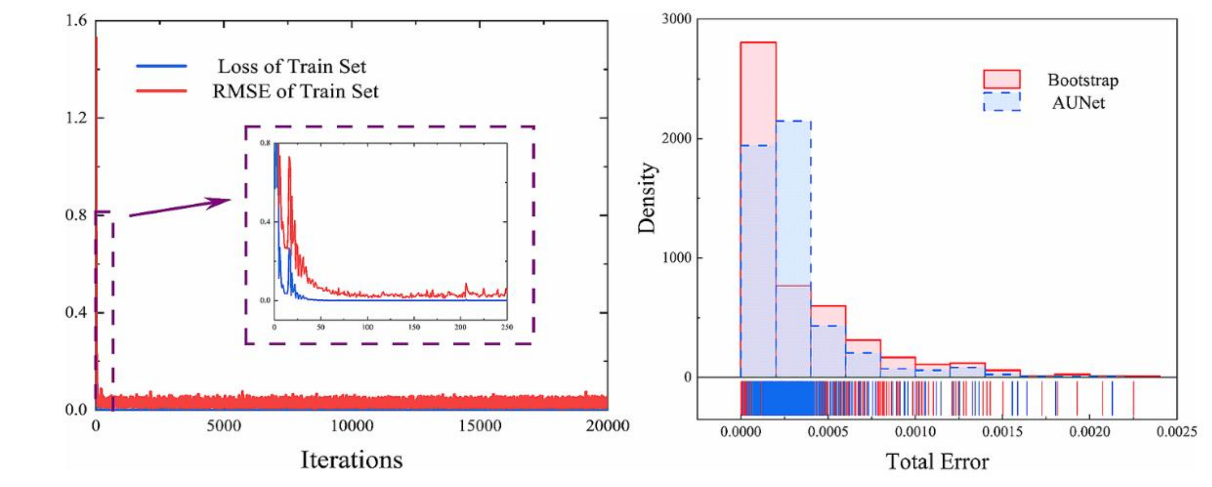

Network Performance

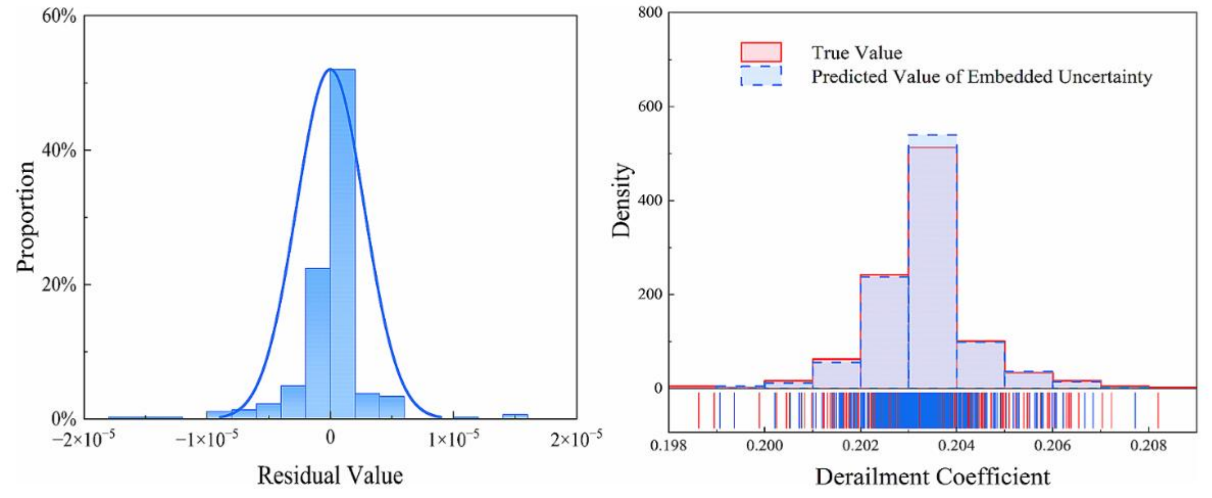

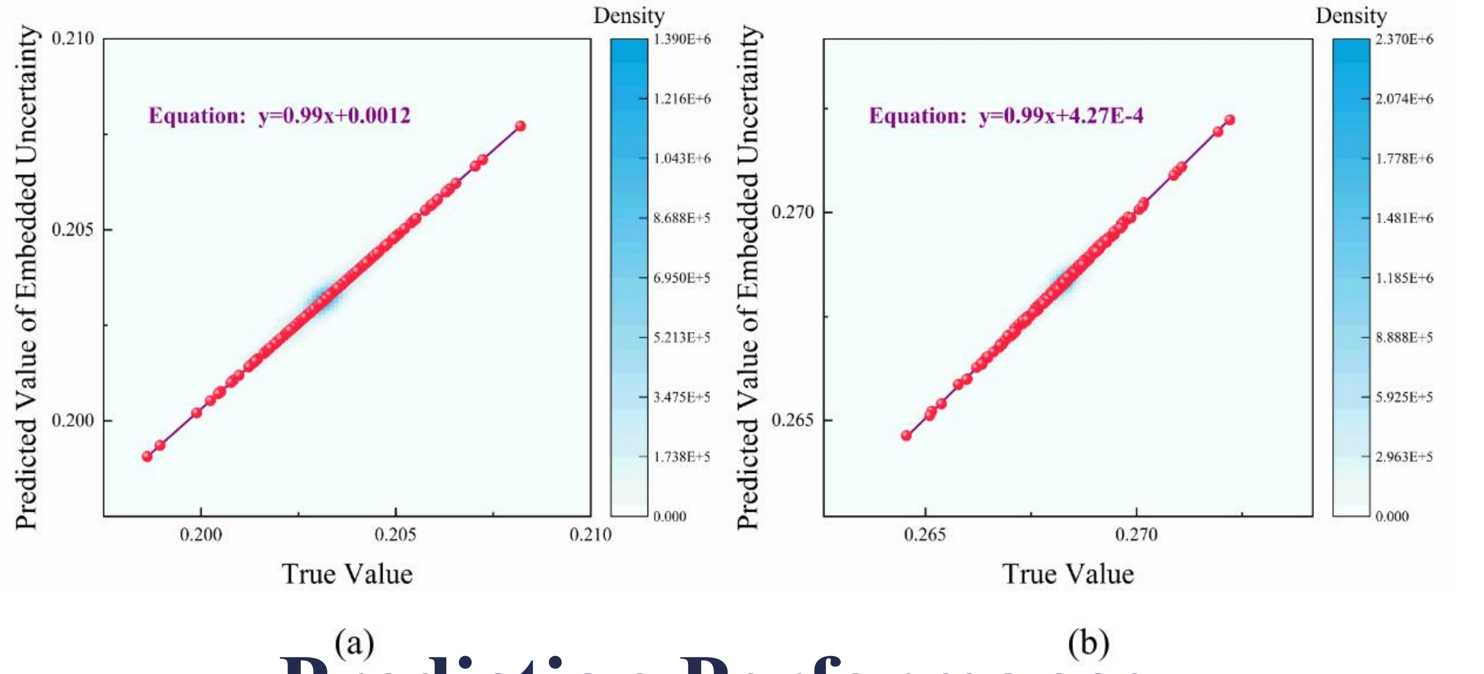

Prediction Performance

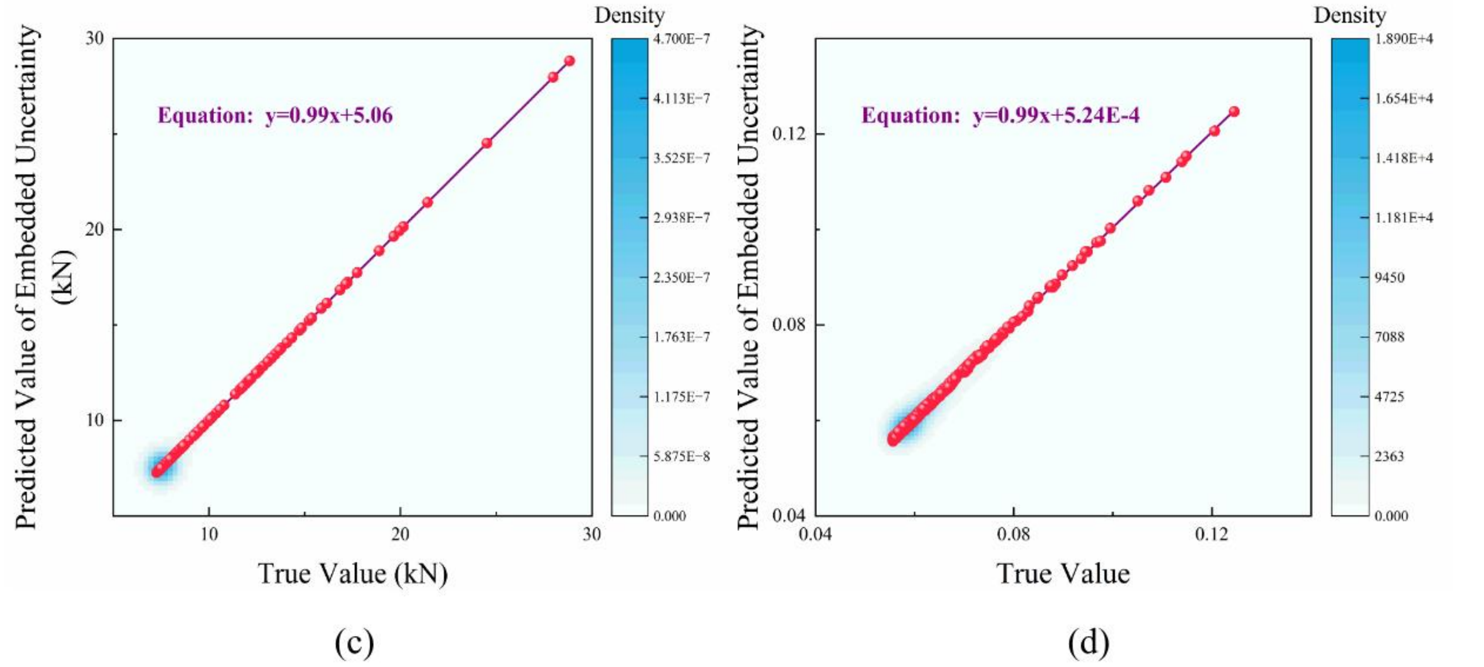

- After uncertainty incorporation, the R^2 and C values for peak derailment coefficient prediction approached 100% and 99%, respectively.

✓ Uncertainty-embedded method **significantly improves** post-earthquake operability peak-response prediction compared with NN surrogate model

Peak Response Prediction Intervals

□ Peak response prediction intervals with different confidence levels were obtained

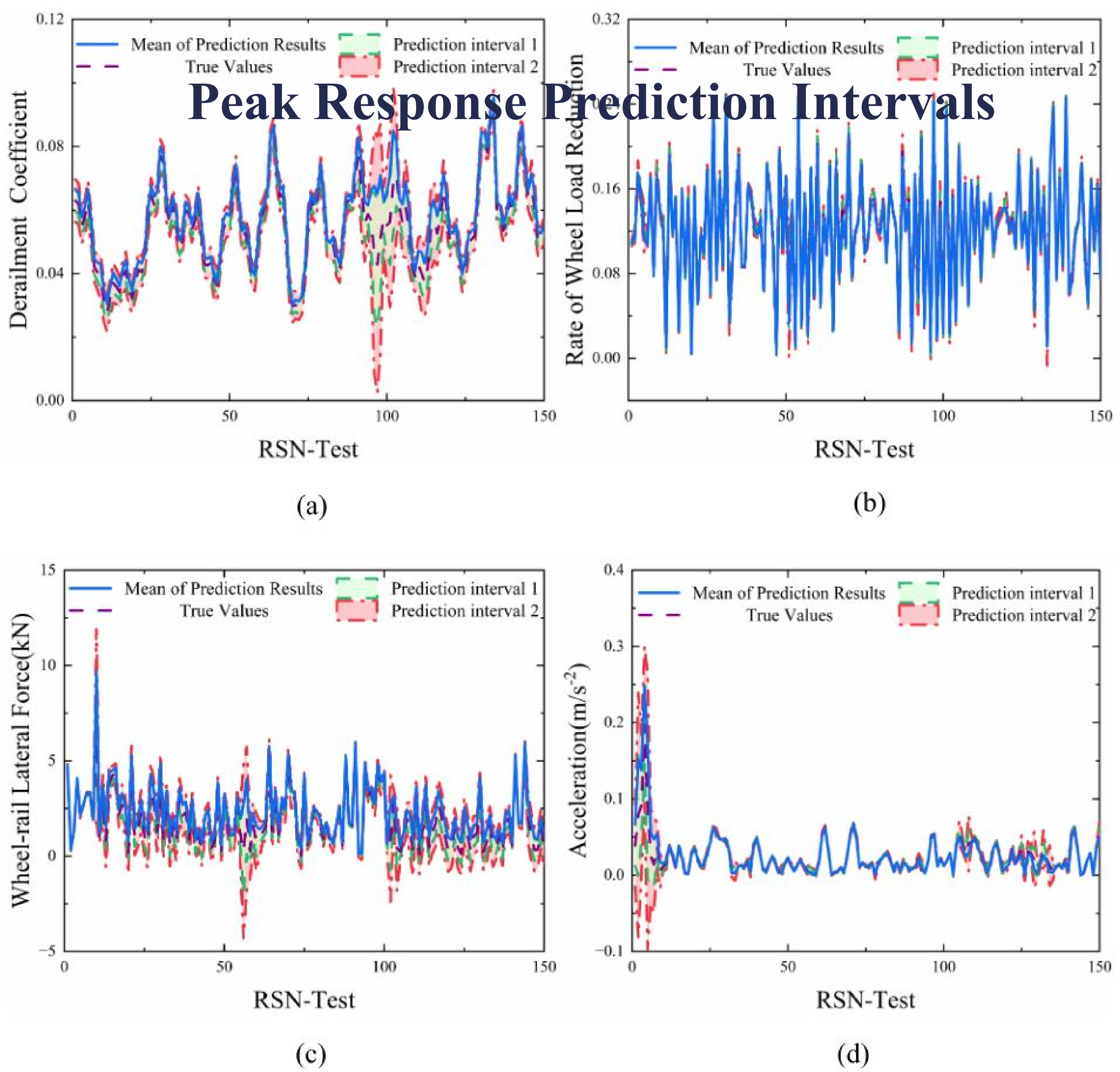

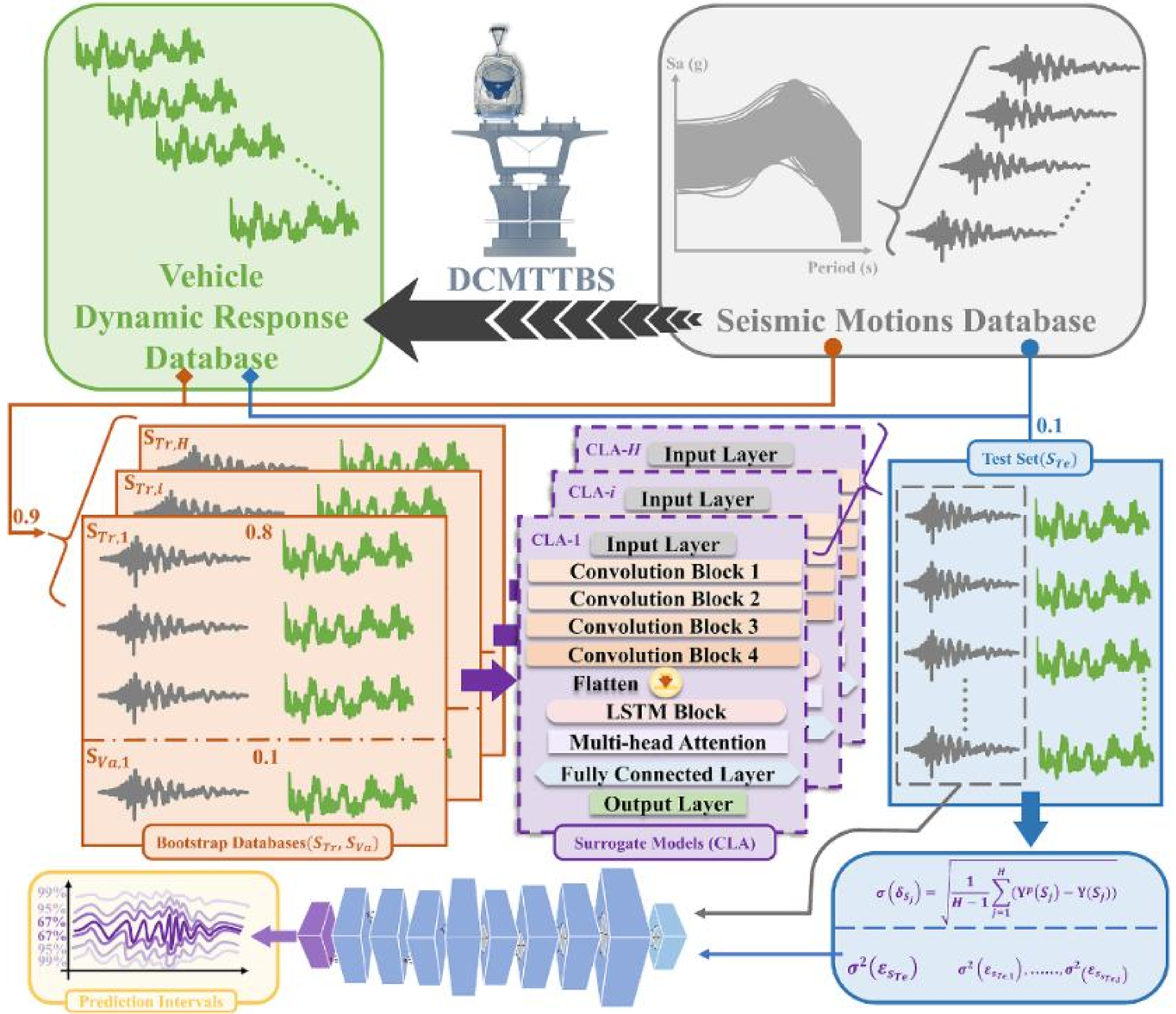

- Uncertainty in post-earthquake train operation indicator peak prediction was quantified, and prediction intervals with different confidence levels were constructed.
- Prediction Interval 2 is recommended as a supplement to point predictions for post-earthquake operation safety, while Prediction Interval 1 can serve as a reference when practical conditions and safety requirements are considered.

✓ The **95% prediction interval** covered all peak values of the post-earthquake train operation indicators in the test set

Presentation Outline

- Background and State of the Art
- Data-Driven Seismic Damage Prediction Method for High-Speed Railway Simply Supported Girder Bridge Systems
- Seismic Response Prediction and Uncertainty Quantification for High-Speed Railway Simply Supported Girder Bridge System
- Seismic Reliability Assessment Method for High-Speed Railway Simply Supported Girder Bridge Systems
- Regional Seismic Reliability Assessment of High-Speed Railway Simply Supported Girder Bridge Systems

- A sample database generation method for regions with different topographic characteristics was proposed based on Latin hypercube sampling and Gibbs hybrid sampling, considering the prior distributions of structural parameters

Structural Priors: $$P(x_r \mid x_{-r}) = \frac{P(x_{-r} \mid x_r) P_{\text{prior}}(x_r)}{P(x_{-r})} \propto \prod_{a=1}^{A} P(x_a \mid x_r) P_{\text{prior}}(x_r)$$

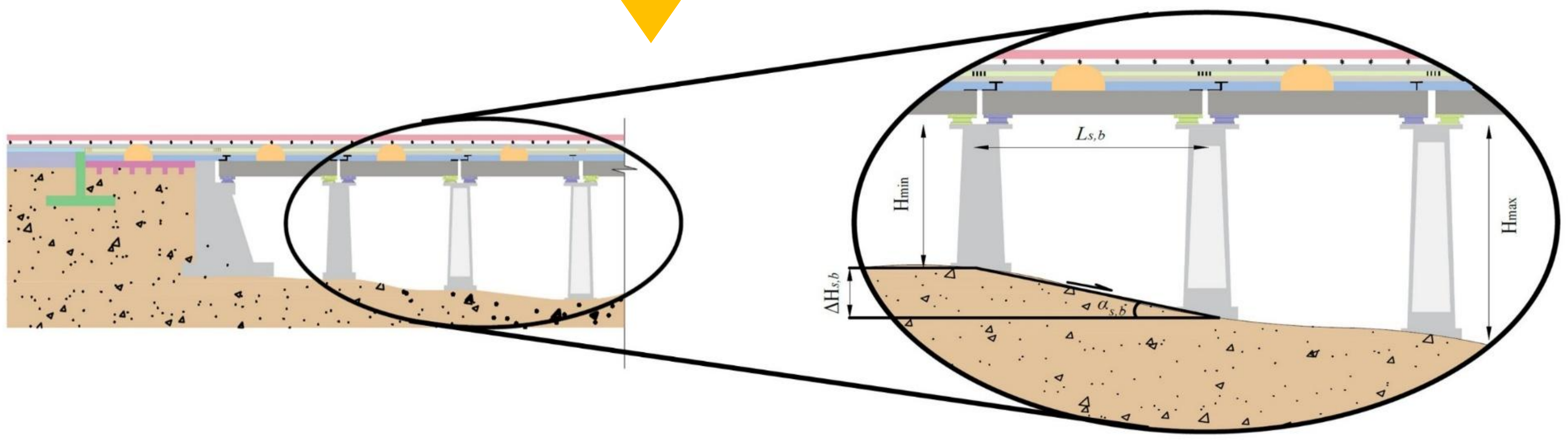

Table 6
Geomorphological featu[illegible]d corresponding pier height constraints in the region.

Geomorphological Feature	D[illegible]ion	Pier Height Arrangement and Combination Limits
Flat Land	$\alpha_{s,b}$<2°, Pier height difference not exceeding 20 m	$\Delta H_{s,b}<L_{s,b} \times \tan(2)$, H_{max}-H_{min}<20 m
Hills	2°≤$\alpha_{s,b}$<6°, Pier height difference not exceeding 150 m	$L_{s,b} \times \tan(2) \le \Delta H_{s,b} < L_{s,b} \times \tan(6)$
Mountainous	6°≤$\alpha_{s,b}$<25°, Pier height difference exceeding 1[illegible]0 m	$L_{s,b} \times \tan(6) \le \Delta H_{s,b} < L_{s,b} \times \tan(25)$
High Mountain Terrain	25°<$\alpha_{s,b}$, altitude exceeding 300 m	$L_{s,b} \times \tan(25) < \Delta H_{s,b}$, Using simply supported beams is generally not advisable.

Notes: 1. Elevation Difference refers to the altitude difference between the region's highest and lowest terrain points. 2. $\Delta H_{s,b}$ is the height difference between adjacent piers for the s-th span of the b-th bridge, $L_{s,b}$ is the span length, and $\alpha_{s,b}$ is the corresponding slope. 3. The mountainous terrain conditions discussed in this section still adopt the slab ballastless track structure form, as researched in this study.

Regional Geographic Information

Algorithm 1. Generation of Pier Height Sample Repository for Bridge Groups in Areas with Different Topography.

1. Inputs
NS - Total number of samples
Burn - Number of discarded samples
PN_b – Number of piers for the b-th bridge
ΔH_{Pier_Range} - Range of pier height differences
σ - the Standard deviation of N

2. Initialization
Initialize the random number generator
Initialize the sample storage matrix, *Samples*

3. Gibbs Sampling
For each pier g ($2 \le g \le PN$) in the b-th ($1 < b < NS$) bridge, perform the following steps:

3.1. Generate the Initial Pier Height State Matrix and Determine the conditional distribution of the initial pier height and the height differences between piers.
From the target distribution of each pier in the b-th bridge (initial pier height: $Hb\ 1 \sim D_b\{u_b, v_b\}$), calculate the initial pier height state matrix $\mathbf{H}_1$(H1 1,…, Hb 1,…, HNS 1) for all bridges in the region. Also, obtain the conditional distribution ($\Delta H\ b\ g, g\text{-}1 \sim N_g\{0, \sigma_{g,g\text{-}1}\}$) of height differences $\Delta H\ b\ g,g\text{-}1$ between the initial pier height $\mathbf{H}_1$ and the other piers $H\ b\ g,g\text{-}1$.

3.2. Obtain Pier Height Arrangement:
```
For (b in 2:(NS)) {
    For (g in 1:(PN_b)) {
        For (k in 1:g) {
            Sample the pier height H^b(k) from the conditional probability distribution
p(H^b (k)| H^b(1),…,H^b(k-1), H^(b-1)(k+1),…,H^(b-1)(g))
        }
    }
    H^(b+1) ← H^b(1,…,g)
}
```

3.3. Update the Sample Matrix
Store the generated pier height combination in the *Samples* and Perform a GR diagnostic value test on the obtained samples to verify whether the maximum pier height difference satisfies the regional topographical conditions. The final set of samples is denoted as *Final_Samples*

4. Output
The final set of pier height arrangements for different topographical regions: *Final_Samples*

✓ **Structural Database Incorporating Topographic Differences and Structural Priors**

□ Evaluated the convergence of the sample database generation method for different topographic regions

$$\hat{R} = \sqrt{\frac{W\left(1+\frac{1}{N_{c,n}}\right)+\frac{B}{N_{c,n}}}{W}}$$

$$W = \frac{1}{N_c}\sum_{n=1}^{N_c} S_{c,n}^2$$

$$B = \frac{N_{c,n}}{N_c - 1}\sum_{n=1}^{N_c}\left(\mu_{c,n} - \sum_{i=1}^{N_c}\mu_{c,n}\right)^2$$

Gelman–Rubin Diagnostic

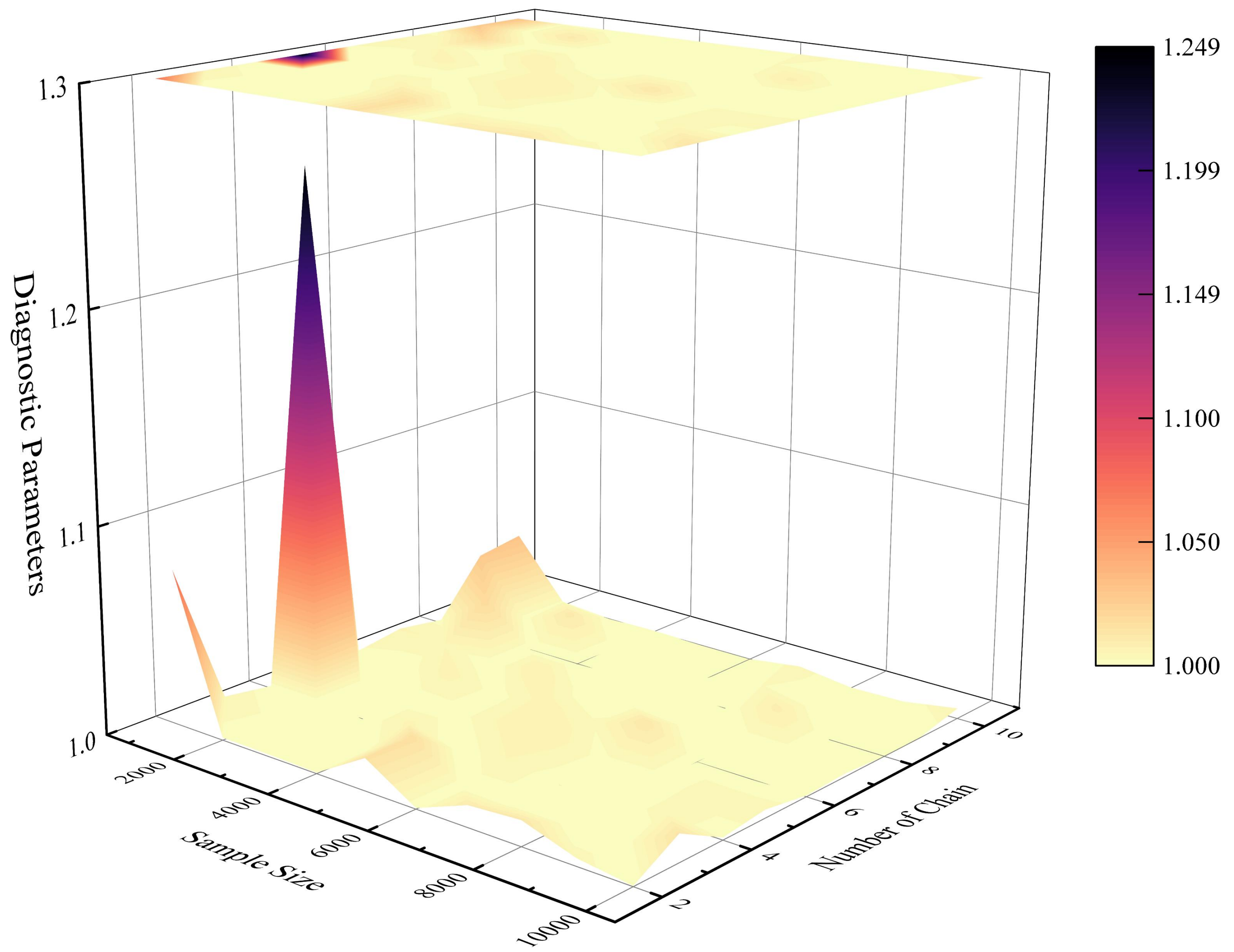

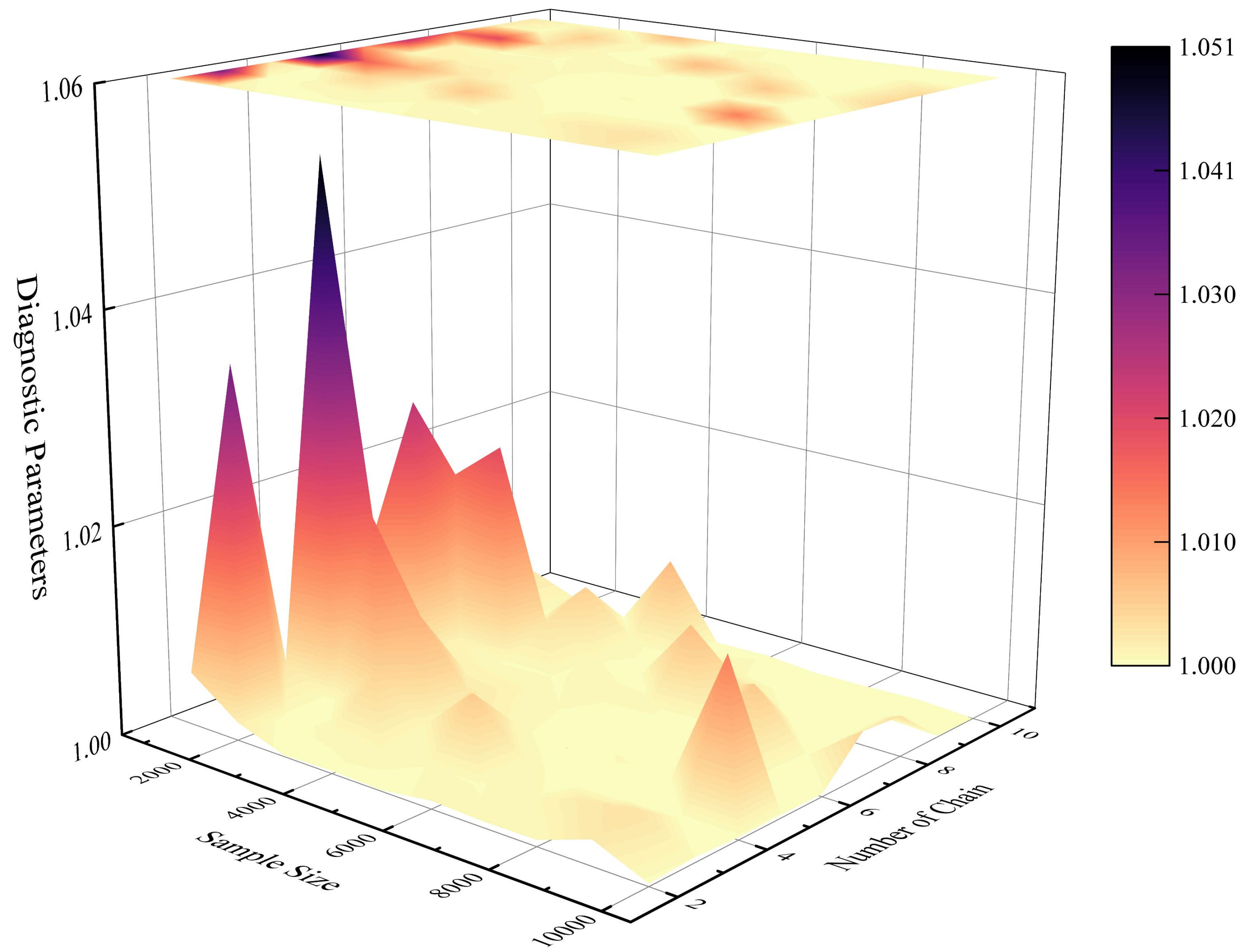

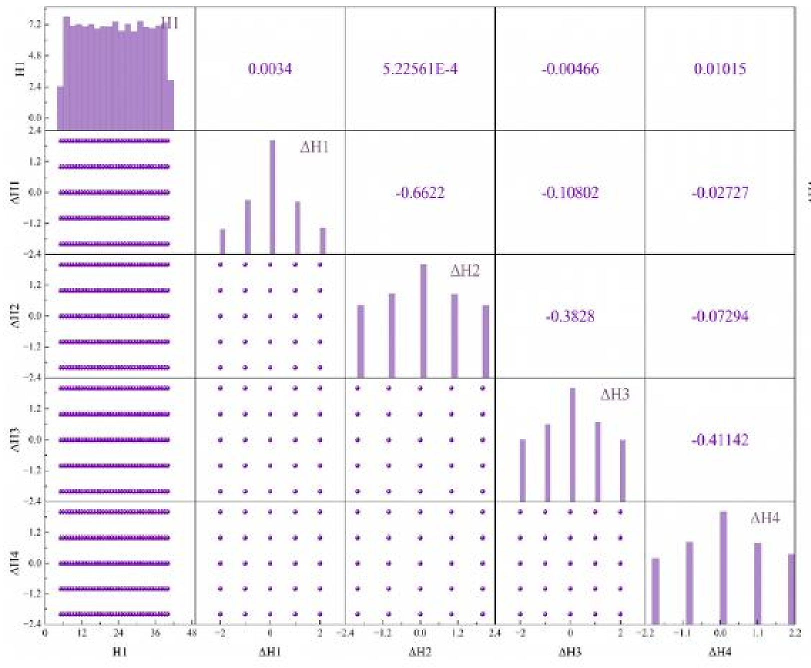

(a)

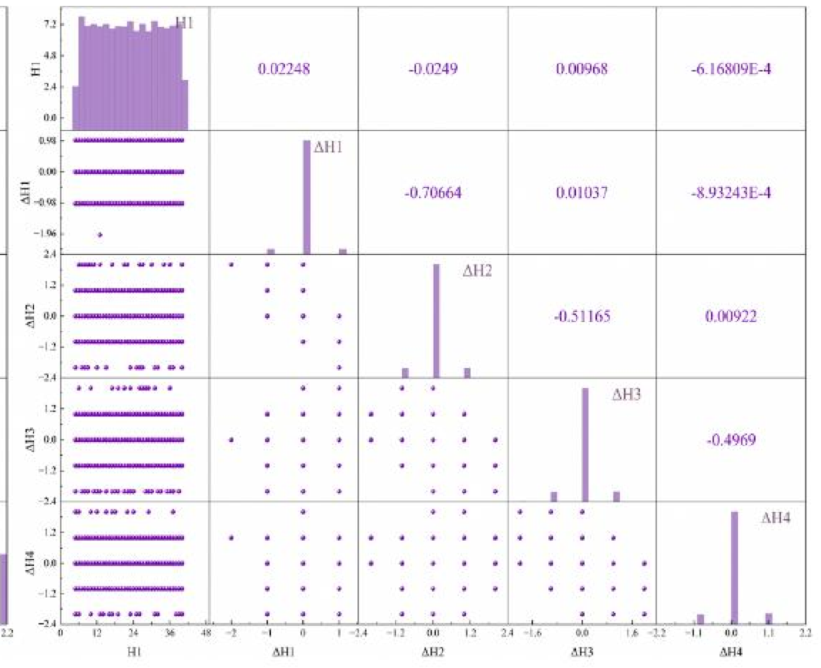

(b)

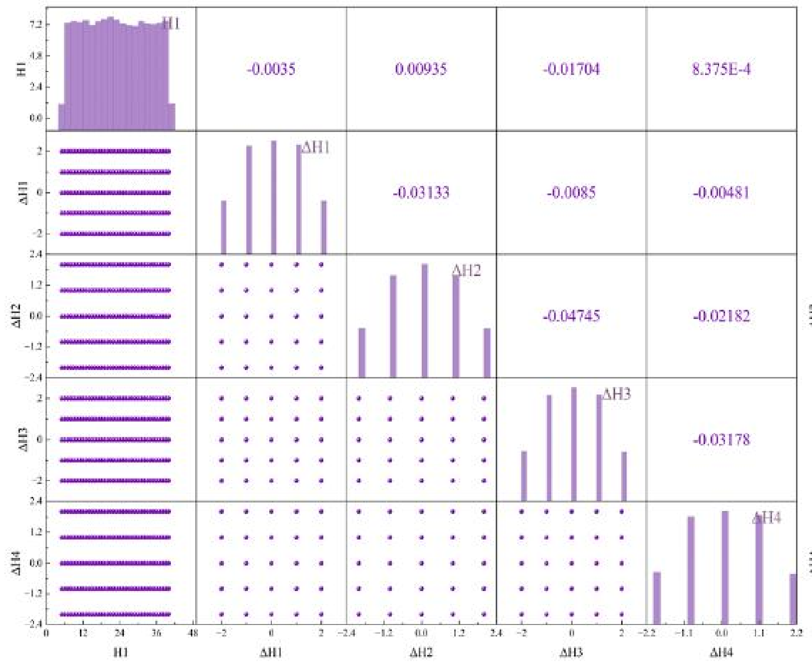

(c)

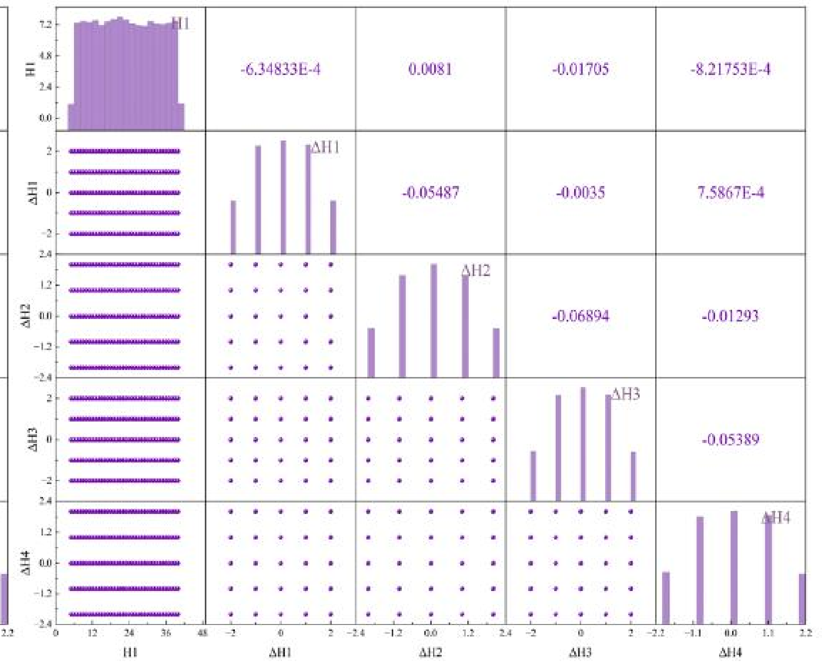

(d)

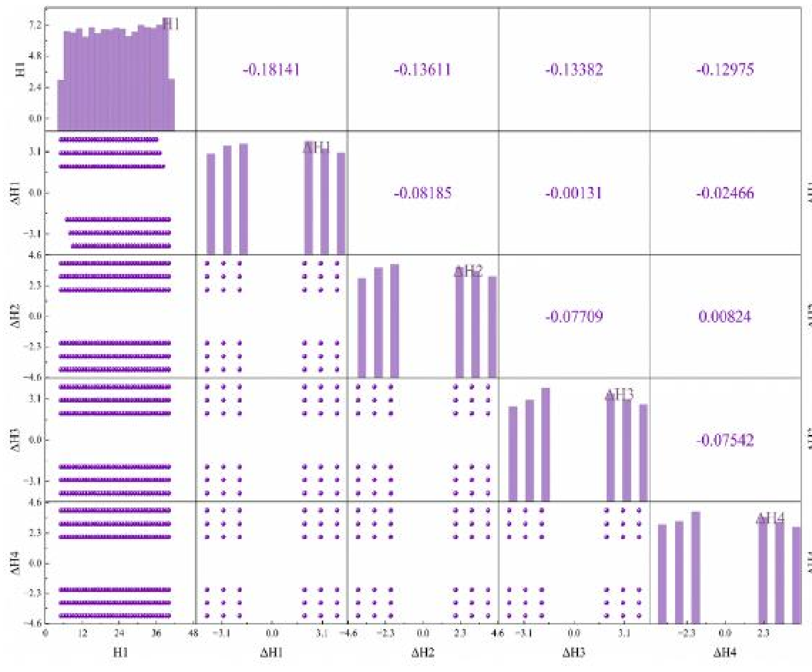

(e)

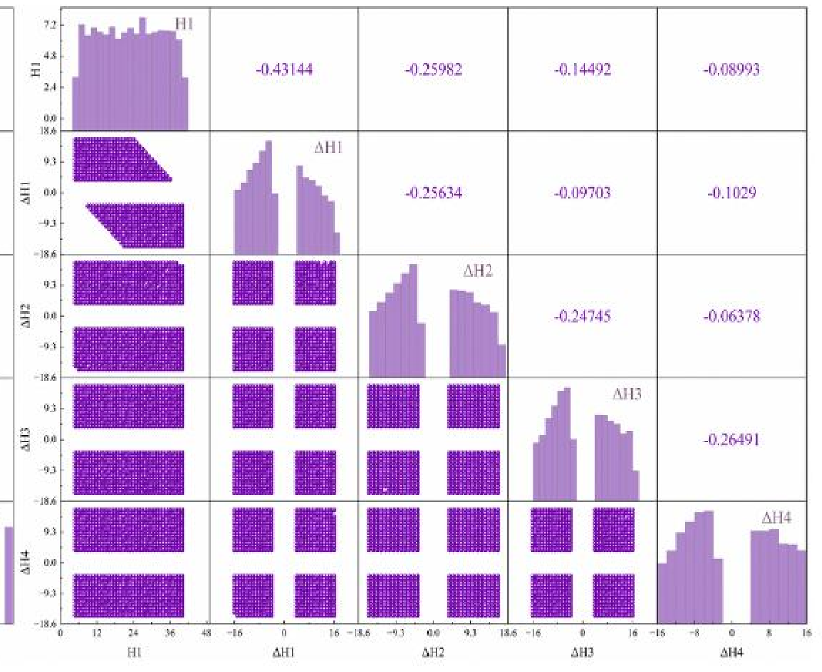

(f)

✓ The **rationality of the construction** method was validated, and the required number of sampling chains and sample size were determined.

Multimodal Feature Fusion-Based Interval Prediction of Post-Earthquake Regional Bridge Operability

Prediction Intervals:

$$\mathbf{X}_{\mathrm{p}}(b) = A^{p}_{\mathrm{RHN}}(b) + \mathbf{K}(b)\sigma(\delta_{\mathrm{RHN}}(b))$$

$$\mathbf{X}_{\mathrm{p,u}}(b) = A^{p}_{\mathrm{RHN}}(b) + \mu(\varepsilon_{\mathrm{RHN}}(b)) + \rho(b)\mathbf{K}(b)\sigma(\delta_{\mathrm{RHN}}(b))$$

$$\mathbf{K}_i(b) = \frac{Y^{p}_{\mathrm{RHN},i}(b) - A^{p}_{\mathrm{RHN}}(b)}{\sigma(\delta_{\mathrm{RHN}}(b))}$$

$$\rho(b) = \frac{\sigma(\Delta_{\mathrm{RHN}}(b))}{\sigma(\delta_{\mathrm{RHN}}(b))}$$

Loss Function:

$$F_{\mathrm{loss,RNUQ}} = \frac{1}{2}\sum_{b=1}^{N_{te}}[\ln(\sigma^2(\varepsilon_{\mathrm{RHN}}(b))+1]$$

$$F_{\mathrm{loss,RAN}} = \sum_{b=1}^{N_{te}}(\mu(\varepsilon_{\mathrm{RHN}}(b))$$

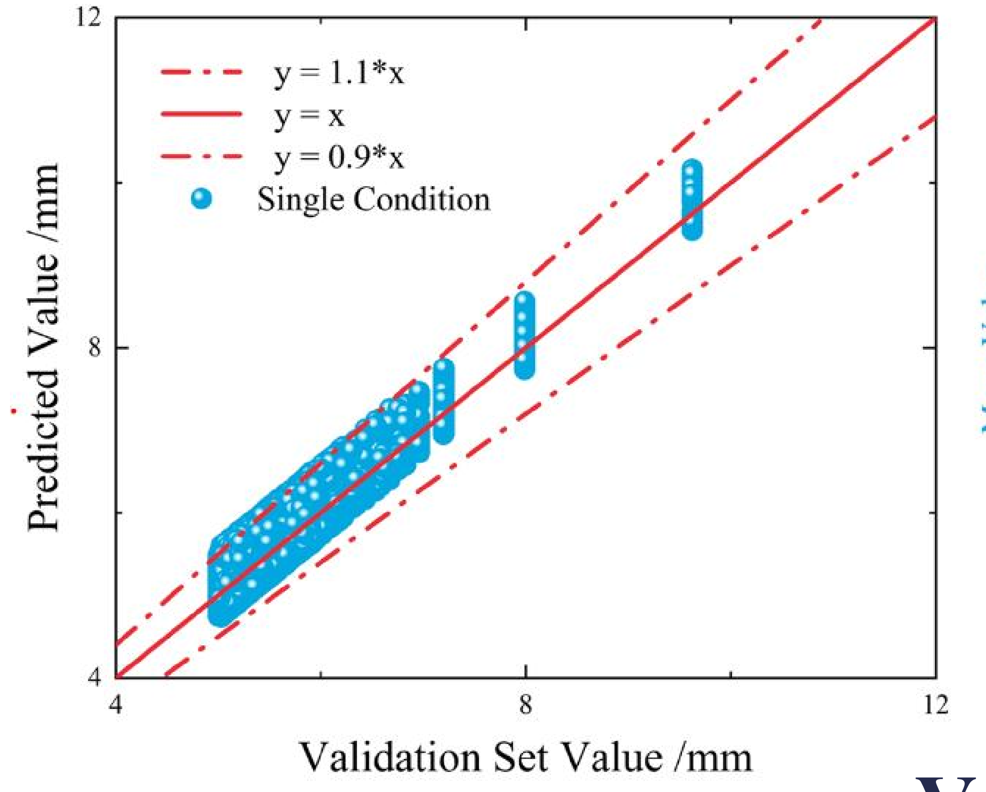

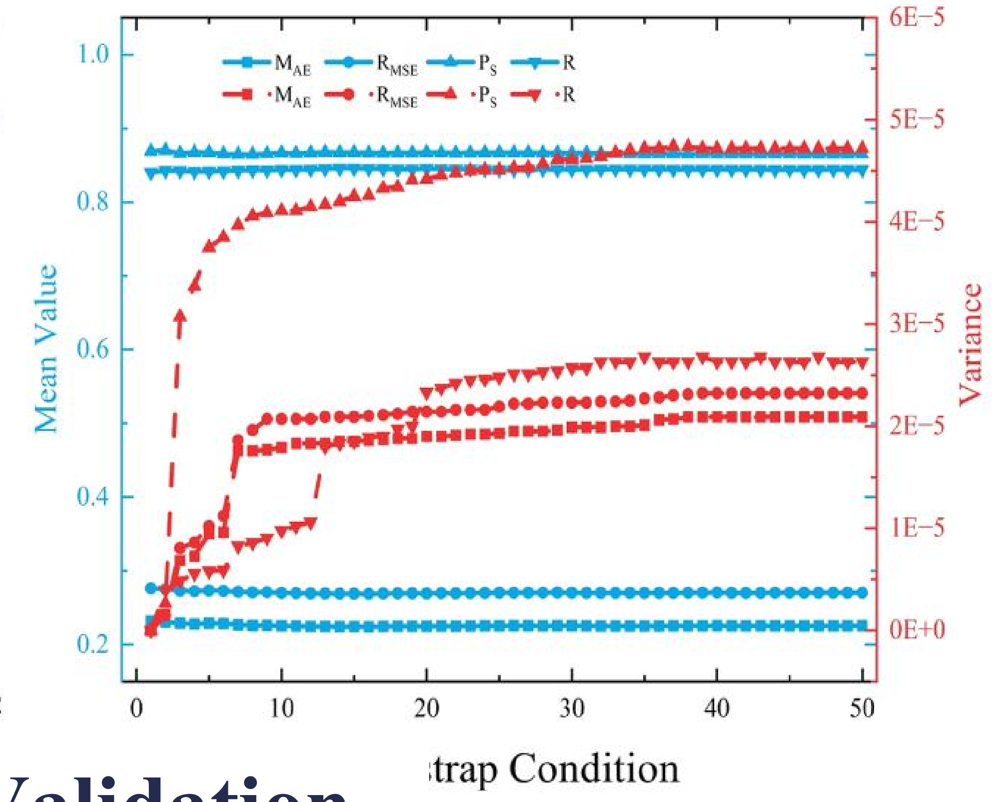

Validation

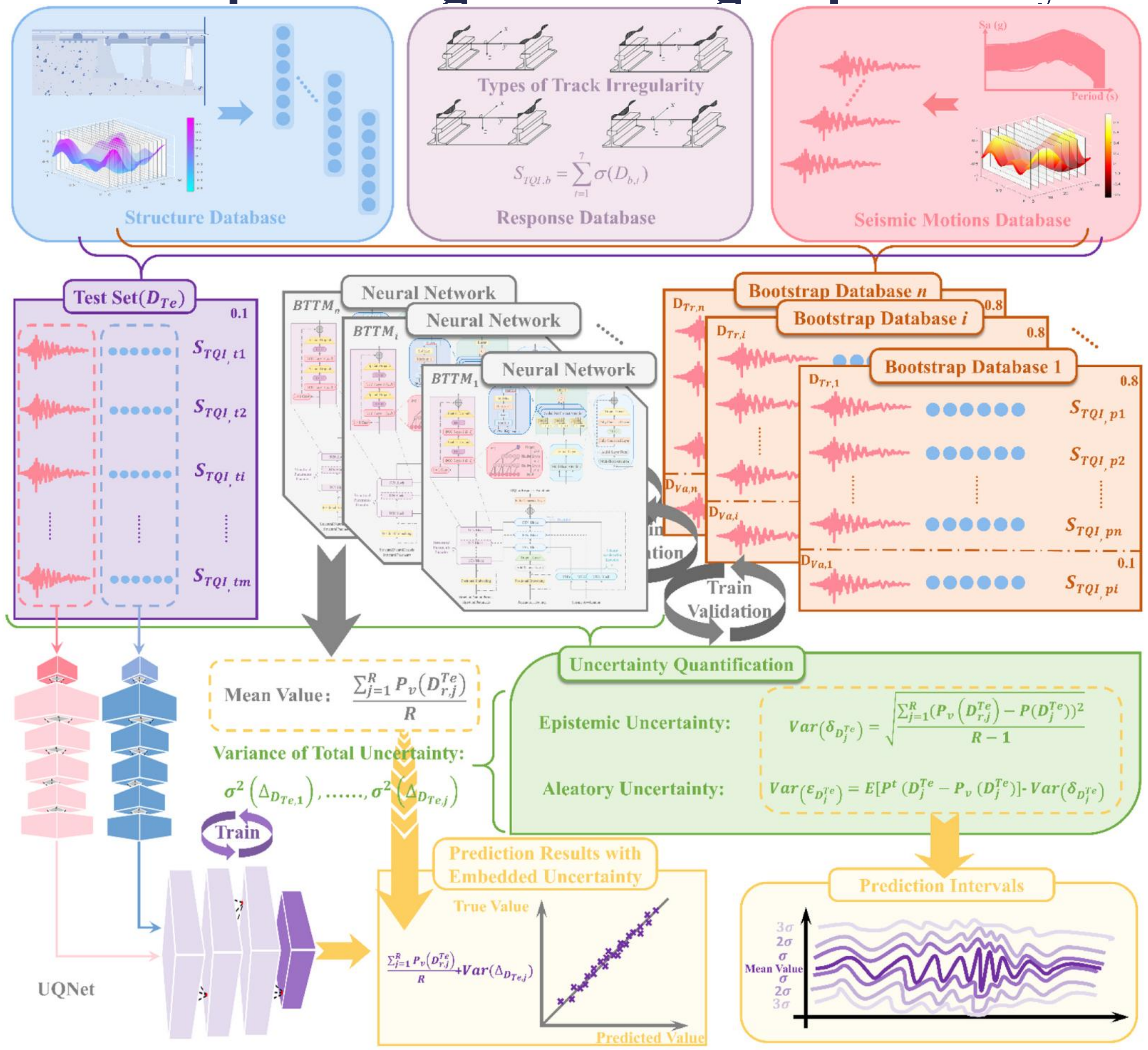

Probabilistic Prediction of Post-Earthquake Regional Bridge Performance

✓ **Multimodal NN Surrogate Model for Rapid Post-Earthquake Operability Prediction of Regional Bridge Groups**

Target Region Overview and System-Level Seismic Reliability

□ Earthquake Magnitude Effects on Regional Bridge Network Operability

Bridge ID	X-Coordinate (km)	Y-Coordinate (km)	Slope α_s(°)
1	74.5	6.5	8
2	75.5	24.2	11
3	79.5	41.0	12
4	76.9	55.8	15
5	41.8	69.6	10
6	-7.6	77.9	9
7	-11.2	62.2	4
8	-1.0	39.3	5
9	10.6	27.1	3
10	6.3	15.4	2
11	17.3	-5.6	5
12	45.3	-7.0	5
13	36.9	22.2	3
14	38.8	35.6	4
15	10.1	48.5	5
16	28.2	61.7	8
Potential Earthquake Source	100	35.6	

Bridge Information

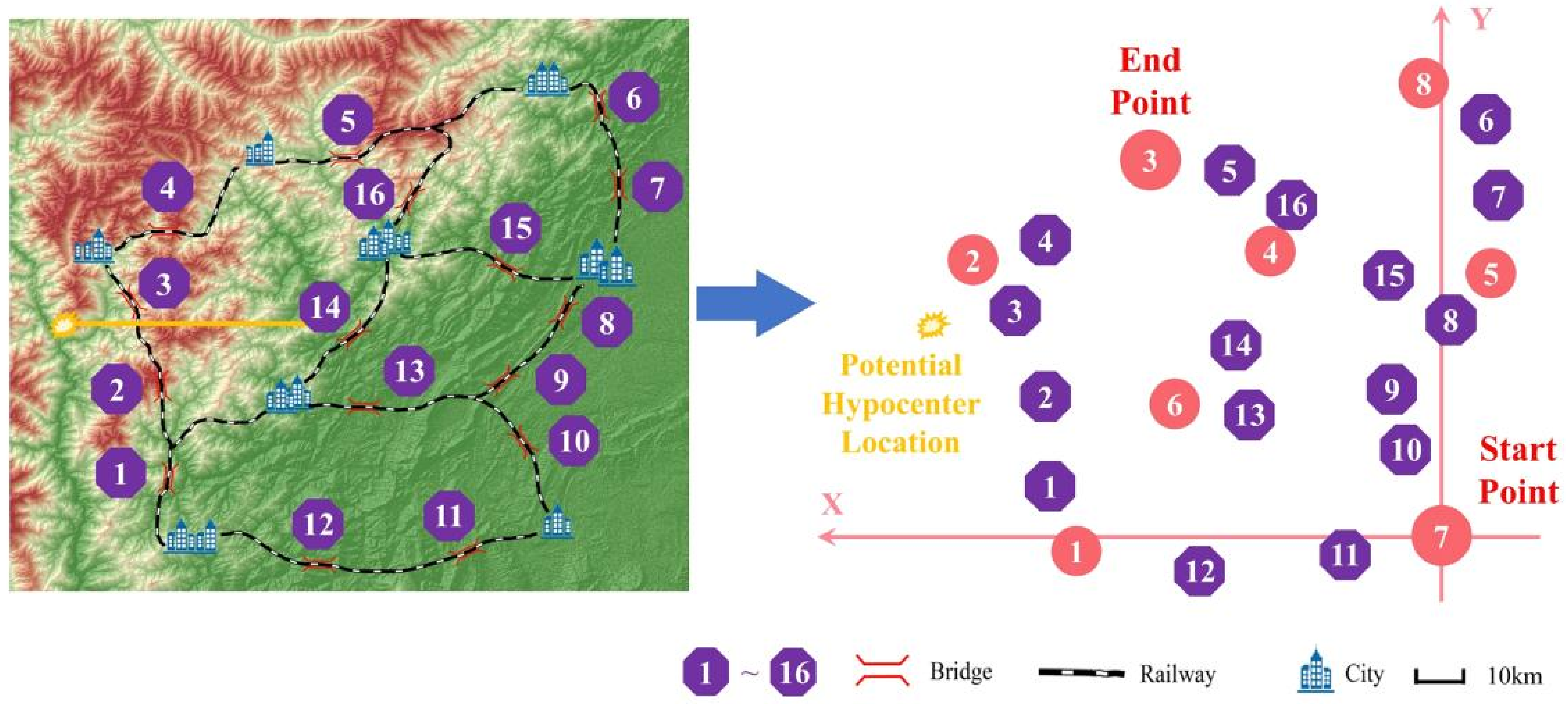

City	1	2	6	7	3	4	5	8
1		72.1	46.6	84.2				
2	72.1		48.9		41.1			
6	46.6	48.9		74.4		45.4	81.6	
7	84.2		74.4				70.3	
3		41.1				70.2		64.8
4			45.4		70.2		54.3	59.6
5			81.6	70.3		54.3		46.9
8					64.8	59.6	46.9	

Railway Line Information

Source–Bridge Site–Topography Ground-Motion Prediction Equation

$$\log(S_{b,i}) = \eta_1 + \eta_2 M_L + \eta_3 M_L^2 + \eta_4 \log(R_b + \eta_5 e^{\eta_6 M_L})$$

$$S_{b,i,t} = \gamma_{b,i,t} S_{b,i}$$

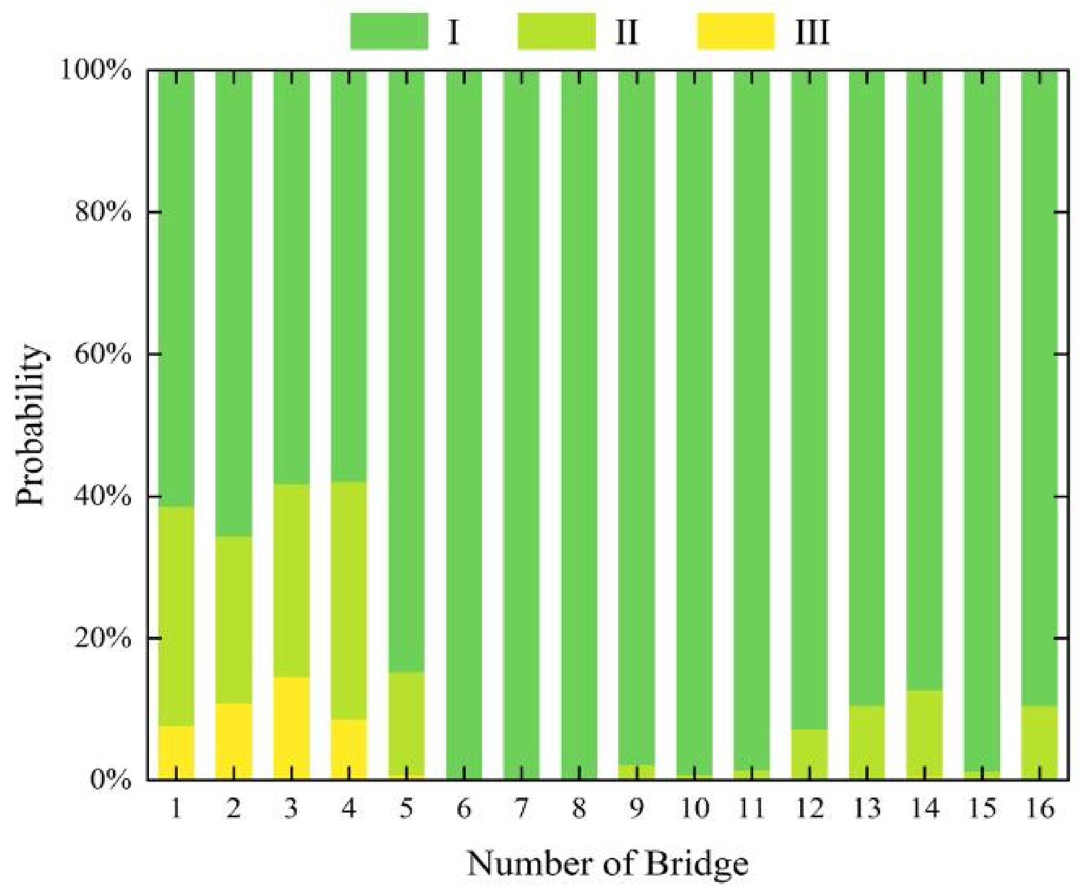

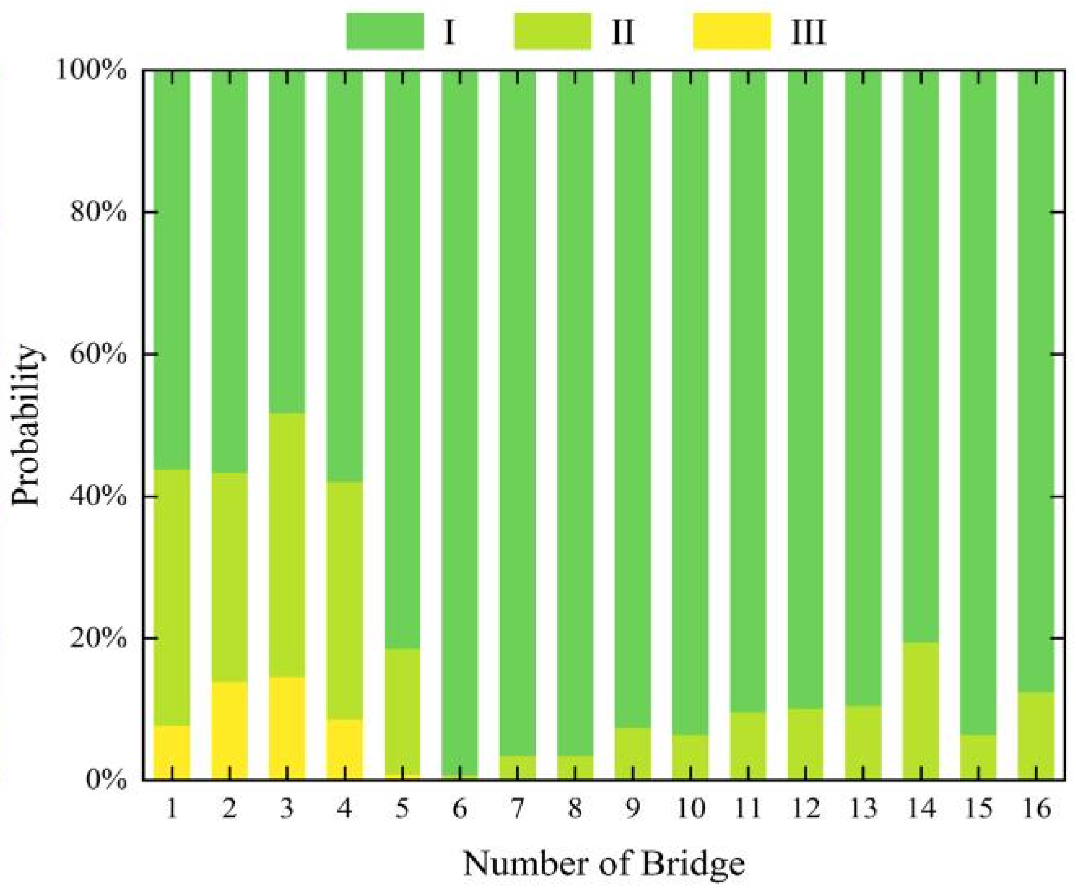

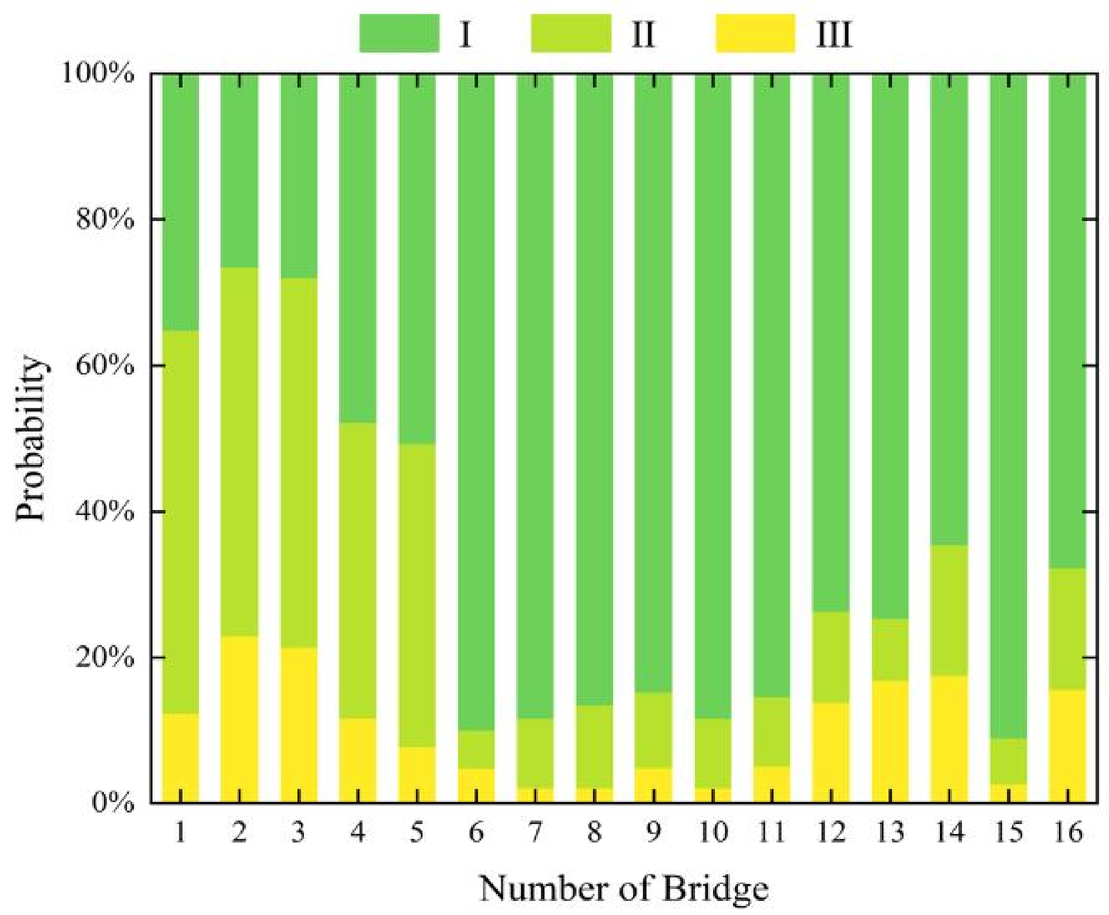

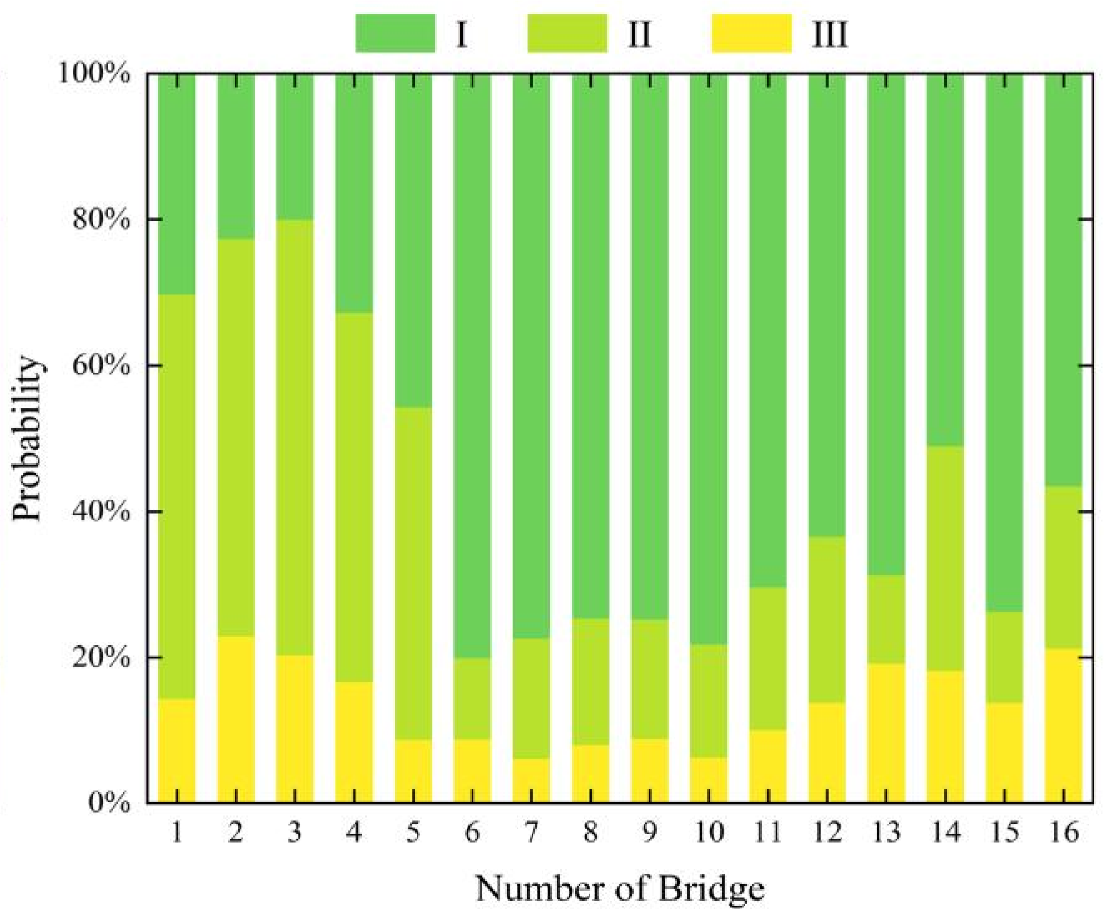

✓ **Determined Post-Earthquake Operability of Regional Bridge Networks**

Earthquake Magnitude Effects on Regional High-Speed Railway Line Operability

$$f_{s_1,v}(L_n)=\prod_{p=1}^{P} f_{s_1,v}(b_p)$$

$$f_{s_2,v}(L_n)=\prod_{p=1}^{P}\left[f_{s_1,v}(b_p)+f_{s_2,v}(b_p)\right]-\prod_{p=1}^{P} f_{s_1,v}(b_p)$$

$$f_{s_3,v}(L_n)=1-\prod_{p=1}^{P}\left[f_{s_1,v}(b_p)+f_{s_2,v}(b_p)\right]$$

Post-Earthquake Operability of Regional Bridge Networks

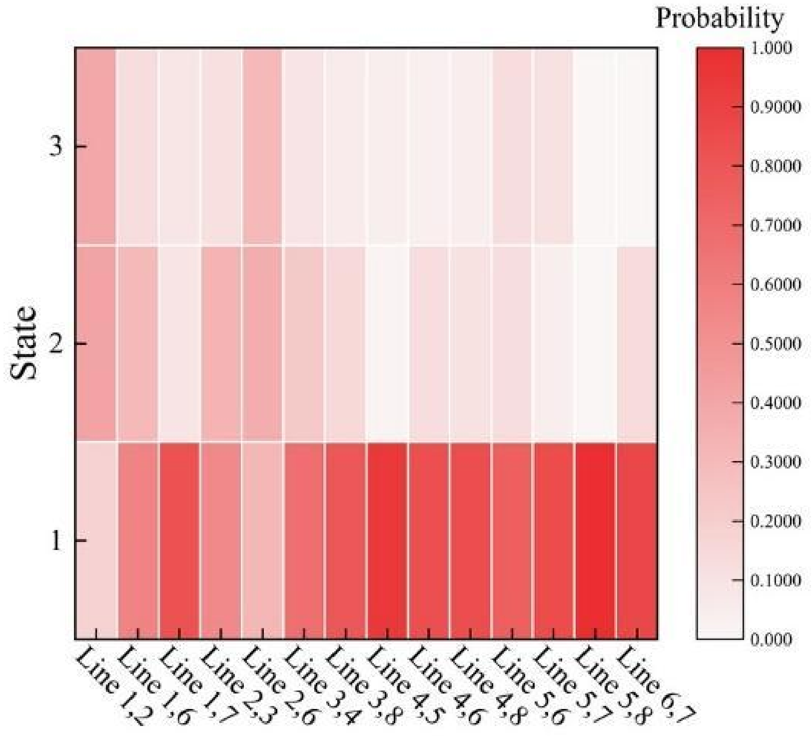

Magnitude 6

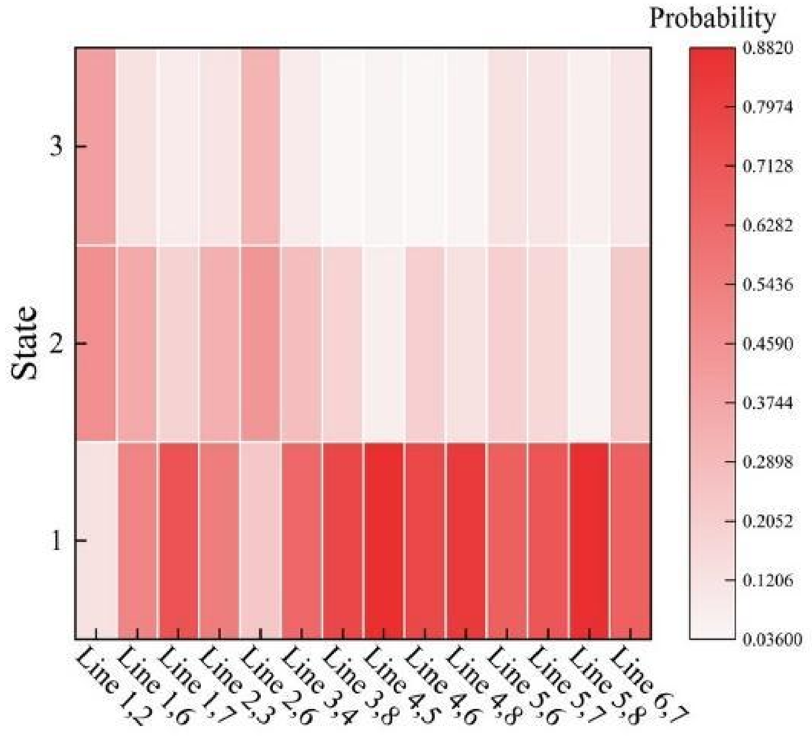

Magnitude 6.5

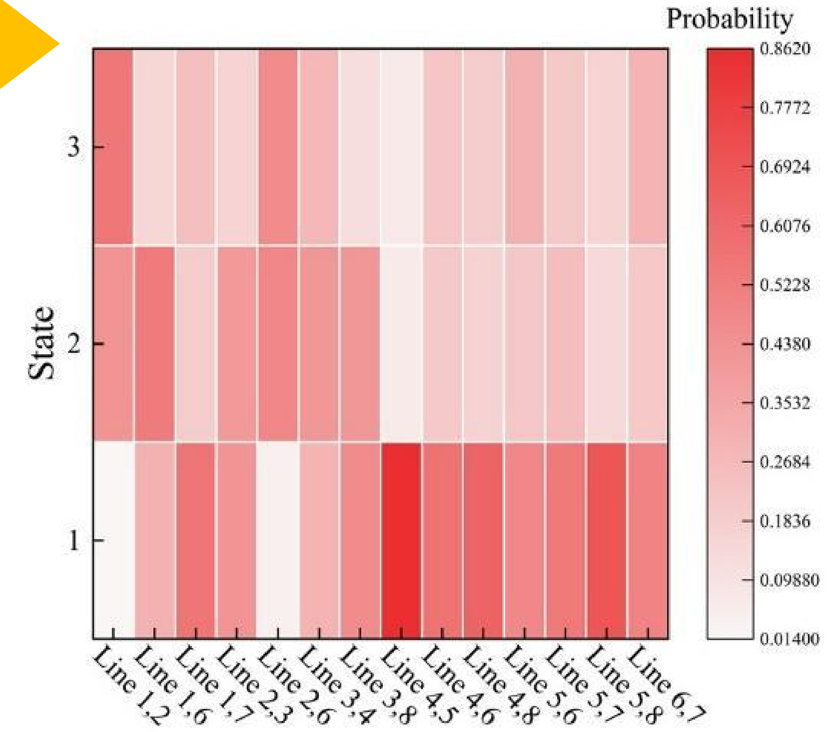

Magnitude 7

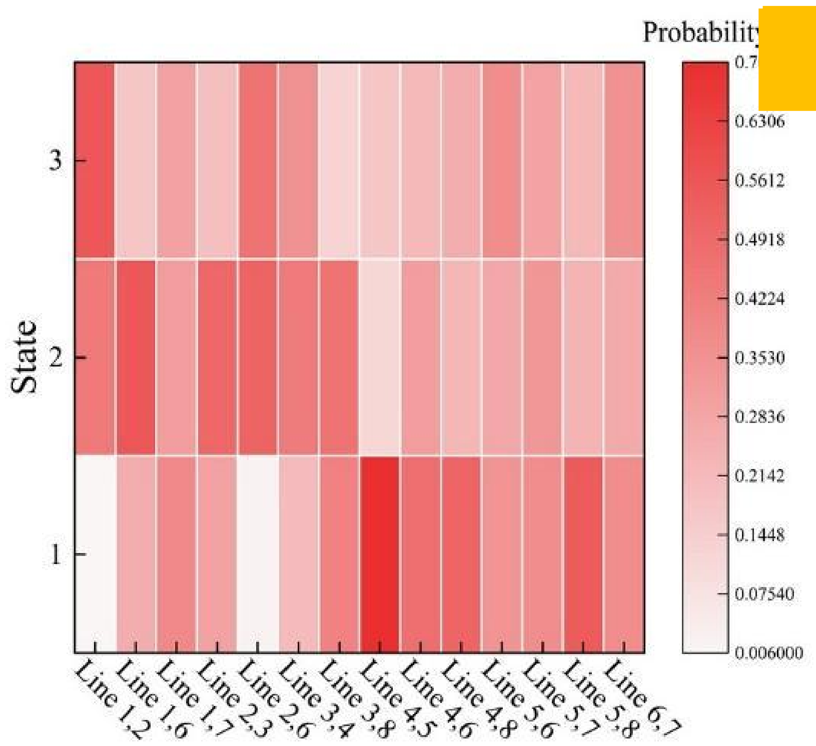

Magnitude 7.5

Probability Distribution of Post-Earthquake Line Operability

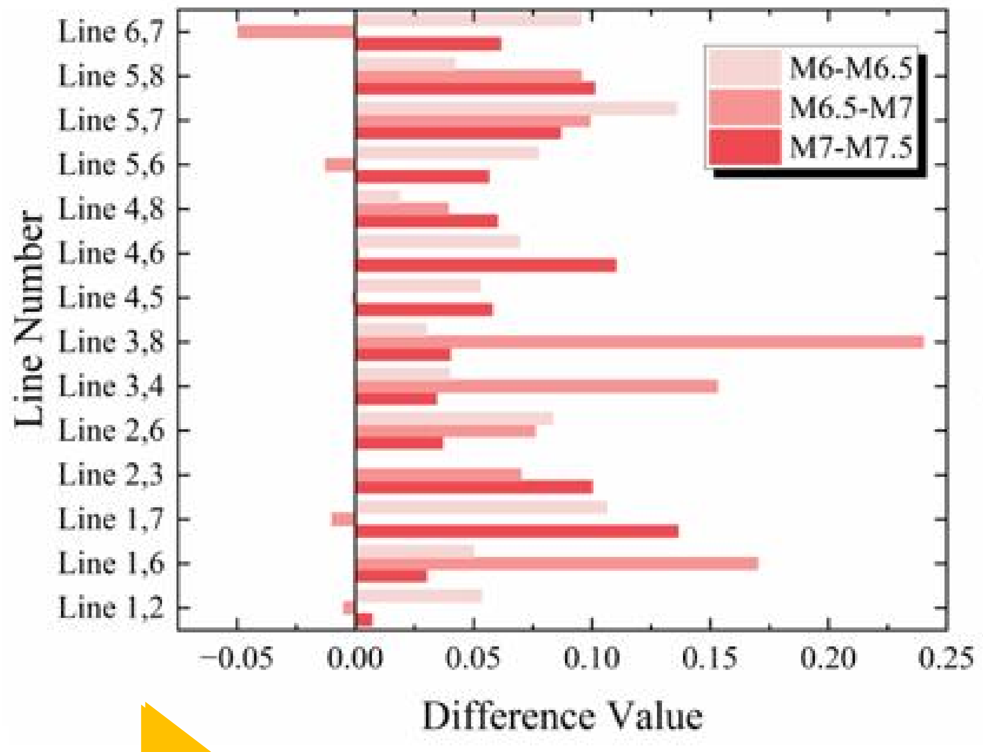

(a) Performance State II

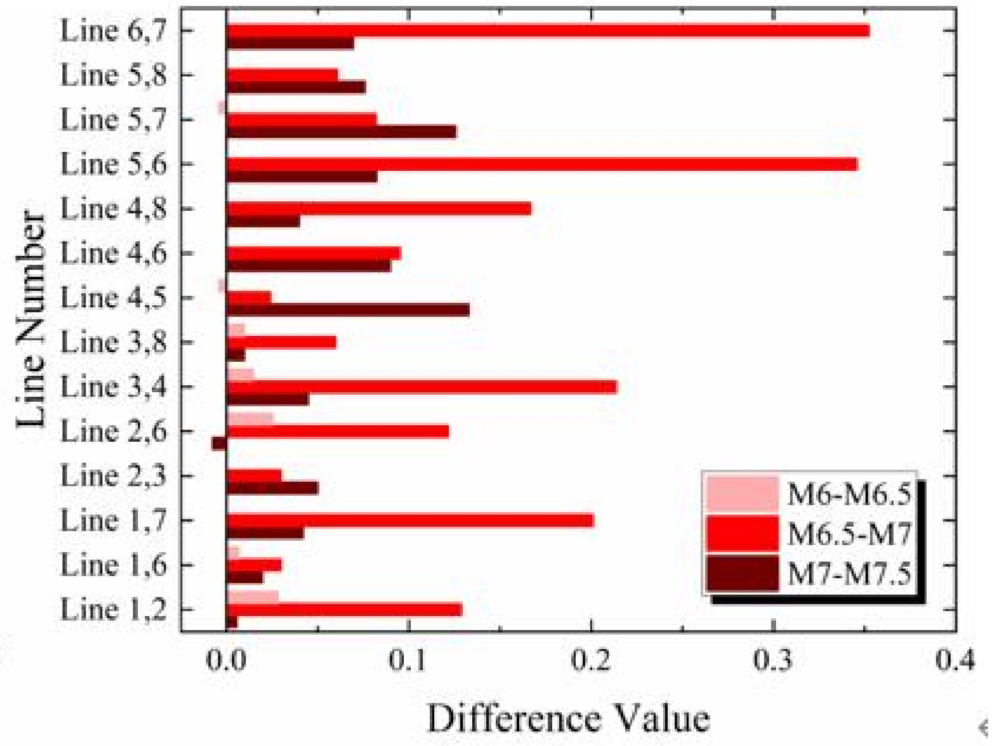

(b) Performance State III

Seismic intensity	Line names
6.5	Line 5-7, Line 1-7
7	Line 1-7, Line 1-2, Line 3-8, Line 3-4, Line 1-6, Line 6-7, Line 5-6
7.5	Line 4-6, Line 5-7, Line 4-5, Line 1-7

Post-Earthquake Priority Railway Lines

✓ Obtained the probability distribution of post-earthquake line operability and identified vulnerable routes under different earthquake magnitudes.

Conclusions

- A regional limited-sample ground-motion generation method was proposed, and the effects of training-set composition on prediction accuracy were revealed. Region-specific network selection criteria and an uncertainty-integrated seismic response prediction framework were developed. Applicability metrics for NN surrogate models were established based on epistemic uncertainty, and the effects of sample size and train speed on peak operability prediction uncertainty were clarified, enabling accurate uncertainty-informed prediction of structural seismic responses and post-earthquake bridge operability

- A geography- and prior-driven generation method for regional HRSBS was proposed, and a multi-source NN surrogate model was developed to couple topographic features with pier parameters. Epistemic uncertainty-embedded prediction intervals for post-earthquake operability were obtained, enabling regional bridge and line performance evaluation and supporting post-earthquake transport capacity assessment.

Limitations

- **Post-earthquake performance of other bridge and track structural forms, tunnel groups, and bridge–tunnel transition sections should be further investigated.**
- **The influencing factors of epistemic uncertainty remain insufficiently discussed. Further studies should focus on reducing, decomposing, and quantifying epistemic uncertainty.**
- **Regional ground-motion parameter attenuation equations should more accurately account for local site effects and near-fault pulse effects.**

Thank You for Your Attention!
Comments and Suggestions Are Welcome.

Lingxu Wu[1] 、Lizhong Jiang[2,3] 、Wangbao Zhou[2]

1. Zhejiang University of Water Resources and Electric Power, Hangzhou, Zhejiang
2. Central South University, Changsha, Hunan
3. Hunan University of Science and Technology, Xiangtan, Hunan

May 2026